The Application of Kinematics to Reproduce Patellar Cartilage and Determine the Compression thereof during Specific Movements

by
Anria Kruger

Thesis presented in partial fulfilment of the requirements for the degree of Master of Engineering (Mechatronic) in the Faculty of Engineering at Stellenbosch University

Supervisor: Dr. J.H. Müller
Co-supervisor: Prof. L. Labey

March 2017

The financial assistance of the National Research Foundation (NRF) towards this research is hereby acknowledged. Opinions expressed and conclusions arrived at, are those of the author and are not necessarily to be attributed to the NRF.

DECLARATION

By submitting this thesis electronically, I declare that the entirety of the work contained therein is my own, original work, that I am the sole author thereof (save to the extent explicitly otherwise stated), that reproduction and publication thereof by Stellenbosch University will not infringe any third party rights and that I have not previously in its entirety of in part submitted it for obtaining any qualification.

March 2017

Abstract

The aim of this study is to investigate the biomechanics of the patellofemoral joint in an *in-vitro* model. The project has three objectives: Firstly, a process needs to be designed that is able to estimate the geometry of the patellofemoral joint cartilage. Secondly, cartilage compression as a result of the investigated movements are determined. Finally, the associated stresses are estimated. The outcome of the objectives will provide information on the degree of cartilage deformation during different functional tasks.

The geometry of the patellar cartilage was estimated through the use of kinematics, the bones from the CT scans of the patella and femur, and the MRI scans of the uncompressed patellofemoral cartilage. This process included reproducing the kinematic models of two knees for a passive and squat motion and then using the results to estimate the patellar cartilage. It was found that the process was able to estimate the geometry of the patellar cartilage through the application of the kinematics and the uncompressed cartilage produced by the MRI scans. It was noted that the cartilage geometry differed between motions and between investigated knees in terms of thickness, but in general conformed to the geometry of patellar cartilage.

The deformation and compression of the patellofemoral cartilage was also determined by comparing the resulting estimated cartilage with the uncompressed cartilage segmented from the MRI scans. The main finding was that compression of the cartilage does result from the application of the investigated movements and that there was a definitive difference between the passive and squat movements.

Finally, the stresses as a result of the different compressions on the cartilage were investigated through FEA. The main findings was that the squat movement consistently resulted in larger stresses than the passive movement and that the stresses recorded on the patellar osseous-cartilage surface interface also produced larger stresses than the stresses found on the cartilage surface.

It was concluded that the designed process was able to determine the geometry of the patellar cartilage by using kinematics and the CT scans of the knee with little input from the MRI scans. Furthermore, through using kinematics, the compression of the cartilage due to these movements could be determined. It was concluded that the squat movement consistently produced larger compressions and stresses than the passive movement. This leads to the conclusion that it would be more appropriate to use the passive compression to modify and improve patellar replacements since it results in less compression and smaller stresses on the patella. Therefore, the replacement can still be modified to improve the geometry and account for some compression in the replacement, but not modified too much through the use of the squat movement to cause excessively larger stresses in the knee.

Uittreksel

Die doel van hierdie studie is om die biomeganika van die patellofemorale gewrig te ondersoek in 'n *in-vitro* model. Die projek het drie hoof doelwitte: Eerstens, moet 'n proses ontwerp word wat in staat is om die geometrie van die patellofemorale kraakbeen te skat. Tweedens word die kraakbeen kompressie as gevolg van die ondersoekte bewegings ook bepaal. Ten slotte, sal die verwante spannings ook bepaal word. Die uitslag van die doelwitte sal dus inligting voorsien oor die mate van kraakbeen vervorming tydens verskillende funksionele take.

Die geometrie van die knieskyf kraakbeen is beraam deur die gebruik van kinematika, die bene gekry vanaf die CT-skanderings van die patella en femur, en die MRI-skanderings van die nie-saamgeperste patellofemorale kraakbeen. Hierdie proses sluit in die reproduksie van die kinematiese modelle van twee knieë vir 'n passiewe en hurk beweging waarvandaan die knieskyf kraakbeen dan geskat word. Daar is bevind dat die proses die geometrie van die knieskyf kraakbeen kon skat deur die toepassing van die kinematika en die nie-saamgeperste kraakbeen van die MRI-skanderings. Daar is opgemerk dat die kraakbeen geometrie verskil het tussen bewegings en tussen ondersoekte knieë in terme van dikte, maar in die algemeen voldoen het aan die geometrie van knieskyf kraakbeen.

Die vervorming en kompressie van die patellofemorale kraakbeen is ook bepaal deur die geskatte kraakbeen met die nie-saamgeperste kraakbeen te vergelyk. Die belangrikste bevinding was dat daar wel kompressie is van die kraakbeen as gevolg van die toepassing van die ondersoekte bewegings en dat daar 'n definitiewe verskil tussen die passiewe en hurk bewegings is.

Ten slotte, die spannings as gevolg van die verskillende drukke op die kraakbeen was ondersoek deur EEA. Die belangrikste bevinding was dat die hurk beweging deurlopend gelei het tot groter spannings as die passiewe beweging en dat die spannings op die knieskyf ossaal-kraakbeen oppervlak koppelvlak tot groter spannings gelei het as die spannings op die kraakbeen oppervlak.

Daar is tot die gevolgtrekking gekom dat die ontwerpte proses wel in staat was om die geometrie van die knieskyf kraakbeen te bepaal deur gebruik te maak van kinematika en die CT-skanderings van die knie met min insette van die MRI-skanderings. Verder deur gebruik te maak van kinematika, was die kompressie van die kraakbeen van die gevolglike bewegings bepaal. Daar is tot die gevolgtrekking gekom dat die hurk beweging deurlopend groter kompressies en spannings veroorsaak het as die passiewe beweging. Dit lei tot die gevolgtrekking dat dit meer gepaslik sal wees om die passiewe kompressie te gebruik om knieskyf vervangings te verbeter aangesien dit lei tot minder kompressie en kleiner spannings op die patella. Sodoende kan die vervanging steeds aangepas word om die geometrie te verbeter en van die kompressie in rekening te neem om die vervanging te verbeter, maar nie so veel te verander deur die gebruik van die hurk beweging as om onnodige oormatig groter spannings in die knie te veroorsaak nie.

Acknowledgements

I would like to acknowledge and express my thanks to the following people for their contribution and support throughout this project:

1. Firstly, I would like to thank my lecturer, Dr. J.H. Müller, for his guidance, support, and patience throughout my project. Thank you for the insight and advice that was always freely available, and the motivation when at times I really needed it.
2. Prof. L. Labey for providing the data needed for my project and also providing insight and advice towards improving the thesis.
3. To my fellow post-graduate students. Thank you for the constant advice and motivation provided throughout the time spent in the office, the coffee breaks when motivation was low, and the great productive working environment.
4. To my family and friends, thank you for providing me with unceasing support and inspiration throughout my post-graduate time-period. To my mom and dad for always pushing me to do better and work harder and for seeing the potential in me. And to my friends for always providing a much necessary break and support when the nights became long.
5. Finally, to the National Research Foundation (NRF) for providing financial assistance towards this research. The Opinions expressed and conclusions arrived at, are those of the author and are not necessarily to be attributed to the NRF.

Table of Contents

List of Figures

Page

List of Tables

Page

Nomenclature

Abbreviations and Acronyms

ADAMS	Automatic Dynamic Analysis of Mechanical Systems
CT	Computed Tomography
FEM	Finite Element Model
MRI	Magnetic Resonance Images
STL	Stereolithography
TET4	Tetrahedral
TET10	Tetrahedron
TKA	Total Knee Arthroplasty
X-rays	X-radiation
3D	Three-Dimensional

Symbols

E	Young's Modulus	[MPa]
Q_1	Lower Quartile	[MPa]
Q_3	Upper Quartile	[MPa]
α_{min}	Minimum Flexion Angle	[°]
α_{max}	Maximum Flexion Angle	[°]
ν	Poisson's Ratio	[-]

Chapter 1

1 Introduction

1.1 Background

In recent years, extensive work has been done on the patellofemoral joint as a whole, focussing on a range of topics such as the design of mathematical models [1], [2], defining the articular cartilage [3]–[7], the anatomy and geometry of the joint [8], patellofemoral biomechanics [9], [10], prosthesis design [11]–[14], injury studies [15]–[17], and more recently statistical shape models of the joint [18], [19]. The majority of studies relating to the geometry of the patellofemoral joint have specifically focussed on describing the trochlear groove, with only a few exceptions focussing on describing any new distinct features on the patellar surface such as the Lambda study [3] and the Wiberg index [20] study. There exists, however, a need to further define and characterise the patella.

As a result there has been a great increase in recent years on research focussing on specific areas of the patella, including the forces on the patella [21], cartilage thickness and deformation [22], [23], and the geometry, anatomy, and position of the patella [24]–[29]. Some of the research is aimed at improving the way that prostheses are designed by providing necessary information to improve the patellar replacement design [30]–[32]. These methods of gathering information can, however, be costly and time consuming to pursue. A significant portion of these methods can also not be performed on a live patient, requiring that the limbs be de-articulated for examination. Investigating the amount of compression, for example, is one of these methods that needs the disarticulation of the limb. Information regarding the compression that patellar cartilage experiences during normal use of the knee could, however, provide better understanding into the shape and thickness of the patellar cartilage and the stresses that the cartilage experiences during normal everyday use.

In order to characterise patellar cartilage accurately, a model of the cartilage needs to be created. This includes building a database of cadaver knees which, preferably, consists of Magnetic Resonance Images (MRI's). MRI scans are able to display not only the bones of a patient, but the surrounding soft tissue including the cartilage. MRI's, however, are more expensive to obtain resulting in rather using Computed Tomography (CT) scans. CT scans are x-rays processed by a computer and does not provide any information on the soft tissue which could aid the investigation. If the cartilage is not available, it has to be recreated in order to determine the compression of the patellar cartilage during movement. A precise construction of the missing cartilage would allow the researcher to collect valuable data regarding the geometry of the patellar cartilage, the compression thereof, and the resulting stresses due to the compression.

Numerous studies on the compression of patellar cartilage have previously been conducted [22], [33], [34], but the main focus usually lies with determining the articular cartilage geometry and thickness under no compression [4], [7], [35]. These studies mainly use MRI's and *in-vivo* and *in-vitro* measurements to obtain the needed information. The existing studies on patellar cartilage compression needs to use multiple MRI scans of the joint while compressed to determine the compression of the cartilage, however, to the researchers' knowledge, no studies exist where CT scans were utilised in the process with little to no implementation of MRI scans. It is proposed that kinematics can be used in an effort to use mainly CT scans as input in determining patellar cartilage compression, taking into account the entire investigated motion. Finally, the compression of the cartilage can then be utilised to provide insight into the stresses that the patellar cartilage undergoes during the investigated movements.

1.2 Aims

This project aims to investigate the biomechanics of the patellofemoral joint in *in-vitro* models. A method needs to be designed in order to recreate model specific patellar cartilage while minimising the use of MRI scans and to broaden the understanding of the compression of the patellar cartilage during normal everyday knee movements. Furthermore, the project aims to investigate the resulting stresses on the patella due to the determined compression.

1.3 Objectives

The objectives for this project are as follows:

1. Estimate the geometry of the patellofemoral cartilage by using limited MRI scans, kinematic models of the knee, and the CT scans of the patellar and femoral bones as inputs for estimating the geometry of the cartilage.
2. Determine the deformation and compression of the estimated patellofemoral cartilage.
3. Determine and investigate the stresses present due to the compression of the patellofemoral cartilage.

1.4 Motivation

An increase in knowledge about the compression cartilage undergoes during normal everyday movement could potentially aid in improving prosthesis design, specifically patellar replacements. Current patellar replacements use standard polyethylene to recreate the patellar cartilage which is very unyielding when compared to actual cartilage. However, during any movement of a normal knee, compression of the cartilage takes place. It is also common for patients to experience patellar pain after a total or partial knee replacement which could possibly be as a result of the rigid uncompressible nature of the material used to replace the elastic compressible cartilage. This means that the compressible nature

of the patellar cartilage is not taken into account when designing patellar replacements which could be one of the causes for patellar pain after surgery. The pain that can still be present after surgery further emphasises the need to investigate the amount of compression that the patellar cartilage experiences during different movements and the effect that this compression has on the prosthesis and thus the comfort for the patient.

Furthermore, replacements are usually designed according to specific predefined sizes and shapes, using very stiff materials (in relation to actual cartilage) to produce the implants. These materials are not very compliant and could result in anterior knee pain after surgery since the implant is not able to compress like it usually does during movement. Investigating the compression of cartilage could deepen the understanding of the type of materials and their biocompatibility that should rather be used for these replacements. It could also give an indication of how much the implants needs to be modified in terms of deformation to improve the design. This could result in a more comfortable patellar replacement which performs in a manner closer to a normal healthy knee. Finally, a better understanding of the compression that patellar cartilage experiences during movement can help deepen the knowledge and understanding of the requirements necessary to potentially improve the knee biomechanics involved in prosthesis design.

1.5 Thesis Outline

This section will briefly outline the contents of each chapter in this thesis.

Chapter Two: The literature review discusses the patellofemoral joint, including the anatomical definitions necessary for the project. Furthermore, the kinematics of the knee joint and the articular cartilage of the patellofemoral joint is discussed. Three-dimensional (3D) modelling techniques and software, and the stresses on the articular cartilage during normal everyday use are also discussed. The chapter concludes with a discussion on existing cartilage estimation models and investigations regarding the compression of articular cartilage.

Chapter Three: This chapter provides a detailed discussion on the materials and methods used in recreating the cartilage of the patella and determining the compression thereof. This includes describing the acquisition of the data used, the creation of the kinematic models, the assumptions made, the designed patellar cartilage estimation model, and the creation of the finite element models. The chapter concludes by describing the various calculations and methods used for interpreting and processing the raw data received from the patellar cartilage estimation model.

Chapter Four: This chapter documents the results obtained from the models, focusing on the geometry of the estimated patellar cartilage, the compression thereof, and the resulting stresses on the patellar cartilage due to the calculated compression.

Chapter Five: A detailed discussion of the results will be provided in this chapter, where the findings will be investigated, discussed, and compared with results from literature.

Chapter Six: The final chapter provides a conclusion for the project, discussing whether the objectives of the project have been achieved, the limitations of the project, any recommendations for future work, and the overall contribution that the project had to the related field of study.

Chapter 2

2 Literature Review

2.1 Anatomical Definitions

This investigation will make use of certain terms of reference to describe and refer to the anatomy of the patellofemoral joint. This section describes and clarifies these terms as described in Wilkie *et al.* [36].

The knee, like the human body, can be separated into three distinct planes of reference. Figure 1 shows these planes.

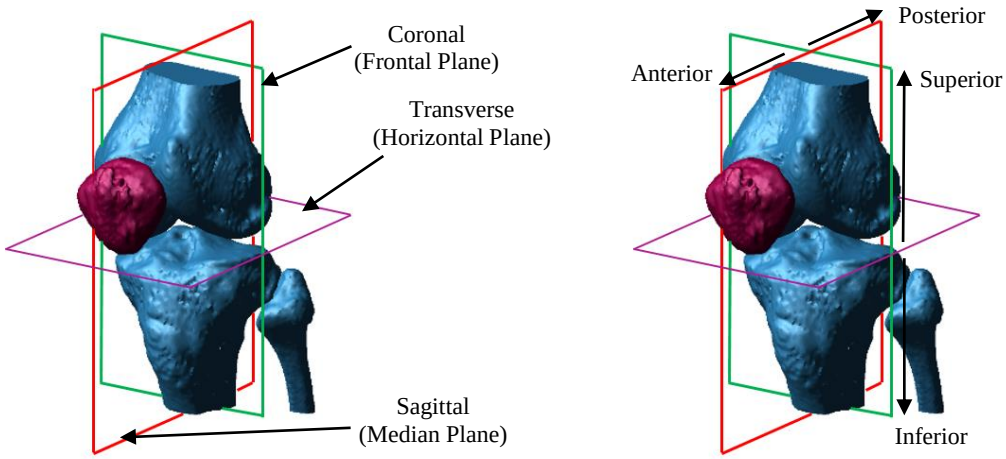

Figure 1: Anatomical references and planes.

Furthermore, the knee can also be divided into its six degrees of freedom. Figure 2 defines these six movements.

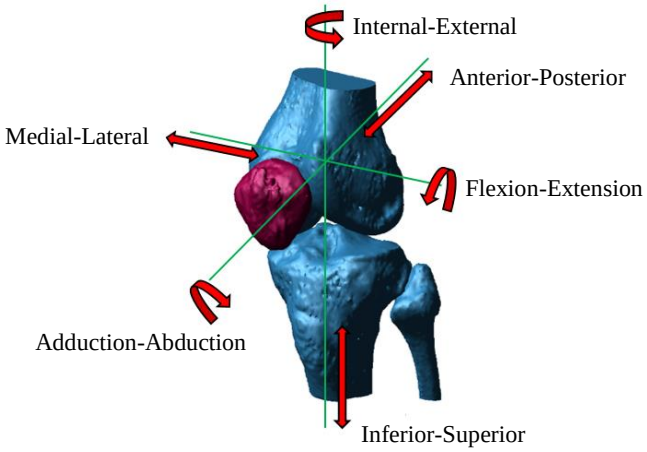

Figure 2: Movements of the knee.

2.2 Anatomy and Function

This section will describe the anatomy and function of the patella (kneecap) and patellofemoral joint separately.

2.2.1 The Patella

The patella plays an integral part in the proper functioning of the knee. Fox *et al.* [27] refers to the patella as a "large, flat, triangular sesamoid bone located anterior to the knee joint". This placement, the composition of the patella, and the relating attachments to the patella allows the patella to facilitate the extension and flexion of the lower limb.

- **Anatomy**

The anterior surface of the patella can be divided into three main parts, namely the superior, mid, and inferior sections (Figure 3). The superior third of the anterior surface is a slightly roughened surface with vertical osseous protrusions which facilitates the attachment of the quadriceps tendon. The middle and inferior thirds both have the same roughened surface as the superior third, however, the inferior section tapers down to pointed apex which facilitates the connection of the patellar ligament.[27]

The posterior surface (Figure 3) is primarily covered by an articular cartilage layer. The inferior apex is the only section of the posterior surface that is not covered by articular cartilage since the patellar tendon requires the roughened surface for attachment.

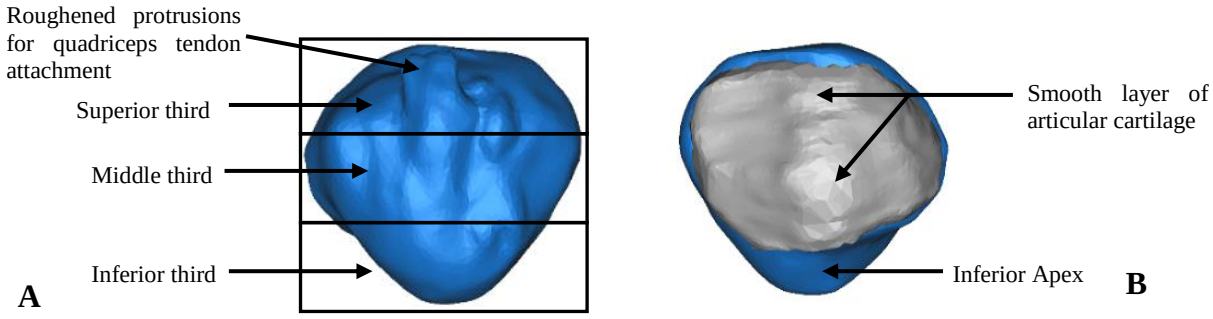

Figure 3: Anterior aspect (A), Posterior aspect (B).

- **Function**

According to Fox *et al.* [27], the patella mainly acts as a structure which increases the lever arm of the extensor mechanism. The patella thus facilitates the extension and flexion of the lower limb via the quadriceps and patellar tendons. The patella then performs as a fulcrum surface for the quadriceps tendon, decreasing the friction on the quadriceps tendon as the knee flexes and extends. [27]

The patella transfers the extensor force over the knee at a larger length from the line of rotation. This results in an improvement in the mechanical advantage of the extensor muscles. Additionally, this increase in mechanical advantage that the patella provides to the patellofemoral joint results in a reduction of 15% to 30% in

the quadriceps force [37] needed for knee extension. Different angles of the knee will result in a change in the mechanical advantage of the patella, with the knee at a more flexed position resulting in a smaller mechanical advantage than when the knee is fully extended [27].

2.2.2 The Patellofemoral Joint

The following section will describe the anatomy and function of the patellofemoral joint and how each component of the joint interlinks and connects with each other and its surrounding components. The patellofemoral joint describes the joint connecting the patella and femur (thigh bone). The joint performs an important function in the stability of the knee as well as facilitating the extension of the lower limb[37]. The patellofemoral joint forms part of the knee (Figure 4).

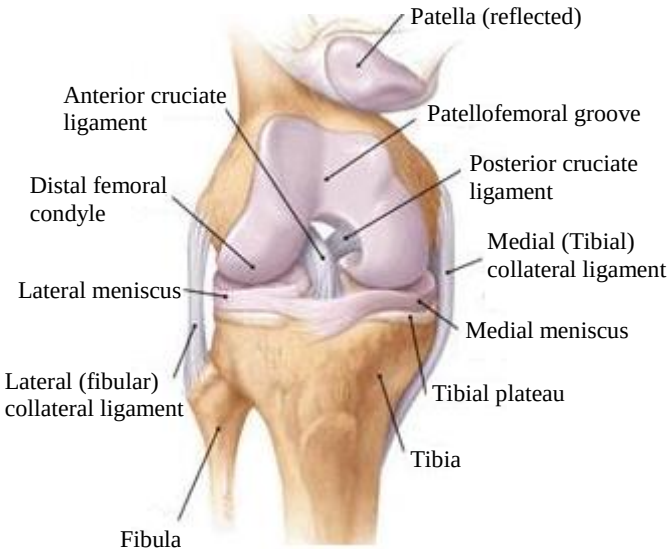

Figure 4: Anatomy of the knee [69]

- **Anatomy**

The femur is the biggest in length and the strongest bone in the body. The superior section, or curved head, of the femur articulates with the acetabulum of the hip [38], while the inferior section of the femur forms part of the patellofemoral joint. The femur has a near cylinder-shaped shaped mid-section which leads down to the inferior section of the femur. The inferior section of the femur interacts with the tibia through two big curved condyles (Figure 5) which are both covered with a cartilage layer. This cartilage layer not only covers the condyles, but also the trochlear groove where the patella articulates with the femur. Just above the femoral condyles are the epicondyles which has various sized protrusions which act as connection points to different muscles and ligaments of the patello- and tibiofemoral joints [39].

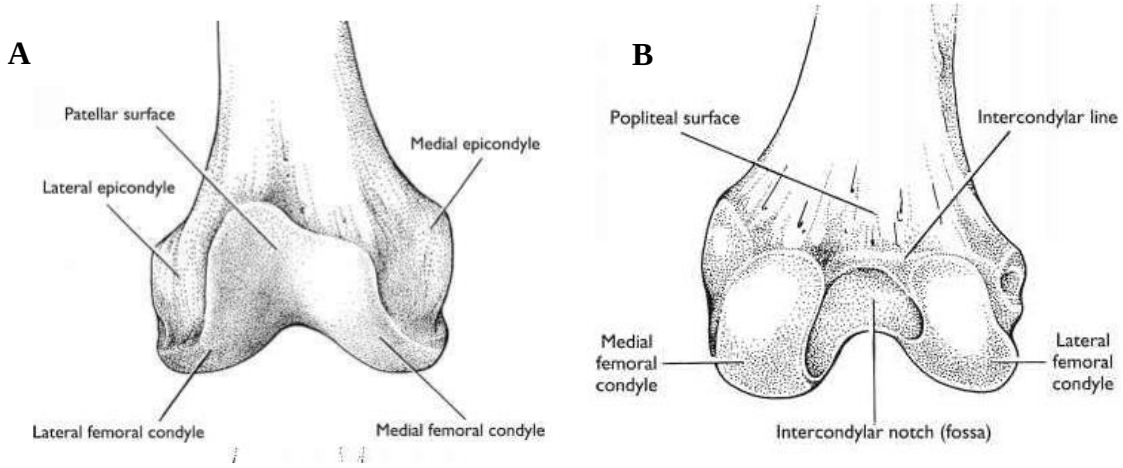

Figure 5: Anterior (A) and posterior (B) views of the distal femur.[39]

There are numerous ligaments and tendons that connect the muscles and bones in the patellofemoral joint. Ligaments are defined as "white fibrous bands of tissue which connect bones" [40], while tendons are "a cord or band of dense, tough, inelastic, white, fibrous tissue, serving to connect a muscle with a bone" [41]. These include the quadriceps tendon which attaches the quadriceps muscle to the superior section of the patella, and the patellar tendon which attaches the inferior apex of the patella to the tibia (Figure 4). The main ligaments in the knee are the posterior cruciate ligament, the anterior cruciate ligaments, medial collateral ligament, and the lateral collateral ligament as seen in Figure 4 [42]. Ligaments especially important to the patella are the medial patellofemoral ligament and the lateral retinaculum. Table 1 names the ligaments mentioned, their origin, insertion point, and function.

Table 1: Ligament descriptions [42]

LIGAMENT	ORIGIN	INSERTION	FUNCTION
Posterior cruciate	Posterior sulcus tibia	Anteromedial femoral condyle	Limits hyperflexion/sliding
Anterior cruciate	Anterior intercondylar tibia	Posteromedial lateral femoral condyle	Limits hyperextension/sliding
Medial collateral	Medial epicondyle	Medial meniscus and medial distal tibia	Holds medial meniscus to femur and resists valgus force
Lateral collateral	Lateral epicondyle	Lateral fibular head	Resists varus force
Medial Patellofemoral	Medial epicondyle	Superomedial aspect of patella	Counterattacks lateral movement of patella
Lateral retinaculum	Iliotibial band	Lateral edge of patella	Helps stabilise patella

The trochlear groove is essential to patellar stability during the movement of the knee and provides a smooth cartilage covered channel in which the patella can travel, providing a means of stabilising the patella during movement. This groove

connects the medial and lateral femoral condyles where it starts out as a shallow, nearly indiscernible, groove on the proximal section of the femoral condyles to a deep channel at the distal ends of the femoral condyles.[43]

- **Function**

The patellofemoral joint allows movement of the patella over the femur and in conjunction with the tibiofemoral joint, forms the knee. The knee can be described as having two main functions [44]:

1. The knee allows movement with minimal forces needed from the relating muscles while providing steadiness to the lower limb for movement over different environments.
2. Secondly, it is able to transfer and absorb loads during normal movement of the lower limb.

2.3 Stresses Experienced by the Patella

The knee joint plays a primary role in moving and supporting the human body. There are numerous forces that act on the joint, collectively allowing the extension and flexion of the lower limb. The main forces that interact with the patella are the quadriceps muscle force, patellofemoral joint reaction force, the tension in the patellar tendon, and the forces in the soft tissue structures on the medial and lateral side of the patella [45]. These forces combined add to the mobility and stability of the joint. During normal everyday movement such as walking, jogging, and sitting, the knee is put under stress.

Numerous studies have been conducted in an effort to determine the stresses, strains and deformations that the articular cartilage undergoes during everyday use. These studies assume the cartilage to be a linear elastic material since applying a 'bi-phasic' material model has proved extremely difficult. The investigations usually apply indentation tests which use a specific sized indenter. The indenter applies a precise reproducible load to a section of cartilage from which various properties can be calculated, including the resulting stresses on the articular cartilage.

Ateshian *et al.*[46] refers to a series of previous investigations from which they established that the stresses found on the articular cartilage of joints can be in the range of 0.2 to 12 MPa. They further state that the majority of the stresses experienced during normal use are more in the range of 0.2 – 2.5 MPa. [46]

Even though the structure of articular cartilage is exceptionally suited towards distributing and minimising the effects of the resulting stresses, the degradation of the cartilage, especially with age, can cause these stresses to produce discomfort and pain in the knee. A thorough investigation into these stresses in the articular cartilage due to normal everyday movement can increase the depth of understanding in terms of patellofemoral pain and injuries by investigating under what circumstances theses stresses would cause pain and injury. For example, stresses in excess of 5 – 7 MPa [47] have been recorded being experienced by patients that suffer from patellofemoral pain. An increase in the knowledge regarding the

stresses and pain experienced by the patellofemoral joint could advance treatment methods and create suitable prevention approaches.

2.4 Knee Joint Kinematics

The primary motion of the knee allows the flexion and extension of the lower limb. This motion can be simplified as a hinge joint in the sagittal plane, however, as seen in Section 2.1, the joint has six degrees of freedom, three translational and three rotational. In full extension, the quadriceps muscles are contracted with the long axis of the femur and tibia line up. As the hamstring contracts the knee will start flexing, moving the patella along the trochlea until the knee has reached full flexion at between 150° to 160° with full extension being at 0°. Figure 6 shows the knee in full extension and flexion during a passive motion of the knee. [44]

A **B**

Figure 6: Full extension (A) and flexion (B) of the knee during a passive knee motion

During maximum extension, the knee is in its most stable and supported position, where the least amount of force needs to be applied by the quadriceps to ensure stability. The motion that the knee experiences most often, takes place during gait. During gait, the knee moves in such a manner as to allow the body to move forward with negligible upper body actions needed. In order to ensure that the toes of the moving limb do not drag across the floor when stepping forward, the knee will flex to about 70°. As the knee moves through the swing phase of the gait, just before the heel hits the ground, the quadriceps muscles will shorten to extend the knee fully which moves the foot forward. This position allows the heel to strike the ground first. Finally, just before the heel strikes the ground, the knee flexes to about 15° to absorb the impact of the motion. [44]

Figure 7 shows the gait of the lower limb for one full cycle from full extension, to flexion, and back to full extension.

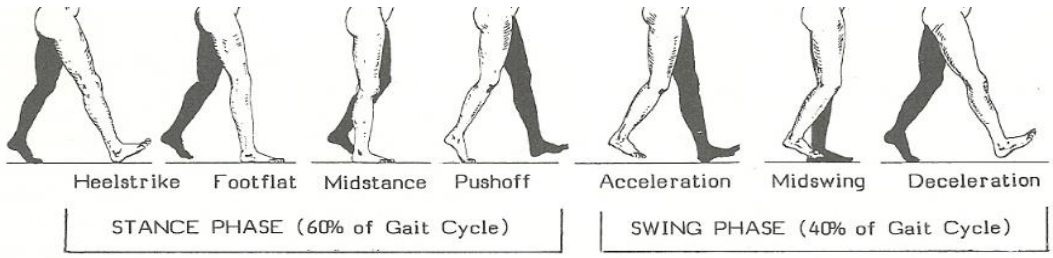

Figure 7: The gait cycle. [70]

- **Articular Kinematics of the Patella and Femur**

The primary articulating areas between the patella and the femur are the cartilage covered posterior surface of the patella (Figure 3, B) and the trochlear groove of the femur. The posterior articulating surface of the patella can be divided into (1) a large, thick, and slightly convex section, (2) a smaller, thinner, and slightly concave section, and (3) a vertical ridge that splits the two surfaces. These three sections share the mirror shape of the trochlear groove and immediate connecting condylar surfaces of the femur. [44]

During the full extension of the knee, the only section of the patella that is in contact with the femur is the distal end of the patella. Very little of the patellar cartilage is in contact with the femur at this point in the motion. As the knee starts to flex, the patella will move along the trochlear groove where more of the patellar cartilage will come in contact with the trochlea and femoral condyles. During deep flexion there only exits contact between the patella and the medial and lateral condyles of the femur and no contact between the patella and trochlea. [44]

Figure 8 shows the contact areas between the femur and patella at various knee flexion angles as the knee experiences motion.

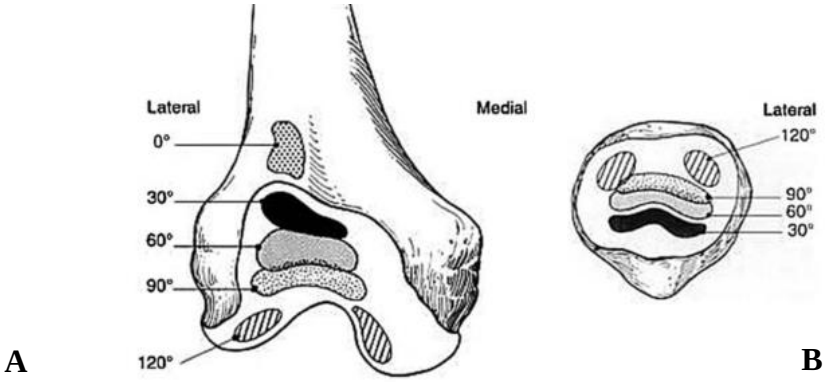

Figure 8: Articulating surfaces of the femur (A) and patella (B) at different angles during motion. [27]

2.5 Articular Cartilage

A detailed description of the thickness, geometry, and location of the articular cartilage of the patellofemoral joint will be given in this section.

2.5.1 Patella

The articulating cartilage of the patella is located on the posterior surface of the patella. The cartilage covers about 80% of the superior section of the posterior patellar surface. Ateshian *et al.*[48] made use of stereophotogrammetry to quantify the articular surface features and cartilage thickness of the knee. Stereophotogrammetry is a technique that uses two-dimensional photographic pictures and suitable mathematical methods to obtain detailed three-dimensional measurements of a specific object. By using this technique, Ateshian *et al.*[48] was

able to measure the underlying bone geometry, cartilage thickness, and cartilage areas. The specific area (A) and the grey shaded topographical map of the cartilage thickness (B) of the patella can be seen in Figure 9 as identified by Ateshian *et al.*

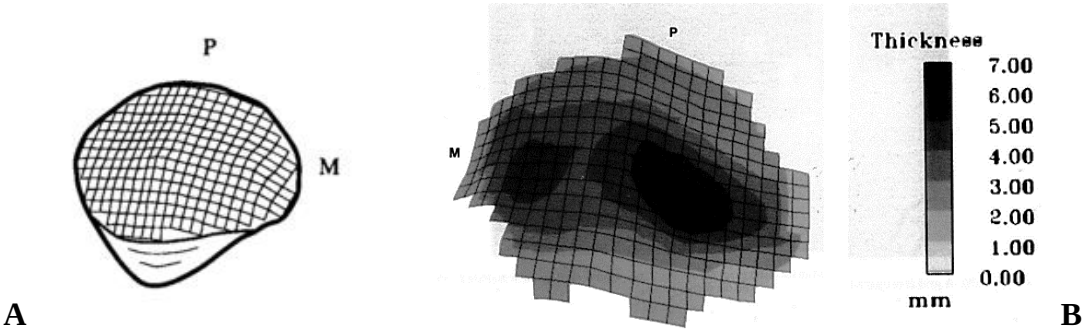

Figure 9: Three-dimensional model depicting cartilage surface area (A) and topographical map of the cartilage thickness (B) of the patella. (M = Medial, P = Proximal) [48]

Ateshian *et al.* calculated the surface area of the patella as 10.7 ± 1.6 cm^2, the mean cartilage thickness as 3.33 ± 0.39 mm, the minimum cartilage thickness as 0.89 ± 0.31 mm, and the maximum cartilage thickness as 5.91 ± 0.87 mm. The thickest part of the patellar cartilage can be located in the middle area of the cartilage surface. More specifically, the lateral third of the cartilage usually has the thickest cartilage, with the cartilage becoming thinner towards the outside edges of the cartilage surface.

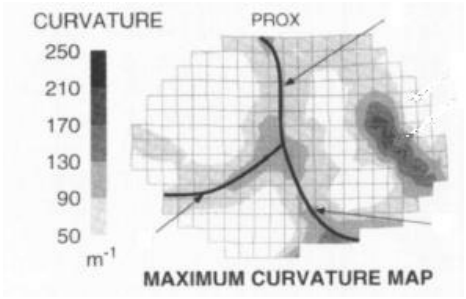

Figure 10: Maximum curvature map of patellar surface. [3]

The surface geometry of the patellar articular cartilage, however, can be further analysed describing its distinctive surface features. These features can increase the characteristics of the surface geometry of the patella. Kwak *et al.* [3] conducted a surface curvature analysis of the human patellofemoral joint where they analytically calculated the curvatures of the patellar and femoral cartilage and used it to classify significant distinct surface structures to aid in the characterising of these surfaces. The patellar surface can commonly be defined as having a mostly convex surface with different elevations and features, however, a more detailed and accurate description would be that the surface of the patella can be defined as having a somewhat convex middle region, and slightly concave outer regions. In some cases, a distinct "tilted lambda ridge" can be identified as seen in Figure 10. [3]

2.5.2 Femur

The articulating cartilage of the femur is situated on both of the femoral condyles and the trochlear groove. On the inferior end of the femur, the thickest cartilage can be located on the trochlea. The trochlea makes contact with the vertical middle cartilage ridge on the patella and helps in guiding the patella over the femur. The cartilage situated on the anterior aspect of the femur has thinner cartilage than the trochlear cartilage. As summarised by Ateshian *et al.*[48], the surface area for the femoral cartilage is 29.5 ± 2.5 cm^2, the mean cartilage thickness is 1.99 ± 0.12 mm, with a minimum of 0.16 ± 0.06 mm and maximum of 3.61 ± 0.3 mm. The specific area (A) and the grey shaded topographical map of the cartilage thickness (B) of the femur can be seen in Figure 11 as identified by Ateshian *et al.*

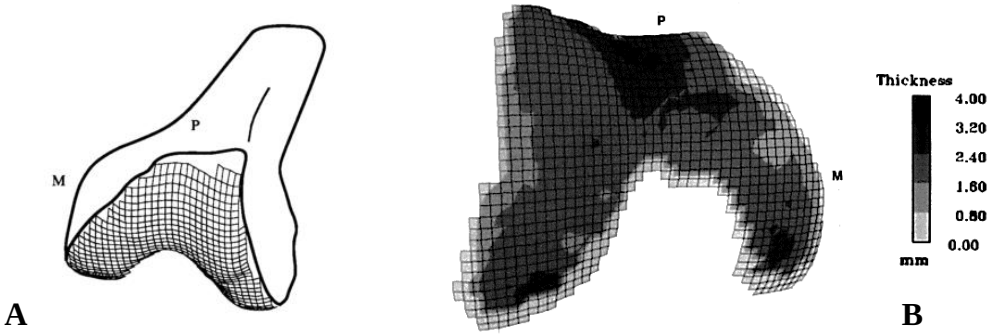

Figure 11: Three-dimensional model depicting cartilage surface area (A) and topographical map of the cartilage thickness (B) of the femur. [48] **(M = Medial, P = Proximal)**

2.5.3 Cartilage in Compression

Cartilage can be described as a porous structure which is composed of a multiphasic structure. The fluid phase consisting of water and electrolytes, and the solid phase consisting of mostly type II collagen. This particular composition is what allows the cartilage to compress. The cartilage also contains varying levels of chondrocytes, proteoglycan, and collagen fibrils. Chondrocytes are cells found in cartilage tissue which maintains the cartilage matrix and makes the cartilage malleable [49]. Proteoglycan are proteins found in cartilage that facilitates the lubrication of the surface [50], while the collagen fibrils are strong fibrous proteins found in cartilage which provides the cartilage with the ability to withstand the forces acting in on it [51]. As a force acts on the patellar surface, the fluid in the cartilage moves out of the cartilage and into the neighbouring tissue which allows the cartilage to compress. The fluid moving into the surrounding tissue causes the tissue to expand which compacts the cartilage. The longer the compression of the cartilage takes places, the greater the effort needed to compress the cartilage further. [52]

The composition of cartilage is not constant and differs layer by layer along its thickness. Cartilage can be divided into four main layers. According to Pal *et al.* [52], "the superficial zone is characterized by flattened chondrocytes, relatively low quantities of proteoglycan, and high quantities of collagen fibrils arranged parallel

to the articular surface. The middle zone, has round chondrocytes, the highest level of proteoglycan among the four zones, and a random arrangement of collagen. The deep zone is characterised by collagen fibrils that are perpendicular to the underlying bone, and columns of chondrocytes arrayed along the axis of fibril orientation. The calcified zone is partly mineralized and acts as the transition between cartilage and the underlying subchondral bones". Mechanical properties of cartilage thus differ with each layer in the cartilage.

The composition of cartilage allows for compression, but varies with time. As mentioned, the more time passes, the more difficult compression becomes. Herberhold *et al.*[33] was able to use 5 cadaver knees to determine the relationship. They observed that within the first minute of compression, only 7% of the total compression had taken place. By the 100th minute of static loading, the compression started to equalise not showing a significant change in compression for the rest of the time period. Cartilage thus follows an exponential trend in the initial stages of the compression after which it equalises not showing any significant increase in compression.

The thickness of the articular cartilage has been thoroughly investigated, however, since most of these investigations relied on de-articulating the knee to measure the articular surfaces, the compression of the cartilage could not be measured. In order to measure the compression, the articulating surfaces needs to be in contact with each other and undergoing a load of some sort, thus in order to measure the compression of the cartilage the knee should not be de-articulated.

2.5.4 Material Properties

The composition of cartilage makes determining some of the material properties problematic since cartilage is a non-linear material. Therefore, this section will focus on the material properties of articular cartilage such as the Poisson's ratio and Young's Modulus which could be implemented to determine the stresses experienced by articular cartilage that is subjected to a load under the simplifying assumption that the articular cartilage is a linear elastic isotropic homogenous material.

In most studies found [53],[54],[55], these properties were determined and calculated by using indentation tests to apply the pressure to the articular cartilage. These tests, however, vary somewhat in terms of the size of the indenter and the amount of pressure being applied to the cartilage. This results in a range of values for both the Poisson's ratio and Young's Modulus, each relating to the tests performed by the individual investigator.

Kempson *et al.*[53], for example, described an experimental procedure where in-vitro indentation tests were performed on articular cartilage of the human femoral head in order to describe the creep modulus of the cartilage. The process involved indenting the cartilage on the femoral head at a reproducible unchanged load for two seconds and then measuring the indentation. Those indentation measurements were then used to calculate the creep modulus. Finally, the investigators used the

measured strains to calculate a range of Poisson's ratios (see Table 2) with a mean value of 0.48. [53]

Another investigator, Hayes *et al.*[54], created a mathematical model for indentation tests of the articular cartilage. They modelled the cartilage as infinite elastic layer connected to a rigid half-space based on the theory of elasticity. The mathematical model that they created was able to use Poisson's ratios in the range of 0.3 to 0.5 (see Table 2) to determine other material properties.

Finally, Hori *et al.* [55] used experimental methods involving compression indentation tests to determine shear and bulk moduli. The main investigation revolved around performing numerous experimental indentation tests on human articular cartilage and comparing it to data, experimental and from mathematical models, of previous investigations in an effort to establish a connection between the material properties. The results from their investigation reported (see Table 2), amongst others, a Poisson's ratio of 0.47, which they compared to studies mentioned earlier in this section. [55]

Table 2: Poisson's Ratios as found in literature.

	Poisson's Ratio (*v*)		
	Mean	Min	Max
Results 1: [53]	0.48	0.43	0.56
Results 2: [54]	0.45	0.4	0.5
Results 3: [55]	0.47	0.418	0.492

Table 2 shows a common tendency for the Poisson's Ratio to be within an approximate range of $v = 0.4 – 0.5$. Hori *et al.* also reported an average Young's Modulus of $E = 5.06$ MPa, however, numerous previous studies [53], [56], provide the Young's Modulus in a range of $E = 6.97 – 11.63$ MPa.

2.6 Three-Dimensional Modelling

Various methods exists with which the patellofemoral joint can be assessed, analysed, and investigated to provide various outcomes that can aid in prosthesis design, injury diagnosis, and data collection . Three-dimensional (3D) modelling provides an extremely powerful platform to achieve these outcomes and has become essential in the medical and engineering field. Through either the use of graphics software, imaging, or scanning, high quality 3D models can be created with relative ease.

2.6.1 Radiography

A radiograph (Figure 12) refers to "a negative image on photographic film made by exposure to x-rays or gamma rays that have passed through matter or tissue" [57]. Radiographs are one of the most common and widely used methods of imaging. However, in recent years investigators have moved to more modern methods such as computed tomography (CT) scans or Magnetic Resonance Imaging (MRI) since radiography only takes single images in one axis at a time and is not able to provide a 3D image of the section being investigated. Even though radiographs are able to image the internal organs, they are much more capable of imaging the osseous structures of the human body.

Figure 12: Radiograph depicting a knee.[71]

2.6.2 Computed Tomography Scan

CT scans (Figure 13, A) are a useful imaging technique which can be used to investigate the osseous structures of the human body. CT scans are able to take a 360 degree scan of the section of the body needed with which it is able to produce multiple detailed cross-sectional images of the body part. CT scans are, however, more suited towards the imaging of osseous structures. [58]

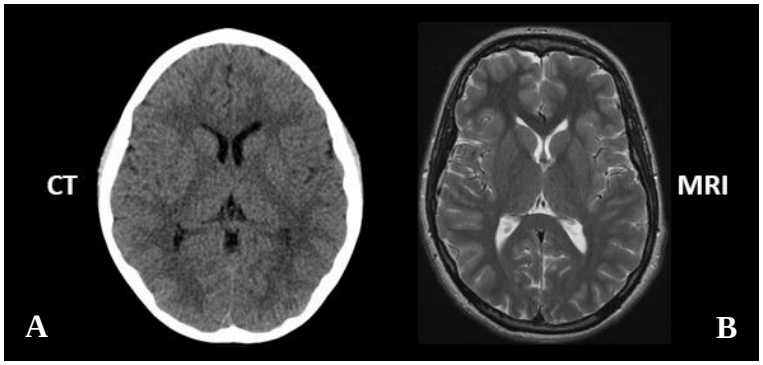

Figure 13: CT scan (A), MRI (B), of the brain.[72]

CT scans are more expensive than radiographs, but are able to produce a much more detailed image which can easily be processed into a 3D model. CT scans, however, lacks in contrast ability which could make it difficult to spot potentially important details and information.

2.6.3 Magnetic Resonance Imaging

Magnetic Resonance Imaging (MRI) uses a magnetic field and radio waves to generate in depth high-resolution pictures. MRI can produce extremely detailed cross-sectional images (Figure 13, B) from which 3D models can be created of the osseous structures and soft tissue of the human body, making it the most ideal method for imaging the internal structure of the human body. [58]

MRI's are, however, much more expensive and time consuming than CT scans and radiographs and since MRI's make use of a magnetic field, anyone with pacemakers and other medical implants would not be able to be scanned in a MRI machine. Even with the disadvantages listed, the increased capability of MRI to image soft tissue and produce highly detailed images, still makes it the leading choice as a diagnostic and imaging tool. The images received from MRI or CT scans can be processed into 3D models (Figure 6) of the particular object.

2.6.4 Mimics/3-Matic

While MRI and CT scans are used for the initial data accumulation, the images need to be processed by computer software into the 3D model needed. Mimics (V16.0.0.235, Materialise, Belgium) is a software specifically designed for medical image segmentation and is able to process data from a range of input formats such as CT, MRI, and 3D ultrasound. The software not only enables the user to create accurate 3D models form the imaging data, but also provides a platform to measure and modify the model. Finally, the software exports the model in a stereolithography (STL) file. [59]

A STL is a file format that is commonly used in 3D modelling. The STL file divides the model surface into triangles where an increase in triangles increases the complexity and detail of the surface being approximated.

While Mimics is an extremely powerful software for segmenting the MRI/CT data, it has limited modification functions. 3-Matic (V8.0, Materialise, Belgium), however offers a great range of functions to modify the 3D model. 3-Matic is exceptionally suited for 3D measurements and engineering analyses, designing patient specific prosthesis, and for preparing the model for finite element analysis. Combined, Mimics and 3-Matic forms a powerful platform to create, modify, and design 3D anatomical models.

2.6.5 ADAMS

Automatic Dynamic Analysis of Mechanical Systems (MSC ADAMS) (V2013.1, MSC Software Corporation, California) is a software mainly used in the modelling of dynamic systems and structures. This allows the user to study and investigate how the model reacts to different loads and forces which makes it an excellent software to study the kinematics of an anatomical model. [60]

2.6.6 MATLAB

MATLAB (V R2014a, Mathworks Inc, Massachusetts) is an extremely powerful software for performing numerical computation. It provides a platform for solving engineering problems by providing a matrix-based MATLAB language to perform calculations.

2.7 Existing Models on Cartilage Estimation

The measurement, analysis, and model creation of articular cartilage could initially only be performed by ex-vivo measurements on cadaver knees. This was a destructive process which required that the knee be disarticulated to reach the articulating surfaces of the cartilage. Radiography allowed the investigator to measure the cartilage without disarticulating the knee, however, the nature and quality of the radiograph proved to be inadequate for cartilage analysis.

When MRI became a common technique for acquiring and creating 3D models, the investigation of cartilage increased. MRI is a highly detailed, but expensive, technique to identify and measure cartilage. However, MRI is still the most common method of measuring and determining the shape, thickness, and location of the articulating cartilage of the patellofemoral joint. Most studies [61], [62], [7], [63], focus on obtaining the MRI images of the joint and using the resulting model to investigate the cartilage. These studies, however, tend to use their own measurement technique which is not always reproducible by other investigators. MRI can be used to determine thickness and volume accurately, but MRI with adequate resolution and proper experience in segmenting the images into a 3D model is essential to ensure an accurate representation of the cartilage [62]. Various studies were able to define the mean articulating cartilage thickness of the patellofemoral joint as seen in Table 3.

Table 3: Comparison of the results of the mean thickness of the patellofemoral articulating cartilage.

	Mean Patellar Cartilage Thickness	**Mean Femoral Cartilage Thickness**
Results 1 [7]	3.05 mm	2.08 mm
Results 2 [48]	3.33 ± 0.39 mm	1.99 ± 0.12 mm
Results 3 [63]	± 4 mm	-

Few studies have, to the investigators knowledge, been conducted on recreating the articulating cartilage of the patellofemoral joint without the use of MRI or existing cartilage in the model where only the bones of the knee are available for use.

2.8 Existing Models on Cartilage Compression

In recent years, the compression of cartilage has been studied quite thoroughly. Originally, compression of cartilage was mainly determined by experiments and indentation tests. These investigations provided valuable information into the

compressional nature of articular cartilage, however, the information provided was still considerably different than the results would have been if the joint was still intact.[33]

MRI provided the investigators with a means of examining the articular cartilage under compression without disarticulating the knee. The knee could thus be put under various static and dynamic loads at different degrees of flexion to more accurately determine the compressional properties of the articular cartilage in the knee. Numerous studies [22], [33], [64], [65], have been conducted where MRI was used to determine the cartilage compression. Since MRI is able to provide detailed information regarding the soft tissue of the human body, it is a perfect tool for investigating the compression of the articular cartilage. MRI also allowed for dynamic force testing by examining volunteers performing certain dynamic movements over a period of time. Eckstein *et al.*[22] used twenty healthy volunteers and had them perform squatting at 90° angle and 30 deep knee bends representing the static and dynamic loading movements. The results showed a reduction in the articular cartilage volume of the patella of -5.9 ± 2.1 % during the knee bends and -4.7 ± 1.6 % during squatting, while the articular cartilage of the patella showed a thickness reduction of -2.8 ± 2.6 % during the knee bends and -4.9 ± 1.4 % during squatting. These actions serve to best represent the compression that the articular cartilage undergoes during normal daily circumstances since the knee mostly compresses the cartilage for a few seconds and not hours. The tests showed the compression during the first 320s of loading.

Chapter 3

3 Materials and Methods

3.1 Overview

This chapter gives a detailed description of the materials and methods used in estimating the articular cartilage of the femur and patella from the CT scans and kinematics of the knee joint as well as the methods applied in the analysis of the resulting data. To the author's knowledge, no studies have been conducted to attempt to recreate the cartilage of the patella with only the 3D models (segmented from CT scans) of the bones of the knee joint. Developing a method of achieving this could decrease the resources needed to produce and analyse the articular cartilage of the patellofemoral joint, because the use of 3D data would remove the need to gather information through destructive invasive experimental techniques. The aim is to use the kinematics of the knee during a passive and squat movement to estimate the cartilage geometry. Since the cartilage will compress during these actions, this method can be further utilised to determine the compression of the cartilage while performing these movements. The flow diagram in Figure 14 depicts the flow of data and the process followed to produce the absent compressed articular cartilage of the femur and patella.

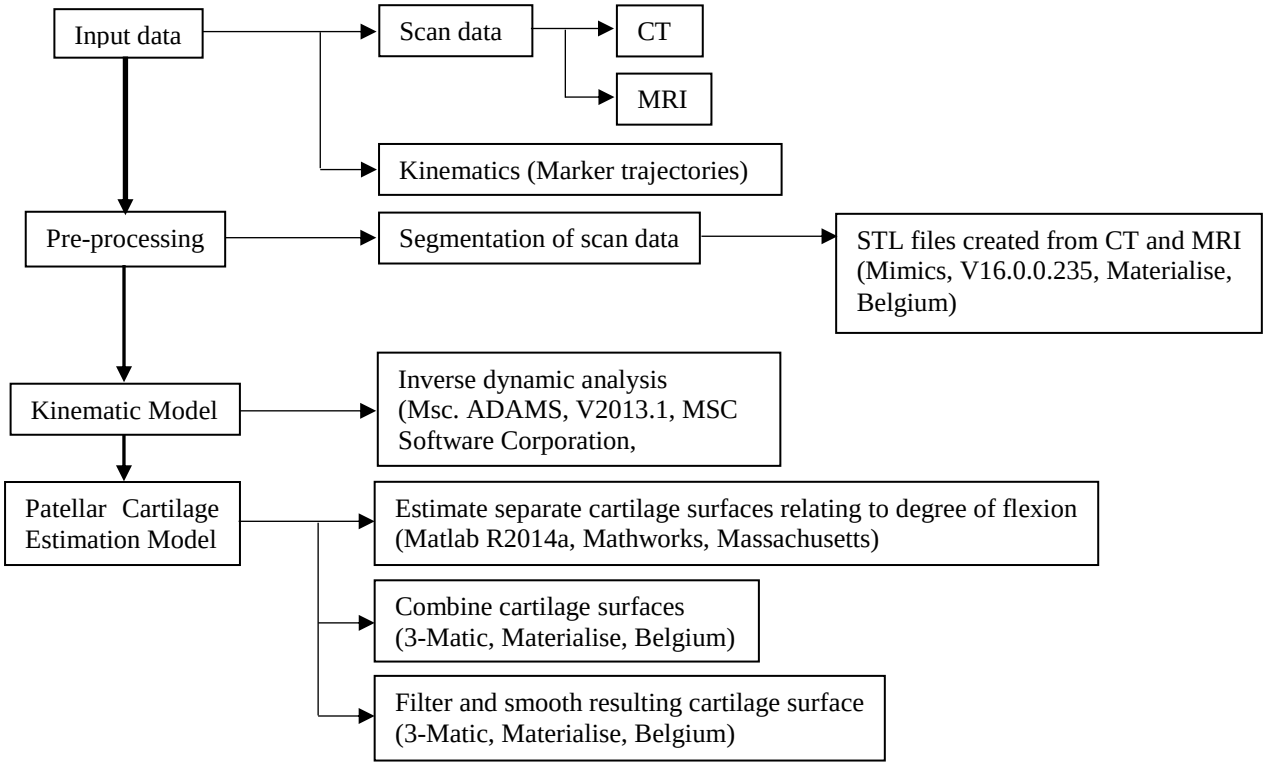

Figure 14: Flow of data and process followed in estimating the patellar and femoral cartilage.

Mainly, the process of estimating the patellar cartilage uses the geometry and thickness of the femoral articulating surface in combination with the kinematics of the knee to form the patellar cartilage. The main theory is that the movement of the femur relative to the patella will shape the cartilage of the patella. The patella receives an overly thick roughly estimated cartilage at the beginning of the process which is then shaped and formed as the femur moves through different degrees of flexion relative to the patella, slicing away the excess cartilage to produce patellar cartilage shaped by the kinematics of the knee joint.

3.2 Ethical Approval

Ethical approval for this project was received from the Local Research Ethics Committee (University of Leuven, Belgium). Furthermore, no test or investigation was done involving any of the following criteria as described by the Stellenbosch University Research Ethics Committee:

- "Any direct interaction with or observation of human participants".
- "The use of potentially identifiable personal health records, information, or tissue specimens, and/or,"
- "Human progenitor or stem cells".

3.3 Assumptions

The following assumptions were made during the estimation process of the cartilage:

1. The femoral cartilage does not compress.

   This assumption would greatly simplify the recreation of the cartilage since the original compressed femoral cartilage is not available during the initial stages of the process and thus it would be difficult to determine the relative compression taking place between the femoral and patellar cartilage and apply it to the designed method. By only focussing on the patellar cartilage, the process is simplified and the total compression can be used throughout.

2. The femoral cartilage conforms to the geometry of the femoral condyles and trochlea.

   This assumption also simplifies the process since the cartilage of every individual femur differs slightly and creating individual specialised geometry for each femur would be time and resource consuming. Assuming conformity, however, could still produce a close likeness as can be seen in the geometry description found in literature [48].

3. The femoral cartilage has the same thickness over the entire articular surface.

   Femoral cartilage does not have the same thickness over the entire articular surface, but assuming the same thickness over the entire articular surface will

give a close approximation to the actual thickness distribution as seen in literature [48] and will aid in simplifying the process of estimating the cartilage geometry.

3.4 Data Acquisition

The data used was obtained from the study done by Delport *et al.*[66]. This section will give a short description of the process followed by the investigators as described by Delport *et al.*[66], providing details on the materials and methods, and the results of the experiment focussing on the data used specifically in this thesis. This thesis primarily made use of the CT scans of the patella and femur, the MRI scans of the patella and femur, and the kinematic results obtained during the investigation.

3.4.1 Data Collection Method

Delport *et al.*[66] aimed at testing whether it would be beneficial for patients undergoing total knee arthroplasty (TKA) to restore the neutral mechanical orientation.

The investigators made use of six fresh frozen cadavers of the lower limb with no known medical problems with the joint. The process was started by obtaining the MRI scans of only the knee joint of the lower limb cadavers. CT scans of the entire lower limb were then obtained. The CT scans had marker mounts (Figure 15) connected to the femur and tibia from which a coordinate system could be defined to aid in describing the alignment and kinematics of the knee joint. [66]

A 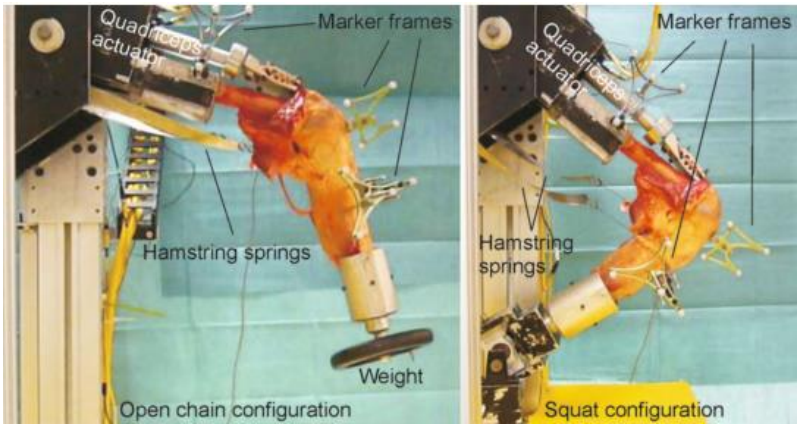

B

Figure 15: The knee kinematics simulator setup. Open chain testing (A). Squatting (B). [66]

The final setup included attaching the knee to the kinematics simulator as shown in Figure 15, which allowed the knee joint to perform various motions such a passive movement and squatting movement from which the specific kinematic data for that movement could be extracted.

The marker frames had reflective round markers attached to the frames which was consistently tracked using six infrared motion capture cameras. The information

recorded from the motion cameras was used to define the trajectories of the markers as the knee joint was put through the mentioned motions resulting in the description of the kinematics of that specific motion of the knee joint. The knee was put through three motions, namely a passive extension flexion motion, an open chain extension, and a squatting motion.

3.4.2 Movements Analysed

The movements mentioned in section 3.4.1 that was used in this investigation will be described in more detail in this section to properly define the movements and describe the kinematics of the knee during the experiment.

Passive Patellofemoral Movement

The passive movement entailed fixing the femur horizontally in the frame and then allowing the tibia to move through the full range of movement without restricting the other degrees of freedom. This means that the tibia and patella with all its related ligaments and tendons would flex and extend to create a cycle of movement which was repeated three times. No extra loads were added to the frame for the passive movement.

Loaded Squat Patellofemoral Movement

The squat movement consisted of performing a squat motion that ranged between 30° and 130° with a vertical ankle load of 133 N applied to the bottom of the tibia where the ankle is located. The tibia fitting was attached to the kinematics structure (Figure 15, B) to replicate the proper form of a squat.

3.4.3 CT Results

The results of the CT scans were accurate enough to enable the investigators to segment precise replicates of the bones of the knee joint. The resulting 3D model provided an accurate bone model, however could not describe or model the soft tissue of the knee joint. Figure 16 shows a final 3D model segmented from a CT scan showing the femoral, patellar, and tibial bones of the knee joint in great detail. The CT scan was detailed enough to depict the osseous protrusions on the femur, patella, and tibia where the ligaments and tendons would attach.

The majority of the data used from the study consisted of the CT scans. The CT scan data was provided in the form of a STL file for the patella and femur which was then utilised in this thesis.

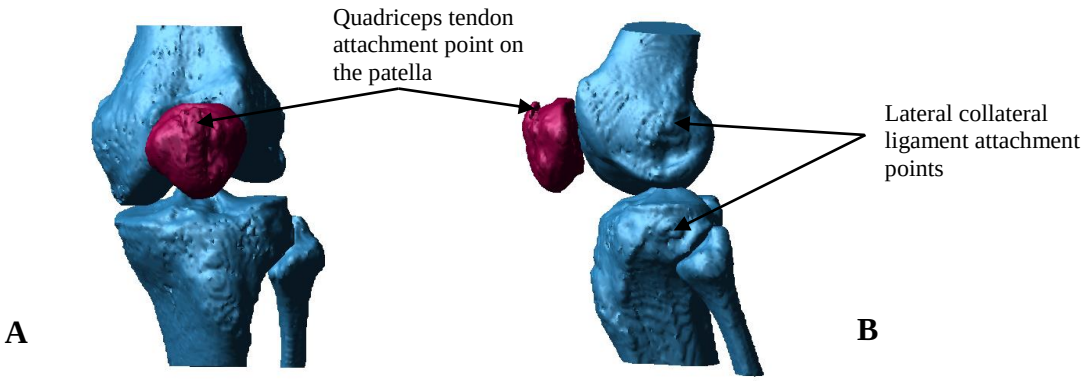

Figure 16: Segmented 3D results of the knee joint from CT scan. Anterior view (A), and lateral view (B).

3.4.4 MRI Results

MRI scans was also conducted on the knee joints. The MRI scan was able to provide detailed data on the soft tissue, especially the articular cartilage, of the knee joint before any loads or motions were applied to the joint. The resulting cartilage was thus the uncompressed cartilage of the knee joint. The segmentation of the MRI was more time consuming and complicated than the segmentation of the CT scans since the segmentation programs are able to very accurately identify the bone on a CT scan, while the soft tissue displayed on a MRI scan needs to be manually identified by the investigator since different types of soft tissue are very similar in contrast to each other on the MRI.

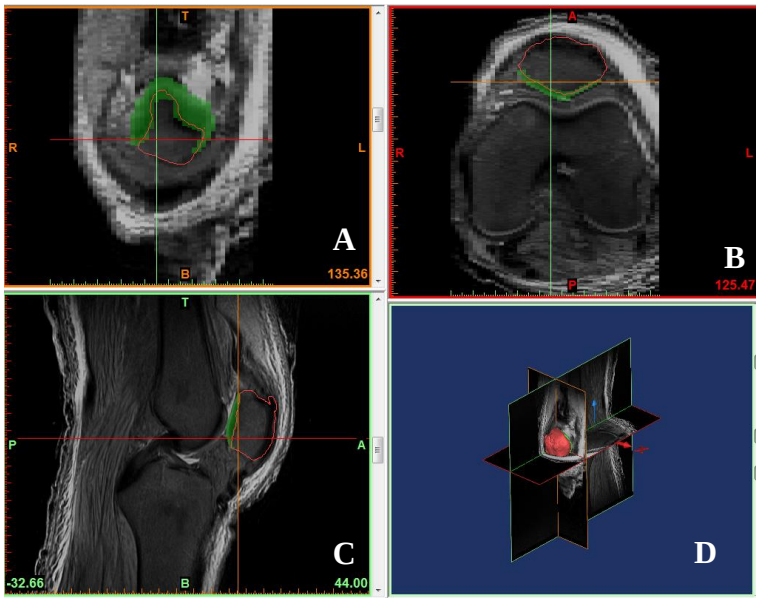

Figure 17: Front view (A), top view (B), side view (C), and 3D section view (D) of the patellofemoral joint of knee 1.

The MRI data of the femurs and patellae for knee 1 and knee 2 was used for the information it provided on the uncompressed articular cartilage of the

patellofemoral joint. The MRI data was provided as the unprocessed MRI scans. These scans had to be segmented manually to extract the cartilage from the MRI data. Figure 17 shows an example of one of the raw MRI sequences clearly depicting the soft tissue. The green highlighted section shows the cartilage as identified on that MRI slice by the investigator while the red outlines the patella bone on the MRI section.

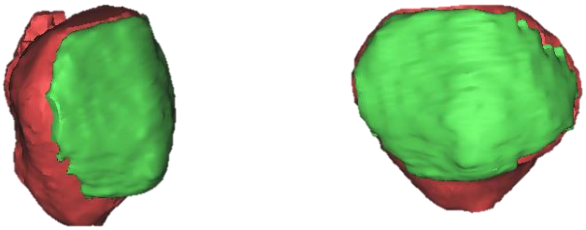

A **B**

Figure 18: Patella as segmented from MRI sequence of knee 1.

Figure 18 shows the patella with cartilage as segmented from that MRI sequence shown in Figure 17.

3.4.5 Kinematic Results

The kinematic data gathered by Delport *et al.* formed the foundation of this thesis since it would be used to test whether the kinematics can be used to recreate the cartilage of the patella and whether it can be used to determine the compression of cartilage during movement. As described in section 3.4.1, the kinematics of the knee movements was tracked by using a system consisting of the kinematic structure, which held the knee cadaver, and reflective markers attached to the kinematic structure. The femur, patella, and tibia each had four reflective markers attached to their section of the kinematics rig which was used to describe the kinematics and trajectories that each of these bones underwent individually in the coordinate system created.

The investigators created a coordinate system which was supplied in the form of a excel sheet containing all the marker coordinates as seen in the defined coordinate system. The X, Y, and Z coordinates for each of the four markers for each of the knee joint structures were provided to be able to define the markers in 3D space relative to their related knee joint structure as they were before any motion took place. This set of data thus defined the coordinates of the knee joint at its original reference point or starting point.

Furthermore, the kinematic data as recorded from the motion capture camera, provided the frame number and all the related coordinates for all the markers at a specific time frame. This data defined the trajectories of the markers of the knee joint as it moves through space.

3.5 Pre-Processing of the STL Files

The first stage in the estimation process is to prepare the received STL files of the femur and patella for further processing. It is essential that any modifications to the STL files that could affect the outcome of the geometry of the final cartilage should be done before continuing to the next step in the process to increase the accuracy and consistency of the end result.

The STL files consisted of the segmented 3D models of the bones of the femur and patella with no cartilage present on the bones. The STL files had small surface abnormalities which was introduced during the segmentation of the CT scans which could greatly affect the accuracy of the estimated cartilage. These surface protrusions needed to be removed to provide smooth even surfaces for inclusion in the rest of the process.

Since the patella and femur were segmented from the CT files, no cartilage was present in the initial STL files. In addition to the initial filtering and smoothing of the STL files, this stage of the process primarily included the addition of roughly estimated cartilage to the femur and preparing the patellar surface for processing.

3.5.1 Processing Segmented CT Scans

Before any material is added to the femoral surface, the original osseous surfaces (segmented from CT scans) need to be smoothed and filtered. The femur showing two enlarged sections of the femoral surface at different angles can be seen in Figure 19. More specifically, Figure 19 highlights the protrusions and nodules that need to be removed from the femoral surface. The entire articular surface of the femur needs to be clear of any inconsistent nodules and protrusions to prevent them from influencing the outcome of the cartilage geometry.

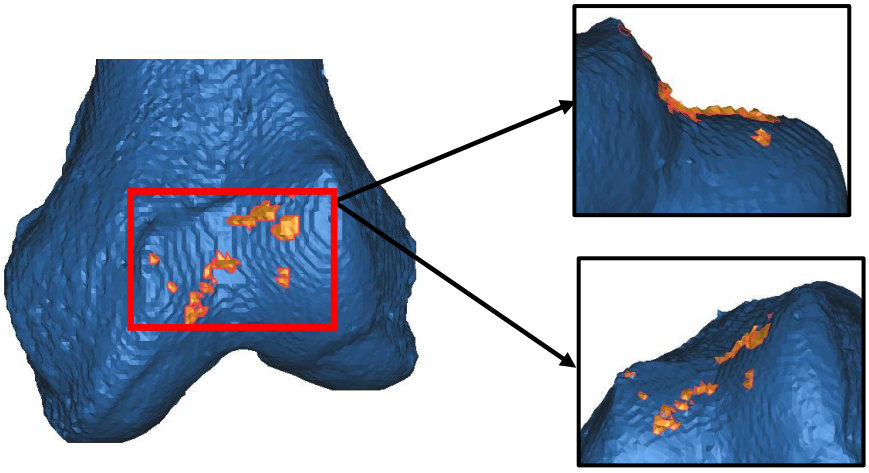

Figure 19: Enlarged sections of the femur indicating the protrusions and nodules which should be removed.

3.5.2 Cartilage Prediction for Femoral Articular Surface

In order to estimate the patellar cartilage, the femoral cartilage had to be predicted. Since the shape and the thickness of the estimated patellar cartilage will be directly influenced by the shape and thickness of the femoral cartilage, this step had to be completed before proceeding to the next section.

There are two main methods of producing a femur with cartilage. The first method involves assuming that the cartilage thickness over the entire articular surface is uniform and that the cartilage conforms to the underlying osseous geometry of the condyles and trochlea. An offset of 1.8mm [48] is then applied, using 3-Matic, to the identified articular surface to replicate the femoral cartilage. The highlighted area in Figure 20 indicates the surface area to be covered by the cartilage. The second method is to segment the cartilage from the MRI scans.

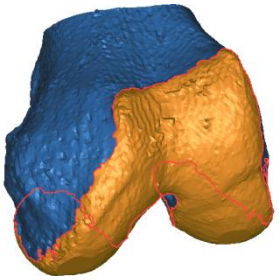

Figure 20: Femoral surface area (highlighted orange) to which the cartilage is added.

After the femoral cartilage has been replicated, the final resulting surface needs to be smoothed and filtered to ensure a clean smooth surface to use in the next stages of the process.

3.5.3 Preparing the Patellar Articular Surface

The addition of material to the patellar articular surface only serves as a base structure from which to form the cartilage of the patella which will be derived from the shape of the opposing femoral surface and resulting kinematics. The initial cartilage being added to the patella at this stage, does not need to be accurate or geometrically specific in any way, the only requirement is that it needs to be thick enough that when the femur and patella are in their articulating positions, the patellar cartilage intersects the femoral cartilage over the entire articulating surface. Figure 21 shows the articulating surface (highlighted) as acquired from literature.

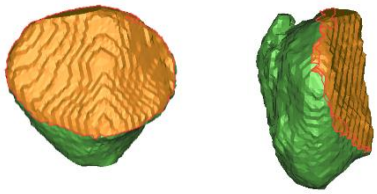

Figure 21: Patellar articular cartilage area (highlighted orange).

Figure 22 shows the patella with the newly added base material intersecting the femoral cartilage.

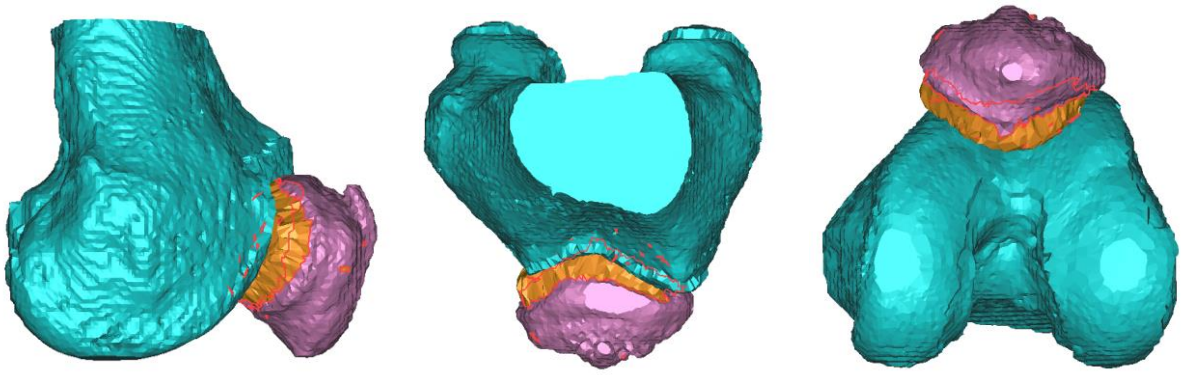

Side View Top View Bottom View

Figure 22: Femoral and patellar cartilage intersection.

The patella and femur modified with the added cartilage material, as described in sections 3.5.1 - 3.5.3, is exported as STL files and forms the base structures to be used in the following steps.

3.6 Kinematic Models

This section details the use of Msc. ADAMS to create a kinematic model from the defined marker trajectories. This includes using the STL files from the femur and patella as prepared in section 3.5 and the marker trajectories defining the movement of the knee joint during a passive and squat movement.

Primarily, ADAMS will be used to articulate the femur and patella into a moving entity through applying the defined trajectories for the passive and squat movement. Firstly, the STL files of the femur and patella, as prepared in section 3.5, needs to be imported into the ADAMS workspace for processing. These parts are already at the correct coordinates in the global coordinate system and relative to each other, and do not need to be moved.

3.6.1 Creating and Connecting the Markers

The markers used in the knee kinematics simulator were not directly connected to the knee joint. Instead, the markers were connected to marker frames which held them at defined locations. The trajectories of these markers where then recorded using the available infrared motion capture cameras. Since the trajectories related

to the markers, the markers also had to be created and added in the simulation to be able to correctly relay the trajectories to the knee joint itself.

The markers can be represented as small spheres, which ADAMS allows the user to create through adding defined bodies to the model. In total, twelve markers should be generated with their coordinates matching the coordinates of the actual physical markers. Initially, when the markers are created in ADAMS, they are not connected to the knee joint in any way, they only have the correct coordinates as given in space. Thus, each one of the markers need to be connected to their relating structure (femur or patella) to be able to use their trajectories. Figure 23 (A) displays the knee joint and the created markers.

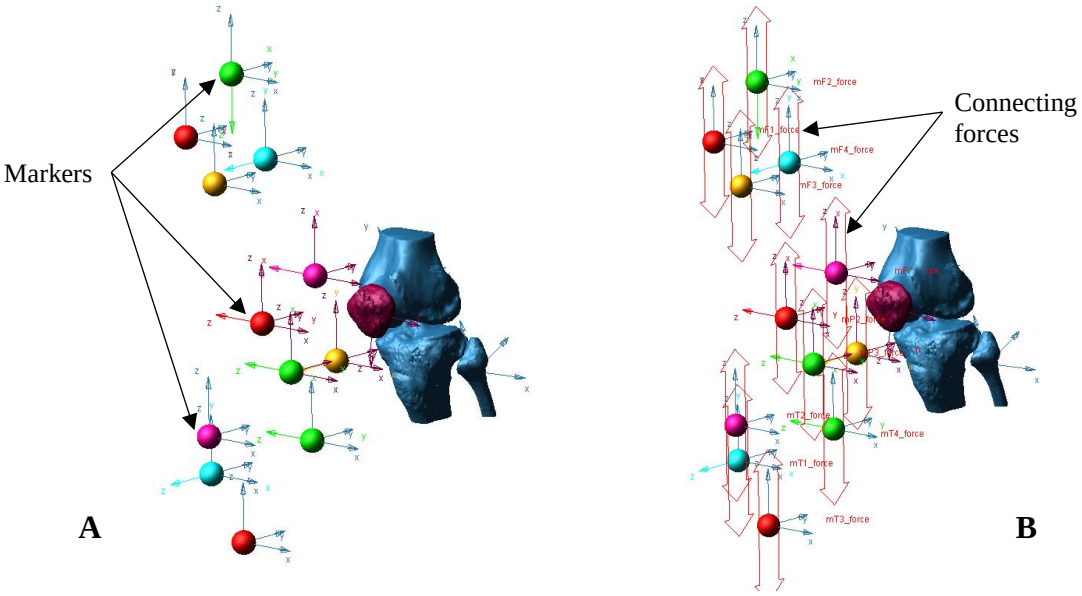

Figure 23: Knee joint with related markers and axis (A). Knee joint and markers with the connecting force (B).

The markers are connected to their related part through the creation of an applied spring-damper force (Figure 23, B) which will result in the trajectories of the specific marker being relayed to the part.

3.6.2 Creating Splines and Applying Motion

This section describes the creation and implementation of splines that define the motion of the three parts in the Cartesian coordinate reference frame over the time period that the motions took place. The splines are created from the trajectories available for the markers. Matlab is used to create individual splines (time and distance) which define the X, Y, or Z position, as tracked over time, for each of the markers. These splines are then imported into ADAMS and applied to the markers. Since the markers are now connected to the parts, the motions are also connected to the parts.

The coordinate system used throughout the project, followed the coordinate system defined by Delport *et al.*[66]. The coordinate system was thus anatomically

determined by the experiment through the use of the CT scans and data markers. The flexion angle used is defined as the angle between the femoral shaft axis and the tibial shaft axis.

Applying the motion to the markers is the final step and by running the simulation, the motion being applied to the knee joint can be viewed. In this thesis, the knee joint for two knees (knee 1 and knee 2) was modelled going through a passive and squat movement.

3.6.3 Saving and Exporting the Model

The Matlab script which shapes the patellar cartilage depends on the femur being at different degrees of flexion in order to ensure that the entire articular surface of the femur is taken into account when shaping the patellar cartilage. During the experiment, the actual flexion for the squat movement only starts at 30°, but this was normalised for all models to zero degrees. The model thus needs to be saved and exported at set degrees of flexion (every 5°), from the normalised zero degrees to the maximum achieved flexion angle. This is done by running the simulation and recording the frame at which the model reaches every successive five degrees of flexion through the use of the measurement tool in ADAMS. The model is then saved at each of these recorded frames, resulting in a set of models each at different degrees of flexion. All the recorded models are then exported for further processing in 3-Matic.

3.7 Patellar Cartilage Estimation Model

This section describes the process of estimating the cartilage from the kinematic models of the femur and patella as prepared in section 3.6 by making use of 3-Matic and author created scrips in Matlab for the mesh deformation.

3.7.1 Pre-Processing STL Files

The prepared kinematic models required minimal processing in 3-Matic before being utilised in Matlab. ADAMS is only able to export the models as parasolid file types, while the Matlab program reads STL files. 3-Matic is thus used to convert the parasolid files exported from ADAMS into STL files which can then be read by Matlab.

3-Matic is used to delete the motion markers that were exported with the femur and patella from ADAMS. The estimation script created in Matlab by the author reads the patella as stationary while the femur moves relative to it, while the model as exported from ADAMS has the femur stationary and patella moving in relation. The final step in preparing these two parts would thus be to globally register the femurs, and their related patella, in relation to the patella at zero degrees by using the global registration tool in 3-Matic. Figure 24 shows three models, each with a patella at a certain degree of flexion as imported from ADAMS. All the femurs are occupying the same space.

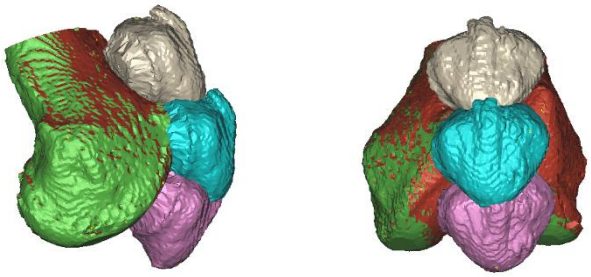

Figure 24: The models as imported from ADAMS.

The global register tool allows the user to choose a stationary object (patella at zero degrees), an object to be moved in relation (a patella at a different degree of flexion), and a move-along object (the femur of the second mentioned patella). The tool then precisely aligns the protruding osseous surfaces (which remains unchanged throughout the whole process) of the two mentioned patellae and moves the femur of the second mentioned patella along, keeping it in the same position relative to its relating patella. Thus, the model which is at zero degrees will be the reference point, while all the other models will be moved relative to it. This means that each patella that is at a different degree of flexion, will be moved to match with the reference patella at zero degrees. The femur of that particular patella will then move with the patella to the reference patella, but still stay in the same place relative to the moving patella. Figure 25 shows the resulting orientation of the model after the global registration. All the patellae are now occupying the same region in space, while their related femurs moved in relation to them.

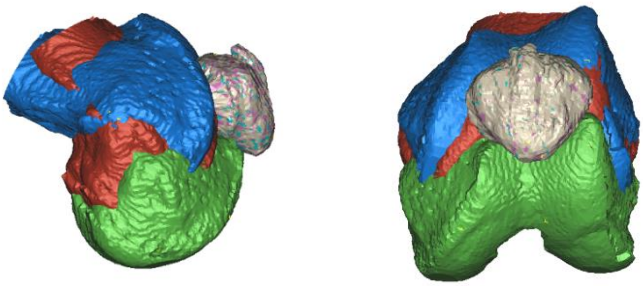

Figure 25: Globally registered patellofemoral models.

The patella at zero degrees and all the globally registered femurs are exported as STL files to be used in Matlab.

3.7.2 Estimation of Patellar Cartilage

This section details the steps followed in the script written by the author in Matlab which produces a set of surfaces to be used to create the patellar cartilage. At this stage in the process, there should be one patella (at zero degrees flexion) with the added material to the articular surface, and multiple femurs each at a different degrees of flexion. Figure 26 provides a flowchart describing the process followed by the Matlab script. The following steps are followed to estimate the patellar cartilage:

Step 1: Import STL files

The first step that the Matlab program performs is importing the applicable STL files into the working directory for further processing. This includes the prepared patella and the relating femurs at the varying degrees of flexion as prepared in Section 3.7. The STL files are voxelised[1] in Matlab through the application of the voxelise.m script as downloaded from Matlabs' open source file exchange platform. The STL files were voxelised in order to form a closed triangular-polygon mesh of the STL files which gives access to an array of data formats that could be manipulated in Matlab. It thus provided a 3D structure consisting of voxels (volume pixels) with coordinates that could be manipulated by the written Matlab script.

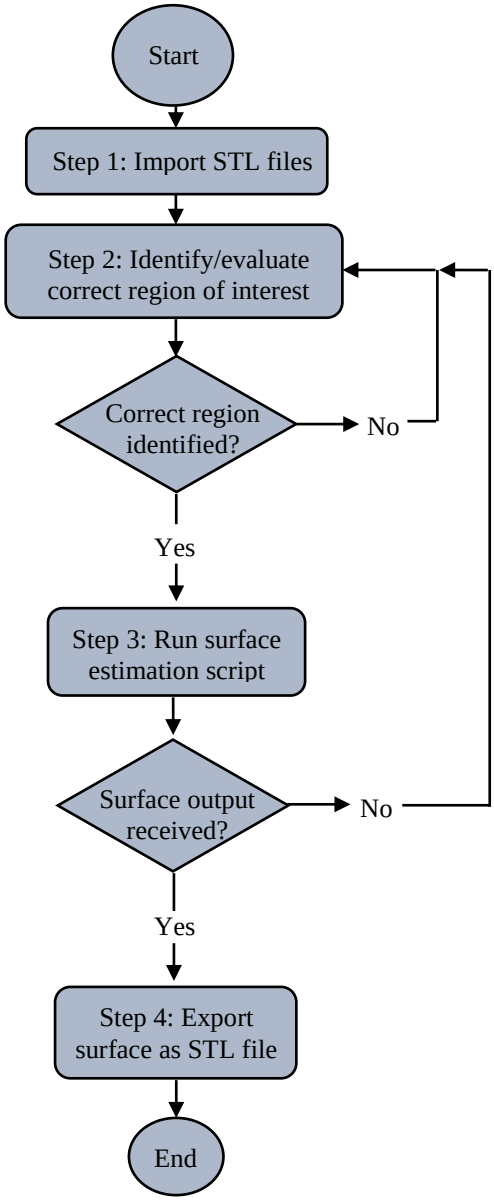

Figure 26: Flowchart describing the steps followed during the estimation of the patellar cartilage in Matlab.

[1]Aitkenhead *et al.*

Step 2: Identify/evaluate correct region of interest

The Matlab program requires that the correct regions on the patella and femur are identified to indicate where the modifications should be made. Correctly identifying the region of interest is of utmost importance to be able to estimate an accurate cartilage surface from the femoral surface. The entire section of the patella containing the added cartilage material needs to be specified in the 3D coordinate system. The rest of the patella should not be added to this specified area. The same area identified on the patella will be identified on the femur since the patella does not rotate or move, this region stays the same throughout the program. Figure 27 indicates the region of interest.

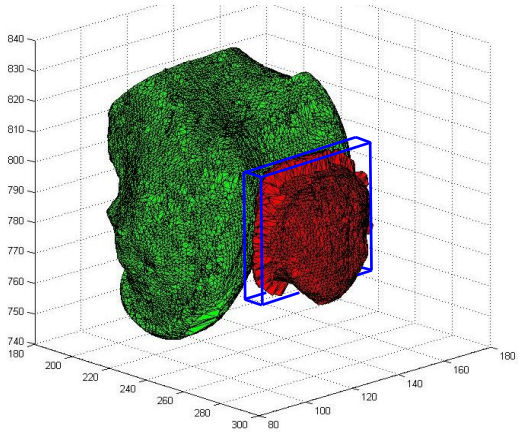

Figure 27: Region of interest for both patella and femur.

Step 3: Run surface estimation script

This step performs the main modifications and mesh deformations and creates the cartilage surface relating to a specific femur at its degree of flexion. Mainly, since the 3D points that the voxelised STL files consist of can be manipulated, the patella structure can be modified by changing the coordinates on the patella that touch or intersect the relating coordinates on the femur, to those intersecting coordinates on the femur. This results in a separate surface the size of the patellar articular cartilage area, but with the shape and position of the opposing connecting area of the femur. The end result for one model (or knee) should be multiple surfaces (Figure 28) that all conform to the intersecting femoral surface of their relating degree of flexion.

Step 4: Export surface as STL file

Once all these separate cartilage surfaces has been created, they are exported as STL files where the final processing of the files can be done in 3-Matic.

3.7.3 Final Processing

This section details the final steps in estimating the patellar cartilage which are done using 3-Matic. The estimated surfaces created in Matlab have to be joined with each other and with the patella to create the final estimated patellar cartilage surface. These surfaces all represent the resulting cartilage of the patella as it connects with

the femur at a certain degree of flexion. In order to create the final surface, these surfaces needs to be joined to take into account the geometrical and compressional effect that the femur has on the cartilage of the patella throughout the entire motion of the knee. This was done by using the glue meshes, wrap, and Boolean Union tool in 3-Matic to join the determined cartilage surfaces and the patella with no cartilage together.

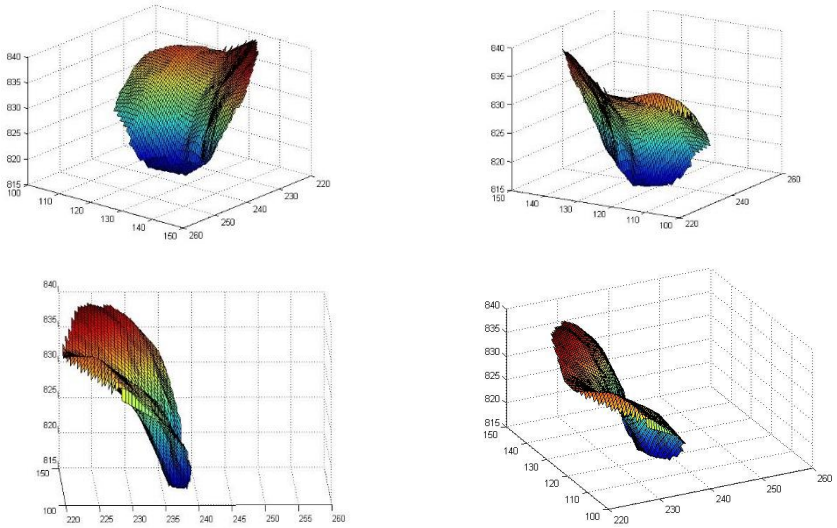

Figure 28: Example of a resulting patellar cartilage surface from one femur at certain degree of flexion.

After the surfaces are joined, each femur at its degree of flexion is checked against the final patellar cartilage surface to ensure that there is no intersection between the two parts. If there are small intersections, they should be removed using Boolean subtraction in 3-Matic. Final smoothing and filtering of the cartilage surface is also done during this stage to end with a smooth cartilage surface. The smoothing of the final patella model was done by implementing the smoothing function in 3-Matic. The smoothing tool in 3-Matic allows the user to modify the type of algorithm being implemented, the smoothing factor and number of iterations. For the most part, a 1st order Laplacian was used since it provides a basic smoothing algorithm which is able to provide good results for most inputs. If the use of this algorithm took away too much material or changed the geometry of the cartilage, a curvature algorithm was implemented which avoids triangles shape influence during smoothing while better preserving mesh shape. The smoothing factor used was also very low (between 0.1 – 0.3) to ensure the preservation of the mesh shape. The final result would be a patella with cartilage that conforms to the surface of the femur where it connects to each other during a specific motion.

3.8 Finite Element Analysis

The final step in the process is to create a finite element model (FEM) of the patellar cartilage in order to determine the resulting stresses from the compression on the cartilage by using a finite element pre-processor (MSC Patran 2014.0.1, MSC

Software, California). MSC Nastran (MSC Software Corporation, California) was used to determine and analyse the resulting stresses. The finite element model will consist of applying a displacement to a chosen section on the patellar cartilage where the displacement will be equal to the actual average cartilage compression of the relating contact area. This process will be repeated for multiple contact areas on the patellar cartilage surface for both models while varying the Poisson's Ratio and Young's Modulus. Varying these values will help to determine how these changes effect the stresses and the resulting effect that the stresses have on the cartilage and underlying osseous surfaces due to the compression.

3.8.1 Preparing Patellar Cartilage

The first step would be to prepare the patellar cartilage by removing the cartilage from the patella bone and re-meshing the resulting cartilage volume in 3-Matic. The entire cartilage volume is divided into three-dimensional linear tetrahedron solid (TET10) elements (1 mm) instead of tetrahedral (TET4) elements since TET10 elements will result in more accurate and refined stress results for complicated 3D structures such as the patellar cartilage. Once the entire volume has been meshed with TET10 elements, the cartilage structure is exported for further processing in MSC Patran.

3.8.2 Creating Finite Element Model

MSC Patran is used as a pre-processor to create the FEM model of the patellar cartilage with Nastran analysing the resulting stresses. In order to reduce the complexity of the analysis, the cartilage will be modelled as a linear elastic isotropic homogeneous material. Material properties for cartilage were researched to establish values for the Young's Modulus and Poisson's Ratio for cartilage, however, it was found that these values vary substantially since the means of determining these values vary between researchers. Various researchers modelled cartilage as a linear elastic material in an effort to determine the Poisson's ratio [53], [54], [55] and Young's Modulus [53], [55] for human articular cartilage. The results vary quite substantially, but there was enough overlapping of results to determine an applicable range for the Poisson's ratio and Young's Modulus which could be used in the FEM analysis. The following range was identified for the Poisson's ratio (v):

$v = 0.4 – 0.48$

The Young's Modulus (E) had a wider range, with the following range identified:

$E = 8 – 12$ MPa

Figure 29 shows the resulting cartilage with the volume mesh as the darker blue lines. Once the cartilage with its volume mesh has been imported into Patran, the material properties (*E* and *v*) is added to the structure.

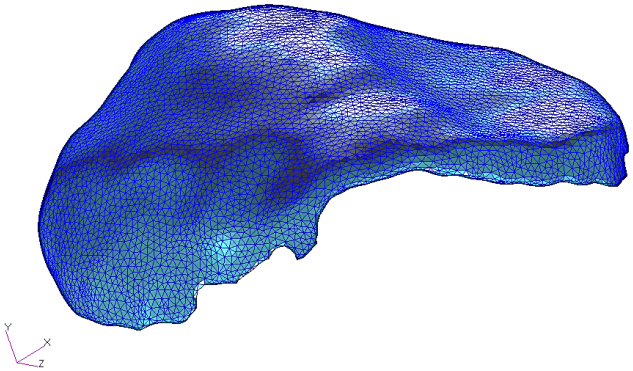

Figure 29: Patellar cartilage with added volume mesh for FEM analysis.

Boundary conditions also had to be added to the model: (1) All degrees of freedom of the nodes situated on the osseous-cartilage boundary of the patellar cartilage had to be constrained, (2) a displacement boundary condition had to be added which accounts for the amount of compression as determined from the inverse kinematic analysis.

The average compression for each specified degree of flexion will be applied to an identified contact area for that degree of flexion. This is done for all the investigated degrees of flexion and their related contact areas which will then be compared to projected contact stresses. Figure 30 shows an example of a displacement boundary condition (light blue) applied to a specific contact area.

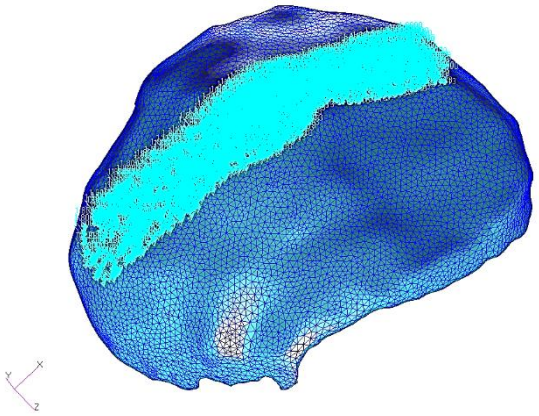

Figure 30: The displacement boundary condition as applied for a specific degree of flexion to its related contact area.

More specifically, the stresses will be determined for each model at flexion angles of zero, 30, 60, 90, and its maximum degree flexion for the passive movement and the same for the squat movements, but starting at 30°. The same analysis is repeated for the Poisson's values of 0.4, 0.45, and 0.48 and Young's Modulus values of 8,

10, and 12 MPa to investigate the effect that these values have on the resulting stresses.

3.9 Data Processing and Analysis

This section details the procedures used to quantify, measure, and process the results. This includes the various calculations and processing done to the results, any methods used to analyse the data, terms and definitions used for the recording of the data, and the presentation of the results.

3.9.1 Measurement Procedure

This section will briefly detail the process used to measure the resulting estimated cartilage surface and quantify the estimated geometry of the cartilage by using the measurement tools in 3-Matic. Mainly, the thickness of the cartilage was of concern. The thickness was able to supply important information from which various investigations could be done, specifically to determine the compression that the cartilage undergoes during the specific motion being analysed.

The first section of the measurement procedure involved moving all the resulting patellar cartilage structures (passive, squat, and uncompressed) into the same space in the coordinate system, overlapping them, and precisely matching the shape and contours of the patellar bone of each patellar structure to each other. The cartilage models were aligned to each other by using the N-point registration tool in 3-Matic. This tool makes use of distinct geometrical features which will be the same on each model. Since the anterior osseous surface of the patella (were the ligaments attach and no cartilage are present) never change throughout the entire process, they were the perfect surfaces to use to align all the patellae together. Using the N-point register tool, multiple easily identifiable distinct points are selected on both patella. When enough points are selected (more than 10 for accurate alignment), the register tool aligns the two patellae exactly. The same is done for all of the remaining patellae for the same knee. This guarantees that the measurements will take place at the same point on each of the patellae and that the specific point and measurement could be comparable to the same point on another patella for the same knee.

The patellae are then sectioned and cut in the coronal plane to provide a straight, consistent edge for measurement of the cartilage which will act as the base reference line. Furthermore, the patellae are sectioned in the transverse plane, dividing the patellae into nine sections (Figure 31) spaced at equal intervals over the cartilage surface. Evenly spaced points (2mm apart) are created on the base reference line, along the transverse axis (y-axis), from which each measurement for each of the patellae will be taken. The points stay at the same position in the medial-lateral direction, but move to the next section in the anterior-posterior direction as every section is finished being measured. Figure 32 displays the measurement layout for a single section. A measurement is taken from a point on the reference line to a point exactly perpendicular to the baseline point on the edge of the cartilage.

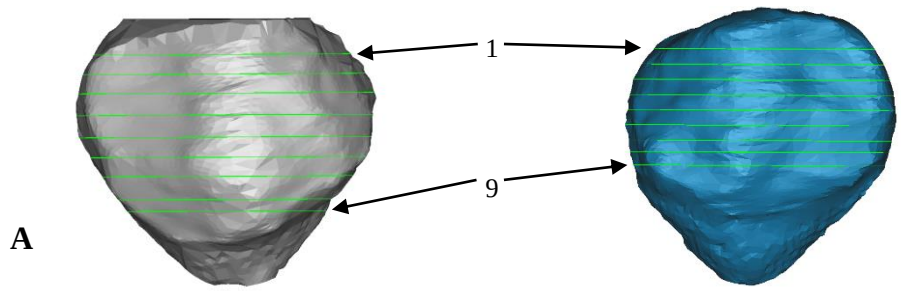

Figure 31: Section numbering for knee 1 (A) and knee 2 (B) during measurement.

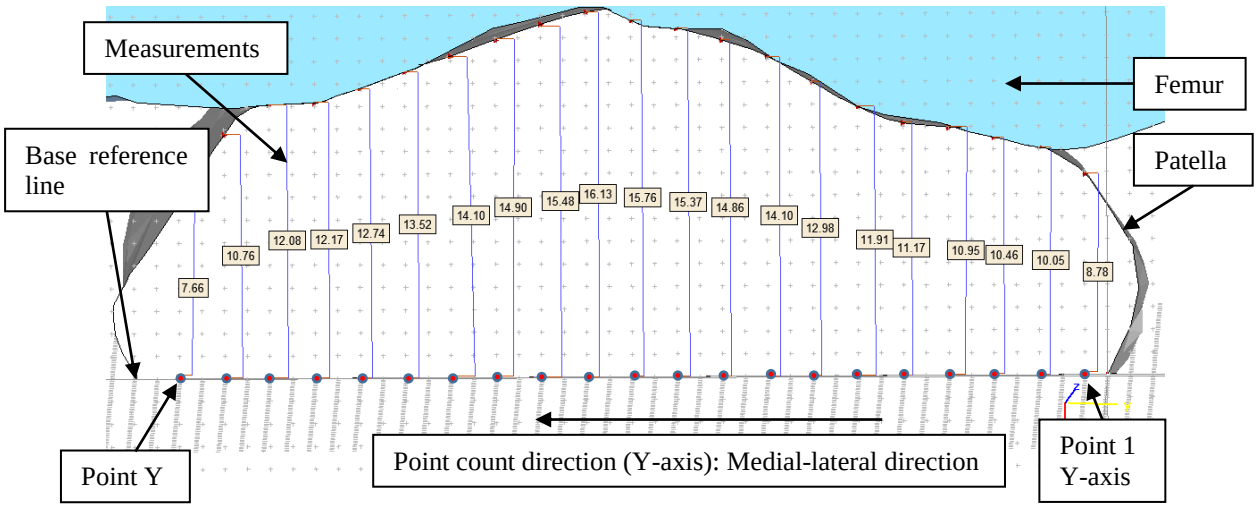

Figure 32: Layout for measuring thickness of femoral and patellar cartilage.

The thickness of the femoral cartilage at the different degrees of flexion also needs to be measured. This data will be important in calculating the relative compression of the femoral cartilage to the patellar cartilage since in the estimation process, it is assumed that the femoral cartilage does not compress. The femurs are all imported and moved to the correct position relative to the patella (correct angle of flexion), where the same sections in the transverse plane, as applied to the patella, are applied to the femur. The measurements are done from the same base reference line situated on the patella, but this time to the edge of the femoral cartilage. The same measurement is then repeated, but from the reference line to the femur without any cartilage present. This will allow for the calculation of the femoral cartilage thickness at that exact point. Both the patella and femoral point numbering start with point one on the right hand side of the patella and with section one starting at the superior end of the patella. This procedure is kept consistent with each of the sections. These steps are repeated for all the sections in the transverse plane for both knees investigated.

3.9.2 Kinematic Model Data Processing

This section details and defines some of the terms used and measured during the recording of the results for the kinematic models. The kinematic models consisted

of a passive and squat movement that was applied to the models for knee 1 and knee 2. The passive movement, as described in section 3.4.2, allowed the knee to move with no added weights and only one out of the six degrees of freedom fixed, while the squat movement (section 3.4.2) allowed movement in all six degrees of freedom with a weight at the point where the ankle is located.

The kinematics results visually demonstrates the resulting motion profiles for the passive and squat motions of knee 1 and 2 which were implemented as an input in the inverse kinematic analysis program.

3.9.3 Estimated Geometry Cartilage Results

Various calculations will be performed after the initial gathering of results in order to quantify and investigate the estimated patellar cartilage. Mainly, calculations will be performed to determine the thickness and compression of the cartilage due to a specific movement. The estimated geometry results provides the estimated geometry of the patellar cartilage while under the assumption that the femoral cartilage does not compress. The results for knee 1 and knee 2 documented, includes the unfiltered thickness results (passive and squat motions) of the models using the femoral cartilage as segmented from the MRI data (Models 1.1 and 2.1) and the models resulting from the application of the femoral cartilage as estimated in 3-Matic (Models 1.2 and 2.2). The filtered results for model 1.1 and 2.1 are also documented and processed.

As described in section 3.9.1, a number of points depending on the thickness of the measured section, will be measured for each section from a predefined base reference line (See Figure 32) which will be kept consistent throughout the analysis. The sectional average cartilage thickness for the patella will be calculated by subtracting the measurement obtained for the patella without any cartilage from the measurement obtained for the patella with cartilage. This calculation will be done for each point on the specific section to get the thickness of the cartilage at that specific point on a specific section. The sectional average will then be calculated by averaging the resulting point thicknesses. The overall average thickness for the patellar cartilage will in turn then be calculated by averaging all the average sectional thicknesses. The same is done for the femoral data.

The percentage values for the amount of cartilage removed during the smoothing and filtering process, and the differences in amount of cartilage between the patellae which used the segmented MRI femur (Models 1.1 and 2.1) to produce the patellar cartilage and the estimated femoral cartilage model (Models 1.2 and 2.2), will also be calculated. The percentage of cartilage removed during the filtering process will be calculated by determining the percentage difference between the overall average patellar cartilage thickness of the unfiltered results and the overall average patellar cartilage thickness of the filtered results. The same percentage calculation will be done between the estimated femoral cartilage results and the segmented uncompressed MRI patellar cartilage results. Additionally, the average error and standard deviation for each section of the patellar cartilage is calculated. The overall averages of these values are also calculated relating to the entire estimated patellar cartilage surface.

The estimated contact areas between the patella and femur during a specific movement will be determined by measuring the distance between the femur at its specific degree of flexion, and the patellar cartilage, for all the points of each section and then estimating whether the measurement taken at that point is less than 0.5 mm. If the measurement is 0.5 mm or less, the assumption can be made that those two points are in contact. Due to the performance of the estimation program, a certain degree of uncertainty is introduced during the final stages of the cartilage estimation when determining the contact areas. This refers specifically to minor surface inconsistencies which could have been overlooked during the final filtering of the surface and could result in a negative result in terms of surface contact between the femur and the patella. By introducing the 0.5mm buffer, it ensures that the contact area is still identified even when there are surface inconsistencies present on the estimated surfaces.

This contact area process will be done for all the points of all the sections resulting in an estimation of the locations and size of the contact areas for each referenced degree of flexion. However, it is important to note that the contact areas will only be determined for the femur at certain degrees of flexion, namely the normalised zero, 30, 60, 90, and maximum degrees of flexion. This could result in areas on the patellar cartilage that do not show any contact since those areas could be related to a degree of flexion that was not investigated.

Finally, the volume of the estimated cartilage for each knee is also determined for all models being investigated (unfiltered and filtered).

3.9.4 Patellofemoral Cartilage Compression Results

The compression results are calculated for the same models as indicated in section 3.9.3. The resulting compression will be calculated in a similar manner to the thickness calculations. The sectional average cartilage compression for the patellar cartilage will be determined by subtracting the measurement obtained for the patella with the estimated cartilage (from the passive or squat movement) from the measurement obtained for the patellar with the uncompressed segmented MRI cartilage. Each compression calculation is done for each point on every section. The sectional average compression is then determined by averaging the compression of all the points of a section. The overall average cartilage compression for the patella is then also determined by simply averaging the sectional averages. Once again, the average error and standard deviation for each section of the patellar cartilage is calculated. The overall averages of these values are also calculated relating to the entire estimated patellar cartilage surface.

3.9.5 Actual Patellofemoral Cartilage Compression

The initial compression calculated refers to the compression as estimated by the estimation program created. This includes the simplifying assumption that the femoral cartilage does not compress. However, by determining the ratio of uncompressed cartilage thickness between the patella and femur, the actual compression of the patellar and femoral cartilage can be calculated.

The cartilage ratio between the patellar and femoral cartilages will be determined by calculating the ratio between the average segmented uncompressed patellar cartilage thickness and the average segmented uncompressed femoral cartilage thickness. This ratio will then be applied to the initial average patellar compression for each movement to determine the actual compression that the patellar cartilage experiences during a specific movement. This actual patellar cartilage compression calculated will then be subtracted from the initial patellar compression, which is the total compression between the patella and femur, to determine the actual compression that the femoral cartilage experiences during a specific movement.

3.9.6 Finite Element Model Stress Results

Finite element models were created for the articular cartilage to investigate the stresses being experienced on the surface of the patellar cartilage where the femur is in contact with the patella, and the underlying stress experienced by the patellar bone due to the compression the cartilage experiences during movement.

As mentioned previously, the stresses are measured at specific degrees of flexion on their relating contact areas at varying Poisson's Ratio's and Young's Moduli. These results are then represented as box and whisker plots to determine the distribution of these values at a specific degree of flexion and compression. Specifically the box of the plot consists of the median value being the middle line of the box, the upper horizontal line the Q3 value and the lower horizontal line the Q1 value. The maximum value can be seen as the end point of the upper whisker, and the minimum value the end point of the lower whisker. The Q3 value represents the upper quartile or the median of all the data above the overall median, and the Q1 value represents the lower quartile or the median of all the data below the overall median.

The mesh convergence for both knees were also determined by running a FEM analysis for a knee keeping all the variables (ν, E, compression, and contact area) the same, but varying the mesh size. This would determine whether the size of the mesh chosen for the stress analysis was small enough to provide accurate results, but not too small as to unnecessarily extent the simulation time. If the determined stress values where in a 15% range of each other, the mesh size chosen was deemed appropriate for the analysis performed.

Chapter 4

4 Results

This chapter will document the results as acquired during the methods explained in section 3. Two knees were investigated, comprising of model numbers S120331 and S120324 which will be referred to as knee 1 and knee 2 respectively. Both of these models were further divided into sub-models consisting of the unfiltered and filtered passive and squat motions. Furthermore, for each model, the actual femoral cartilage as segmented from the MRI's (Models 1.1 and 2.1) was used as well as the femoral cartilage as estimated by the author in 3-Matic (Models 1.2 and 2.2).

4.1 Kinematic Motion Profile Results

Figure 33 and Figure 34 shows the motion profiles produced by the kinematic trajectories for knee 1 while performing the passive and squat motions. These motions were used as an input to the inverse kinematic analysis.

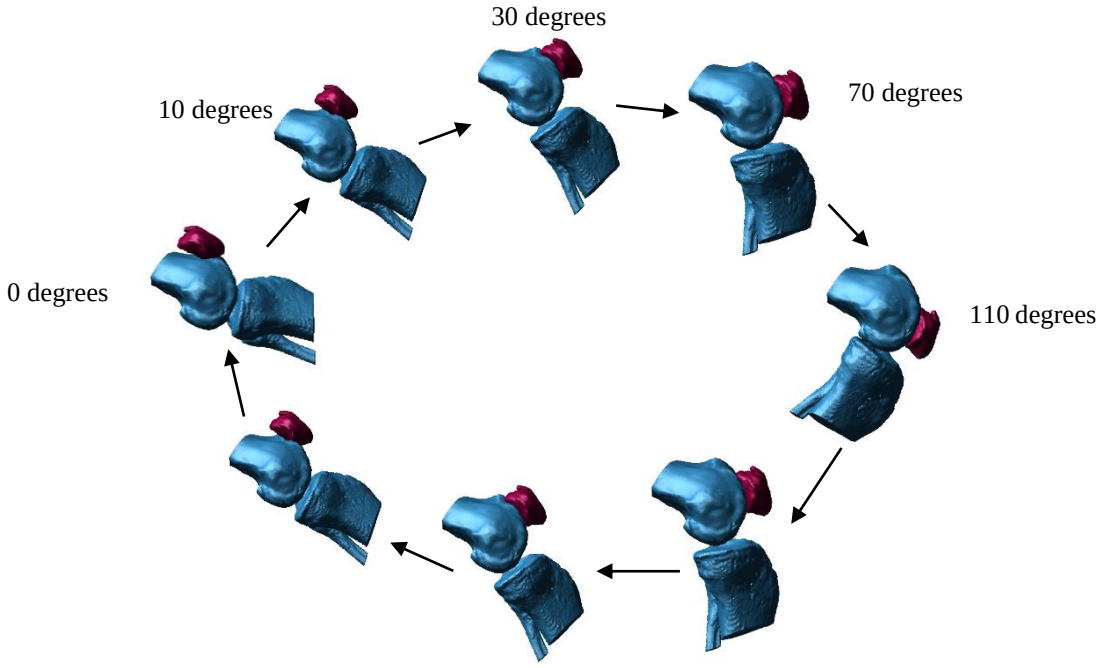

Figure 33: Passive motion profile for knee 1. This shows the actual degrees of flexion.

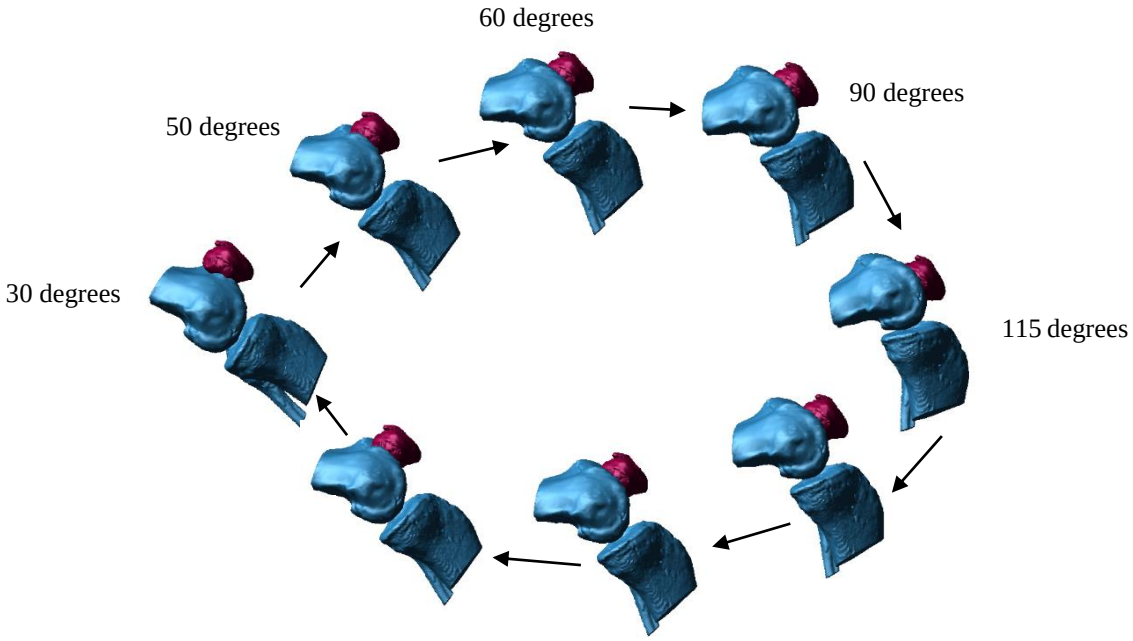

Figure 34: Squat motion profile for knee 1. This shows the actual degrees of flexion.

Figure 35 and Figure 36 shows the motion profiles produced by the kinematic trajectories for knee 2 while performing the passive and squat motions.

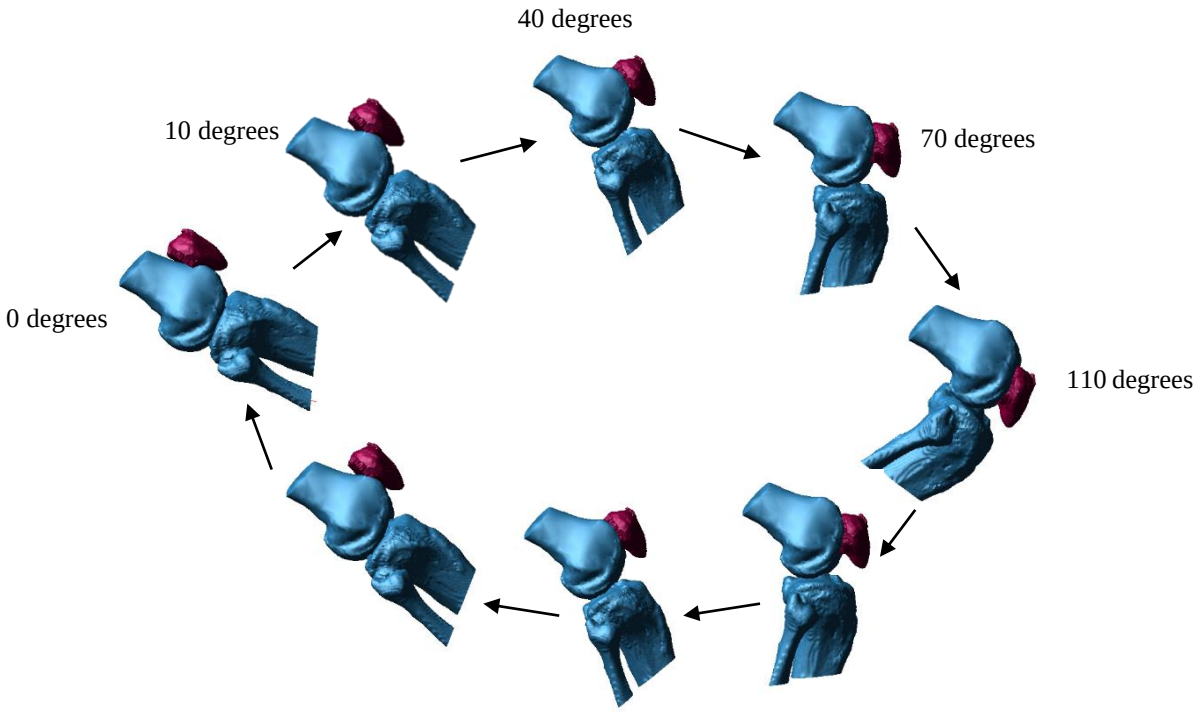

Figure 35: Passive motion profile for knee 2. This shows the actual degrees of flexion.

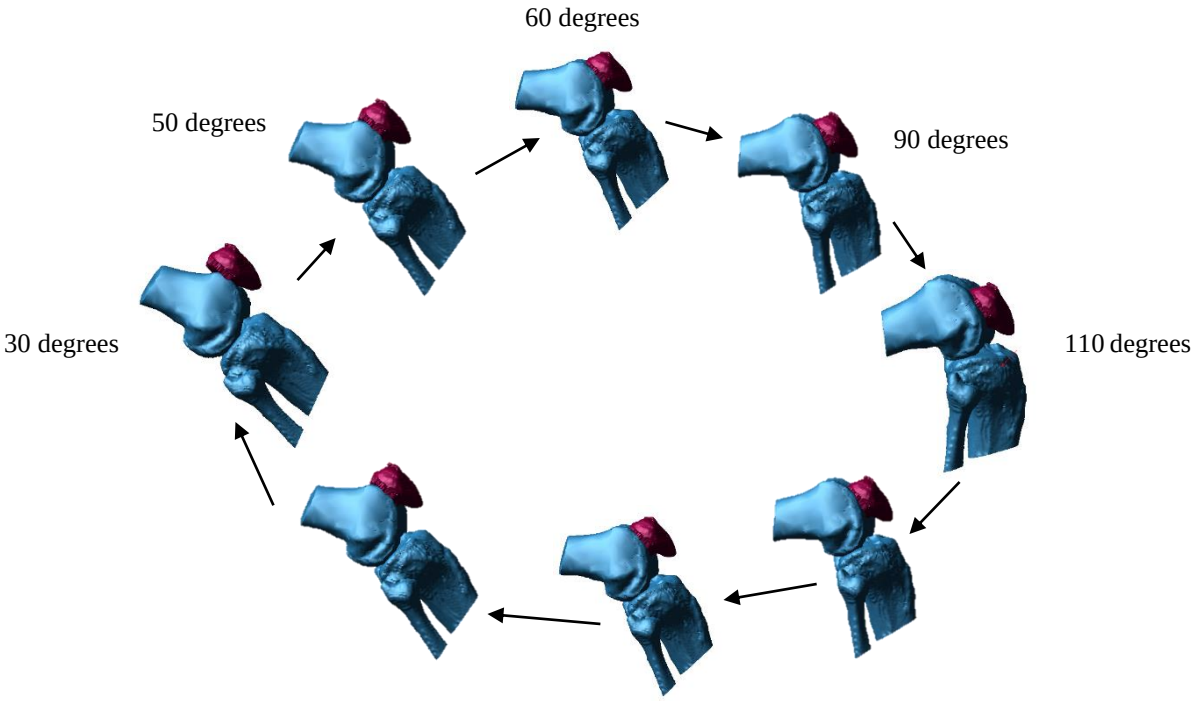

Figure 36: Squat motion profile for knee 2. This shows the actual degrees of flexion.

4.2 Estimated Geometry Results

The following section details the estimated geometry as produced by the inverse kinematic analysis.

4.2.1 Segmented Uncompressed MRI Results

The results obtained from segmenting the available MRI scans for knee 1 and knee 2 will be detailed in the following section. These results shows the uncompressed cartilage for the investigated knees.

- **Knee 1**

The final results for the segmented patella and femur for knee 1 can be seen in Figure 37. The blue structures represent the osseous structures of the femur and patella, while the grey structures represent the cartilage as segmented from the available MRI data.

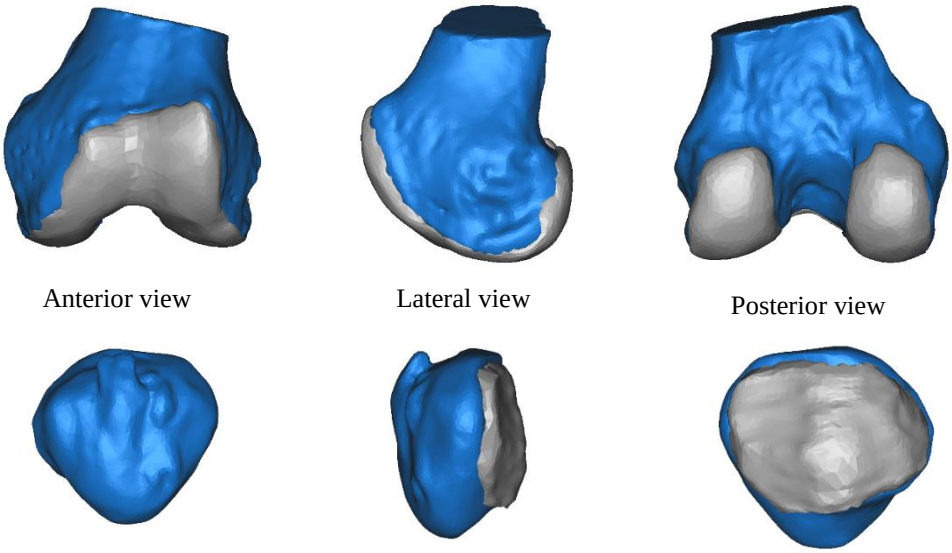

Figure 37: Anterior (Left), lateral (middle), and posterior (Right) views of the femur (top row) and patella (bottom row) displaying the final segmented cartilage for knee 1.

The chart in Figure 38 compares the sectional average thickness of the segmented cartilage of the patella and the relating thickness per section as found in literature [48]. The same comparison was done for the segmented femoral cartilage and can be found in Appendix A.1, Figure 66.

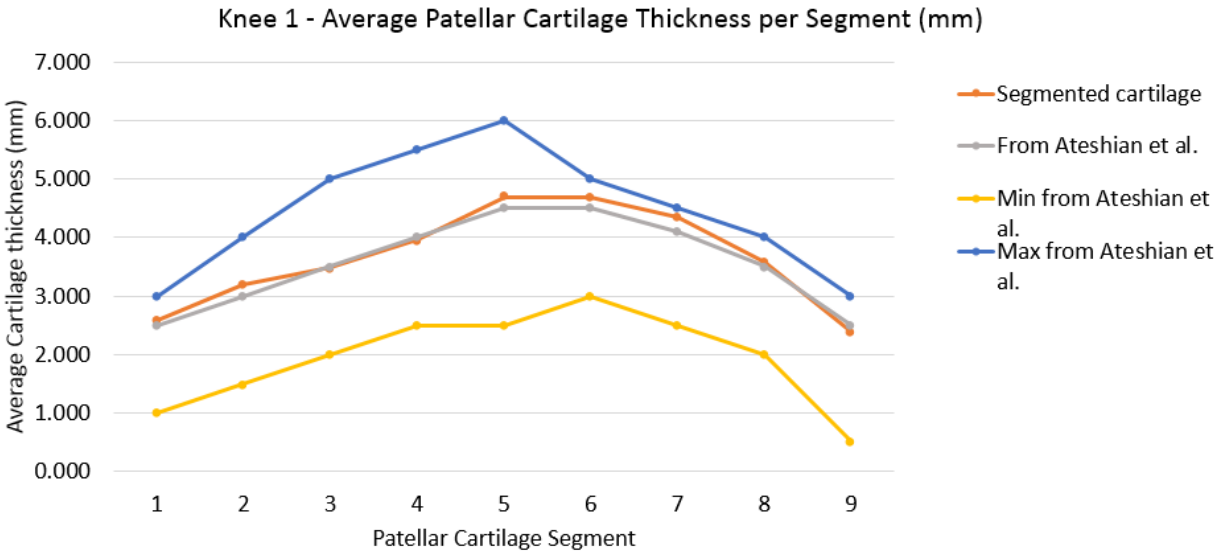

Figure 38: Chart comparing the average, minimum and maximum cartilage thickness per section as found in literature, to the average cartilage thickness of knee 1 segmented from the MRI data for the patella.

Table 4 displays the average error and standard deviation for every section of patellar cartilage for knee 1.

Table 4: Sectional average error and standard deviation for the uncompressed cartilage of knee 1.

Section	Average Error (mm)	Standard Deviation (mm)
1	0.14	0.51
2	0.18	0.74
3	0.13	0.59
4	0.17	0.76
5	0.19	0.86
6	0.28	1.26
7	0.18	0.77
8	0.13	0.53
9	0.22	0.84
Average	0.18	0.76

Finally, the total overall average thickness for the segmented uncompressed cartilage was calculated as 3.657 mm for the patella and 2.013 mm for the femur, with an average standard deviation of 0.76 mm.

- **Knee 2**

The patella and femoral cartilage of knee 2 was also segmented. The final results as segmented from the MRI data can be seen in Figure 39.

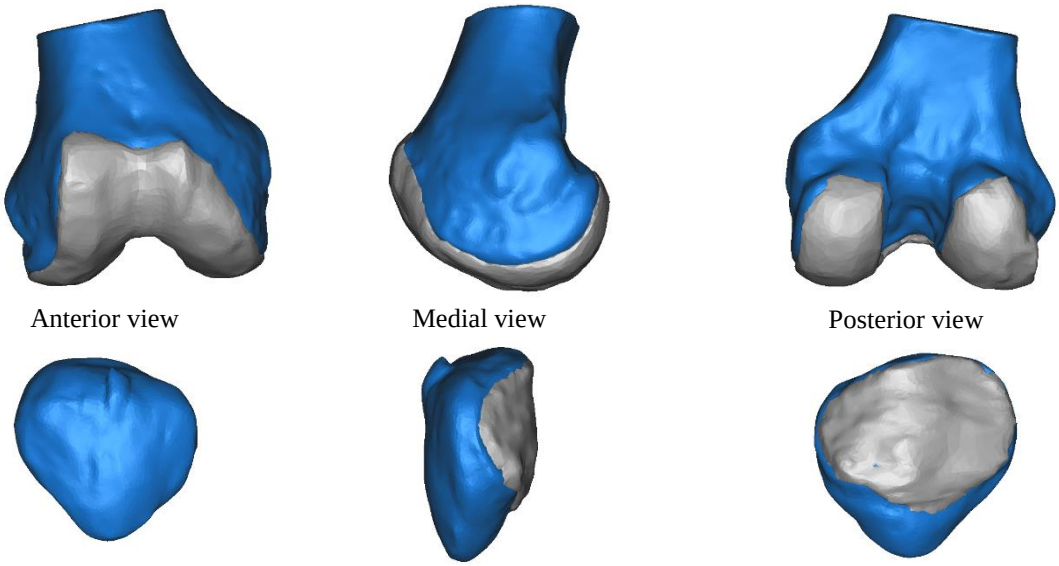

Figure 39: Anterior (Left), medial (middle), and posterior (right) views of the femur (top row) and patella (bottom row) displaying the final segmented cartilage for knee 2.

Figure 40 shows the graph comparing the averages found in literature [48] to the average thicknesses calculated for the segmented patellar cartilage. The section averages for the femur can be seen in the chart found in Appendix A.2, Figure 67.

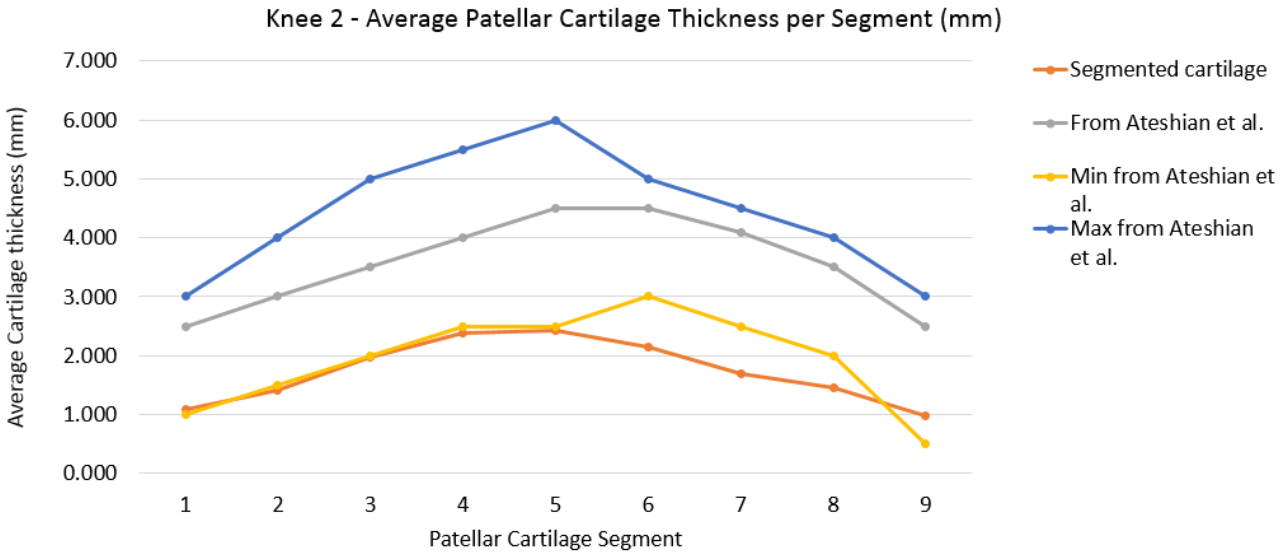

Figure 40: Chart comparing the average, minimum and maximum cartilage thickness per section as found in literature, to the average cartilage thickness of knee 2 segmented from the MRI data for the patella.

Table 5 displays the average error and standard deviation for every section of patellar cartilage for knee 2.

Table 5: Sectional average error and standard deviation for the uncompressed cartilage of knee 2.

Section	Average Error (mm)	Standard Deviation (mm)
1	0.13	0.57
2	0.14	0.6
3	0.15	0.67
4	0.16	0.76
5	0.17	0.83
6	0.17	0.82
7	0.19	0.91
8	0.15	0.7
9	0.15	0.7
Average	0.16	0.73

Finally, the total average thickness for the segmented uncompressed cartilage was calculated as 2.237 mm for the patella and 2.01 mm for the femur, with an average standard deviation of 0.73 mm.

4.2.2 Cartilage Estimation Results for Knee 1

This section details the cartilage geometry results obtained by the application of the inverse kinematic analysis for knee 1. This includes the results obtained by the application of the passive and the squat motion profiles. Model 1.1 refers to raw unfiltered results obtained by using the femoral cartilage segmented from the MRI scans, while Model 1.2 refers to the raw unfiltered results obtained from applying the femoral cartilage as estimated in 3-Matic.

Figure 41 and Figure 42 shows the estimated patellar cartilage results for knee 1 for the passive and squat motions respectively.

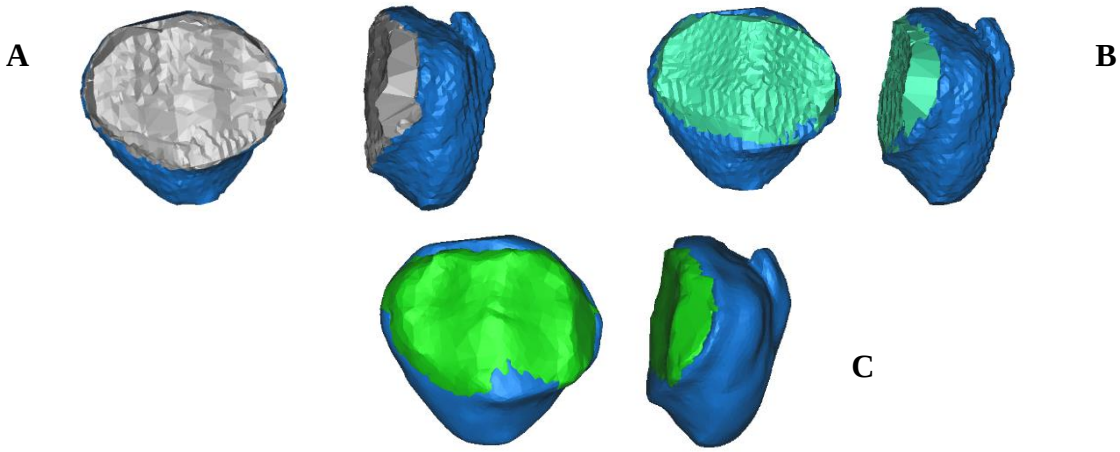

Figure 41: The results obtained for the patellar cartilage thickness for the passive movement – knee 1, with (A) Model 1.1, (B) Model 1.2, and (C) filtered results for Model 1.1.

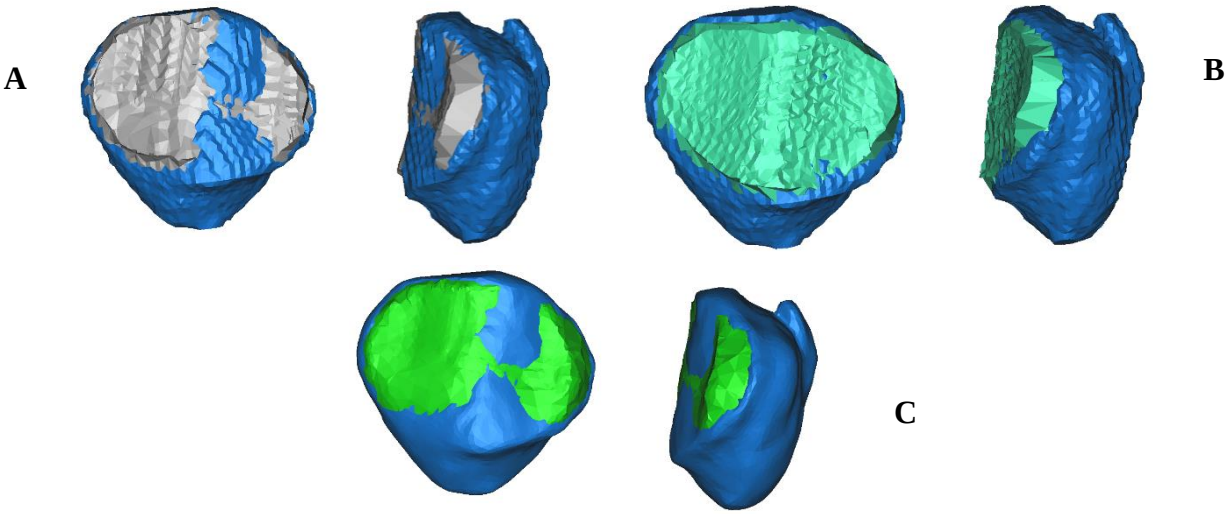

Figure 42: The results obtained for the patellar cartilage thickness for the squat movement – knee 1, with (A) Model 1.1, (B) Model 1.2, and (C) the filtered results for Model 1.1.

Unfiltered Results – Knee 1:

The graph in Figure 43 (A) shows the unfiltered patellar cartilage thickness results for Model 1.1 per section of the patella, comparing the passive motion with the squat motion results. Figure 43 (B) indicates the same results, but for Model 1.2. Refer to Figure 31 for the patella sections.

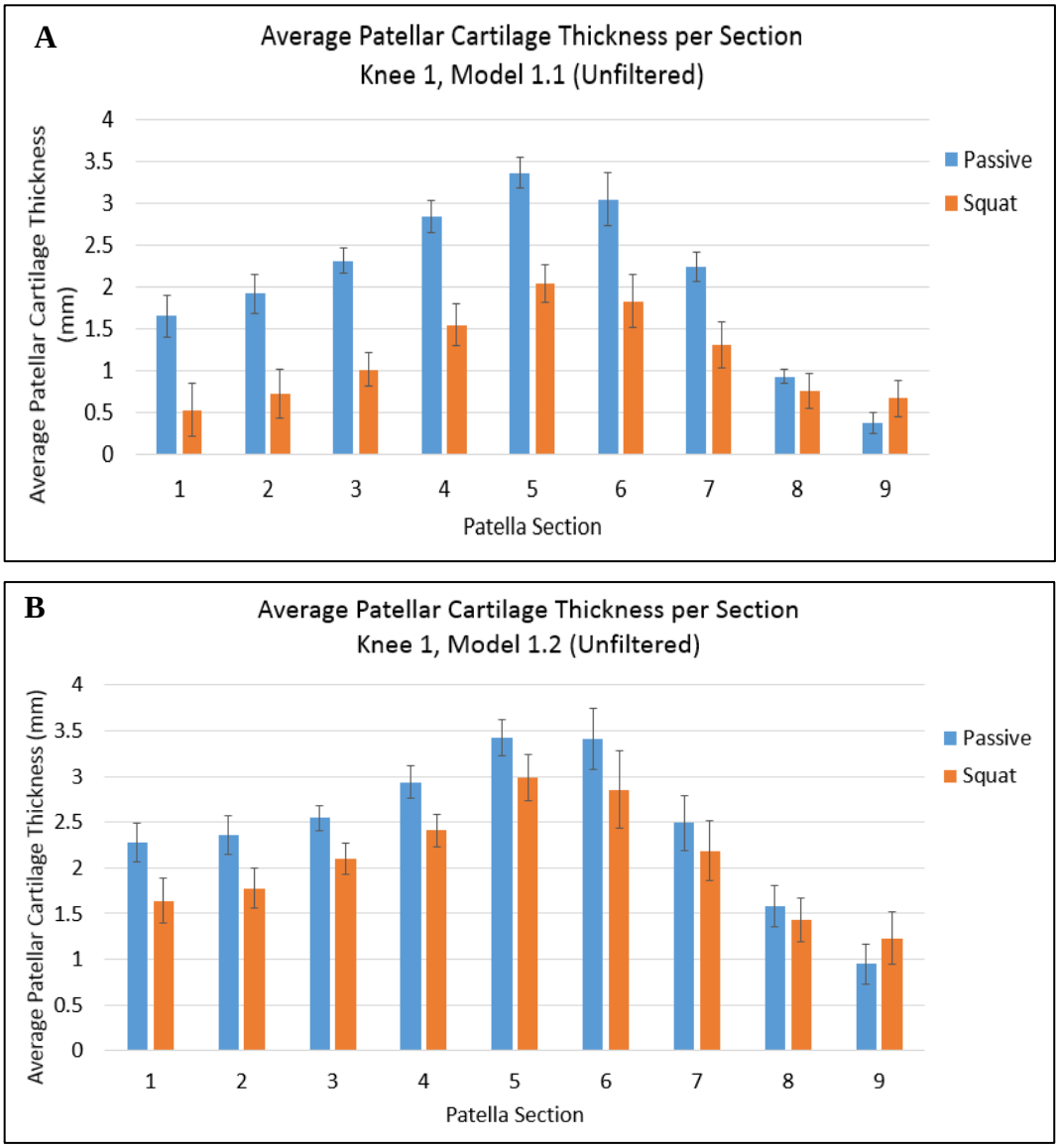

Figure 43: Average unfiltered patellar cartilage thickness results per section for knee 1 comparing the passive and squat motions, for (A) Model 1.1 and (B) Model 1.2 and showing the average error bars for each section.

In Appendix B.1 the sectional average cartilage thickness results for knee 1 can be seen in Table 11, showing the passive and squat results for both models 1.1 and 1.2.

The graph in Figure 44 (A) shows the unfiltered average patellar cartilage thickness results per section for the passive motion profile, comparing the results for model 1.1 and model 1.2. Figure 44 (B) displays the same results, but for the squat motion profile.

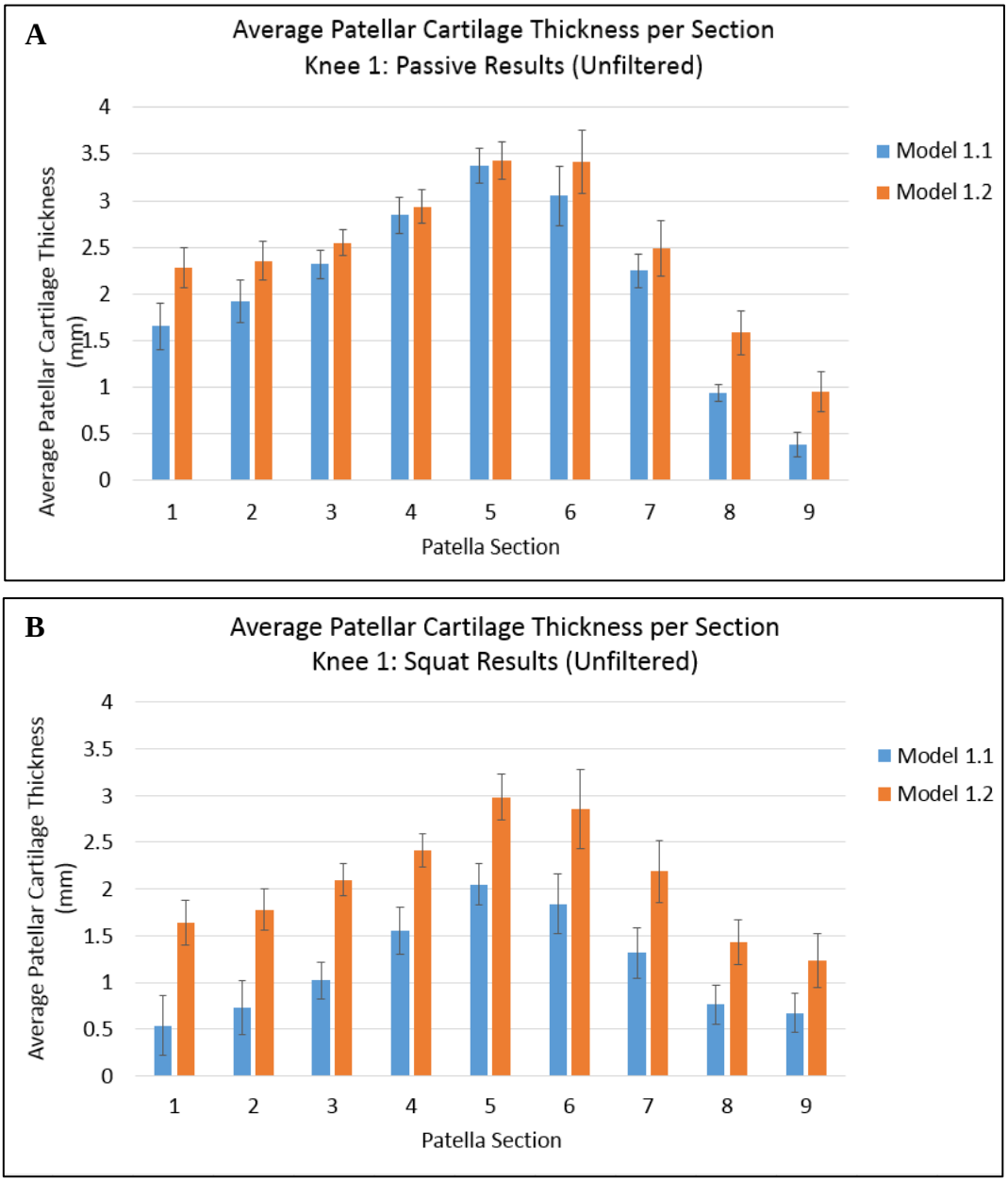

Figure 44: Average unfiltered patellar cartilage thickness results per section for knee 1 comparing models 1.1 and 1.2, for (A) the passive motion and (B) the squat motion and showing the average error bars for each section.

The unfiltered average error and standard deviation for each section of the patellar cartilage for models 1.1 and 1.2 can be found in Appendix B.1, Table 12 and Table 13 respectively. The filtered results for model 1.1 can be seen in Appendix B.3, Table 18.

Filtered Results – Knee 1:

The graph in Figure 45 shows the filtered patellar cartilage thickness results for Model 1.1 per section of the patella, comparing the passive motion with the squat motion results. The graph also indicates the relating filtered sectional thickness values for the uncompressed cartilage (from MRI scans) of knee 1.

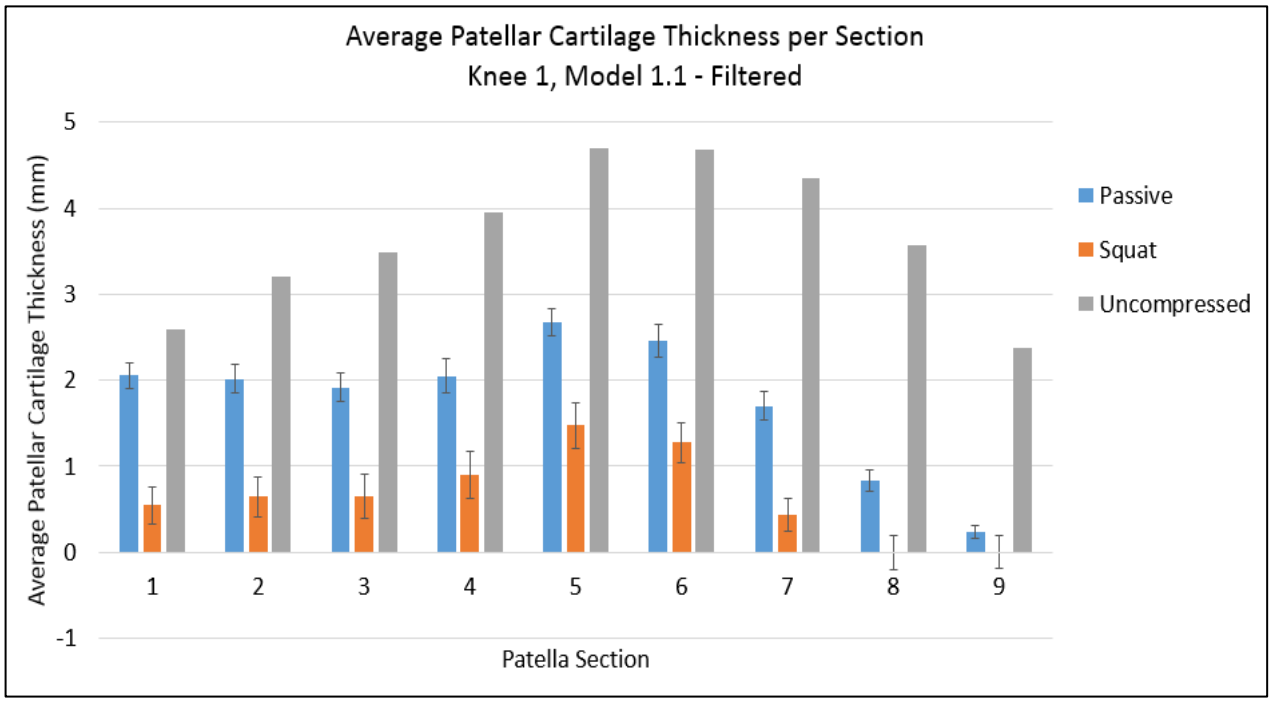

Figure 45: Average filtered patellar cartilage thickness results per section for knee 1 comparing the passive and squat motion results and showing the average error bars.

Figure 46 displays the unfiltered vs. filtered results for model 1.1.

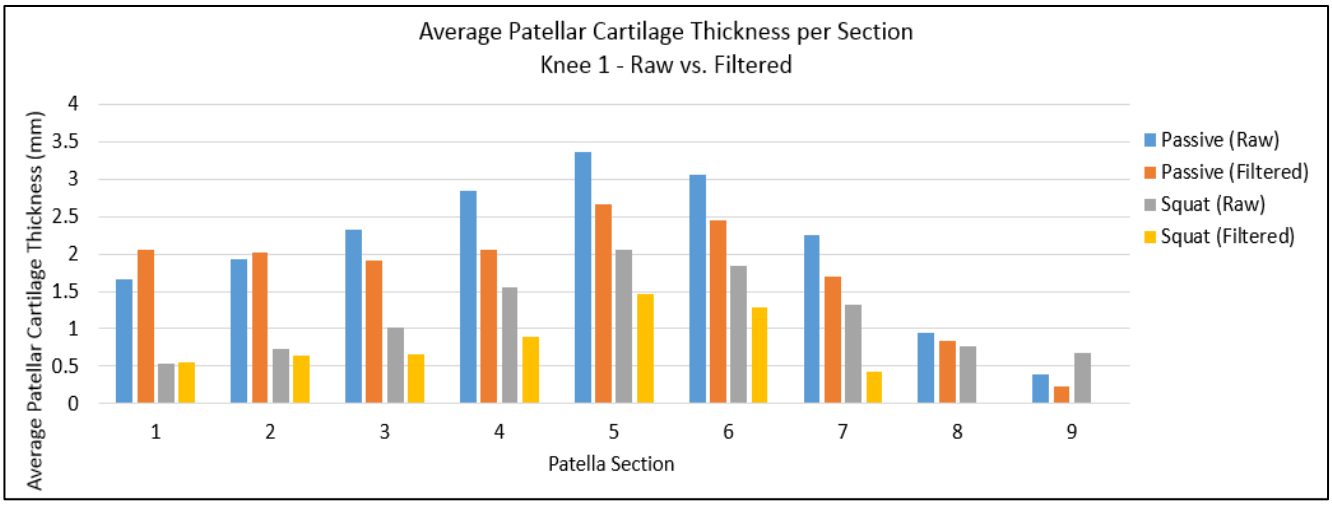

Figure 46: The average patellar cartilage thickness results per section for knee 1, model 1.1. The graph compares the unfiltered vs the filtered results for both the passive and squat motion.

In Appendix B.3, Table 17, the filtered sectional patellar cartilage thickness results for model 1.1 can be viewed. Table 6 summarises the average values calculated for all the cartilage sections for knee 1 (unfiltered and filtered results).

Table 6: Summary of the average values calculated for the patellar cartilage thickness results for knee 1.

	Passive			Squat		
	Model 1.1 (Unfiltered)	**Model 1.2 (Unfiltered)**	**Model 1.1 (Filtered)**	**Model 1.1 (Unfiltered)**	**Model 1.2 (Unfiltered)**	**Model 1.1 (Filtered)**
Average Cartilage Thickness (mm)	2.082	2.442	1.771	1.165	2.068	0.658
Cartilage Volume (mm^3)	1932.840	2359.670	1802.210	1332.770	1949.460	962.580
Average Error (mm)	0.190	0.230	0.160	0.250	0.260	0.230
Standard Deviation (mm)	0.820	0.960	0.660	1.080	1.100	0.970

The results for the passive motion showed that an average of 14.95% (or an average of 0.311 mm) of the cartilage was removed during the filtering and smoothing step for the model 1.1. Also, the patellar cartilage resulting from the use of the model 1.1 had on average 14.74% (or a thickness average of 0.36 mm) less cartilage than the patellar cartilage resulting from using model 1.2.

The results for the squat movement showed that an average of 43.52% (0.507 mm) of cartilage was removed during the filtering and smoothing step for the model 1.1. Also, model 1.1 had on average 43.67% (0.903 mm) less cartilage than model 1.2. Finally, the estimated contact areas for the passive and squat motion of model 1.1 (knee 1) can be seen in Appendix C.1 and C.2, Figure 68 and Figure 69.

4.2.3 Cartilage Estimation Results for Knee 2

This section details the cartilage geometry results obtained by the application of the inverse kinematic analysis for knee 2. This includes the results obtained by the application of the passive and the squat motion profiles. Model 2.1 refers to raw unfiltered results obtained by using the femoral cartilage segmented from the MRI scans, while Model 2.2 refers to the raw unfiltered results obtained from applying the femoral cartilage as estimated in 3-Matic.

Figure 47 and Figure 48 shows the estimated patellar cartilage results for knee 2 for the passive and squat motions respectively.

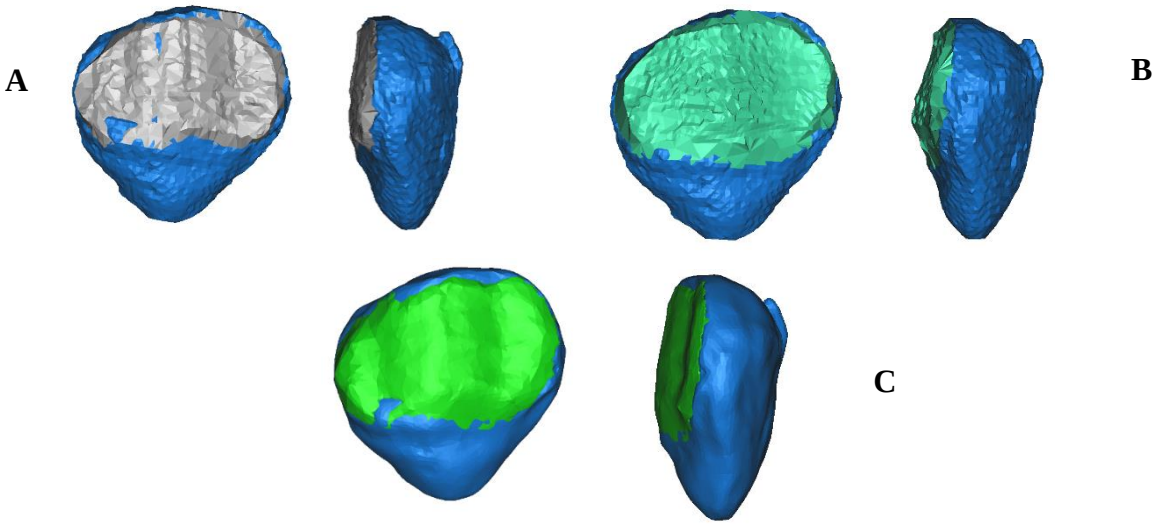

Figure 47: The results obtained for the patellar cartilage thickness for the passive movement – knee 2, with (A) Model 2.1, (B) Model 2.2, and (C) filtered results for Model 2.1.

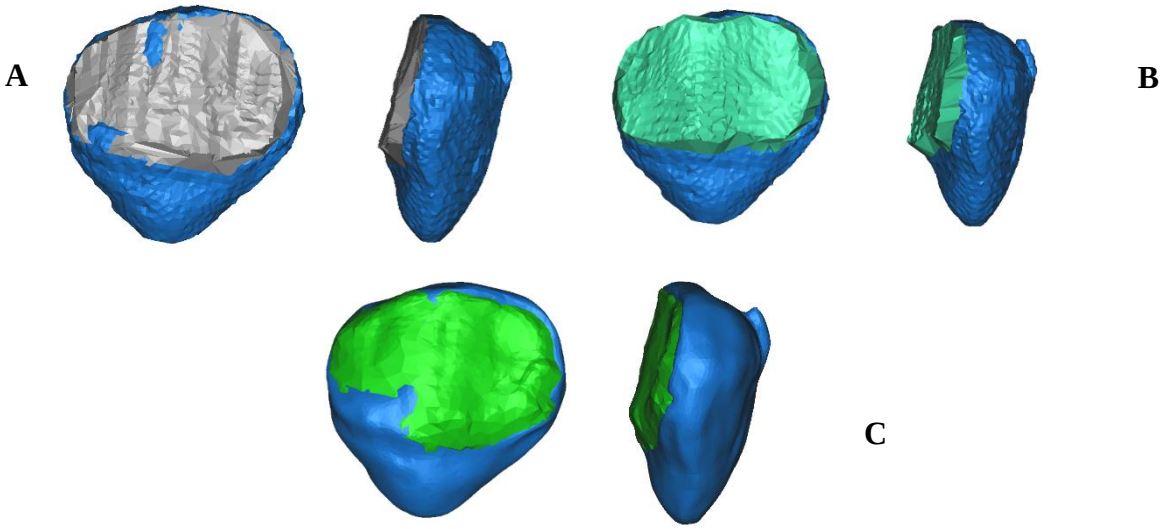

Figure 48: The results obtained for the patellar cartilage thickness for the squat movement – knee 2, with (A) Model 2.1, (B) Model 2.2, and (C) filtered results for Model 2.1.

Unfiltered Results – Knee 2:

The graph in Figure 49 (A) shows the unfiltered patellar cartilage thickness results for Model 2.1 per section of the patella, comparing the passive motion with the squat motion results. Figure 49 (B) indicates the same results, but for Model 2.2.

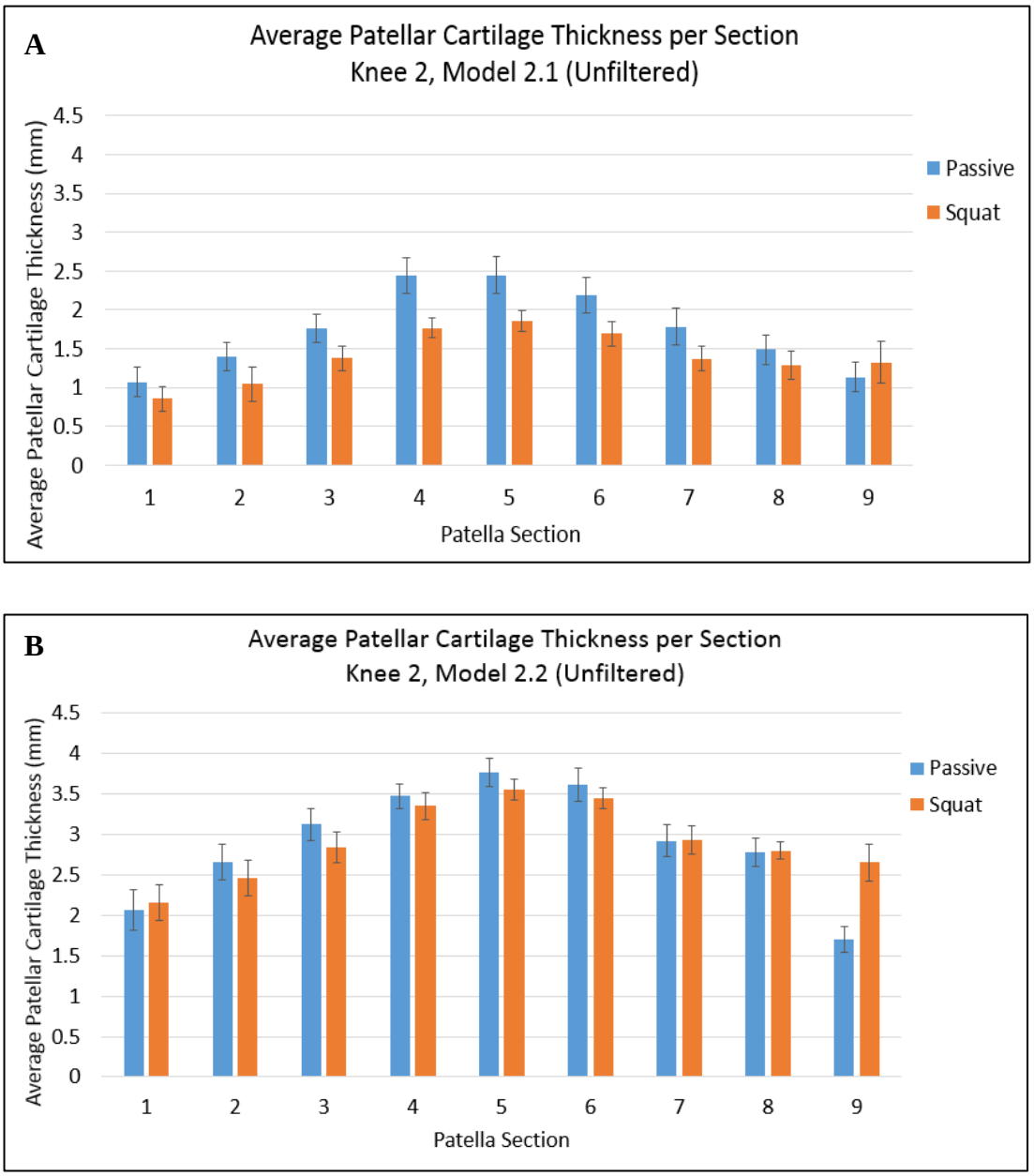

Figure 49: Average unfiltered patellar cartilage thickness results per section for knee 2 comparing the passive and squat motions, for (A) Model 2.1 and (B) Model 2.2, and showing the average error bars for each section.

In Appendix B.2 the sectional average cartilage thickness results for knee 2 can be seen in Table 14, showing the passive and squat results for both models 2.1 and 2.2.

The graph in Figure 50 (A) shows the unfiltered average patellar cartilage thickness results per section for the passive motion profile, comparing the results for model 2.1 and model 2.2. Figure 50 (B) displays the same results, but for the squat motion profile.

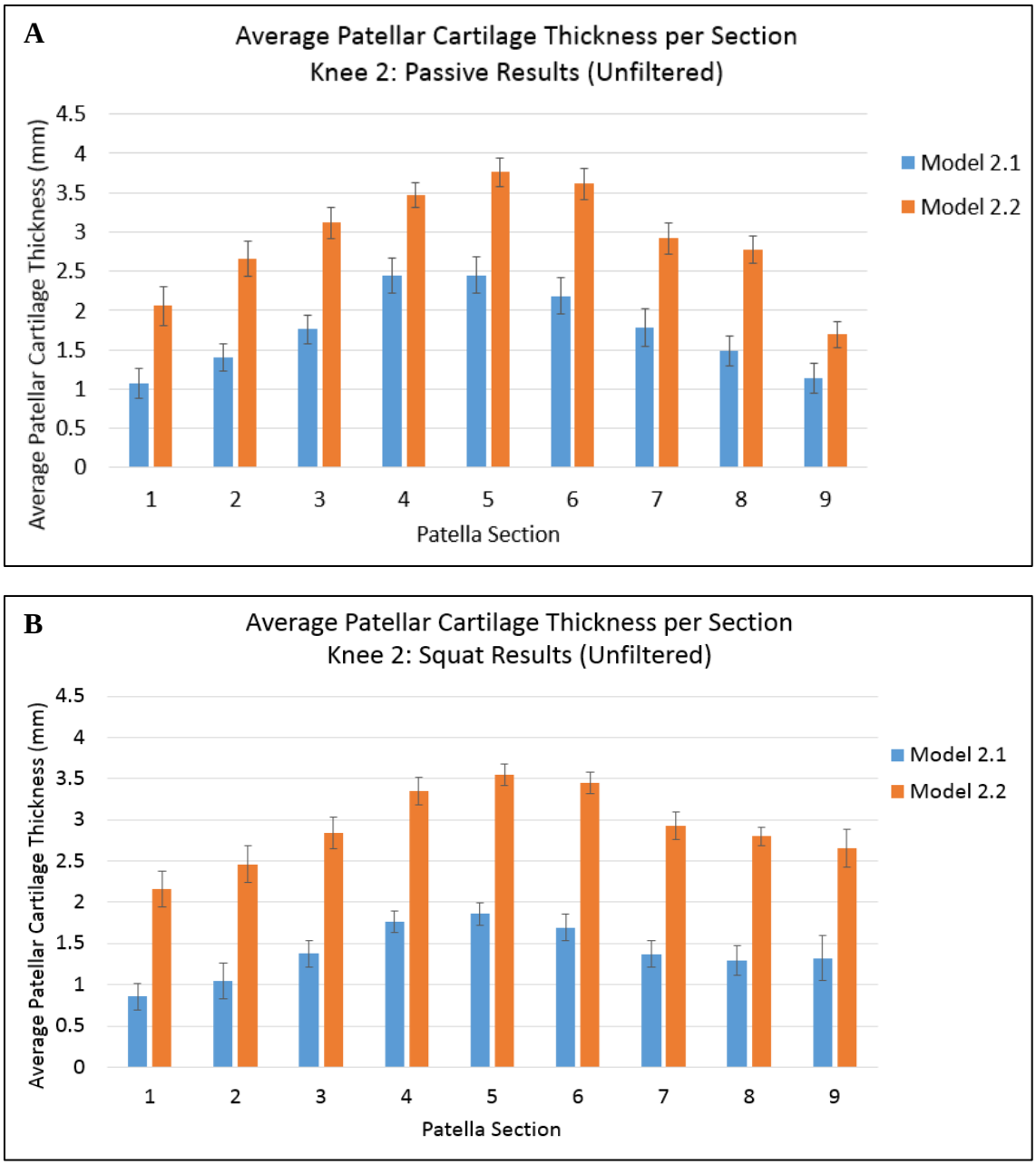

Figure 50: Average unfiltered patellar cartilage thickness results per section for knee 2 comparing models 2.1 and 2.2, for (A) the passive motion and (B) the squat motion, and showing the average error bars for each section.

The unfiltered average error and standard deviation for each section of the patellar cartilage for models 2.1 and 2.2 can be found in Appendix B.2, Table 15 and Table 16 respectively. The filtered results for model 2.1 can be seen in Appendix B.3, Table 19.

Filtered Results – Knee 2:

The graph in Figure 51 shows the filtered patellar cartilage thickness results for Model 2.1 per section of the patella, comparing the passive motion with the squat motion results. The graph also indicates the relating filtered sectional thickness values for the uncompressed cartilage of knee 2.

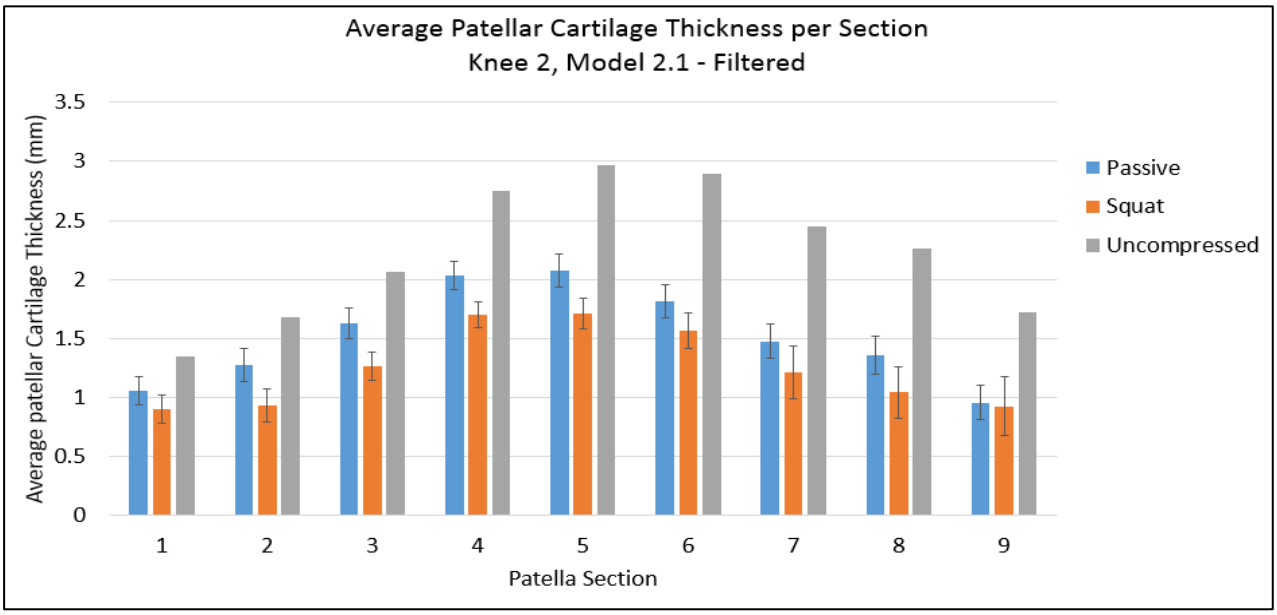

Figure 51: Average filtered patellar cartilage thickness results per section for knee 2 comparing the passive and squat motion results and showing the average error bars.

Figure 52 displays the unfiltered vs. filtered results for model 2.1.

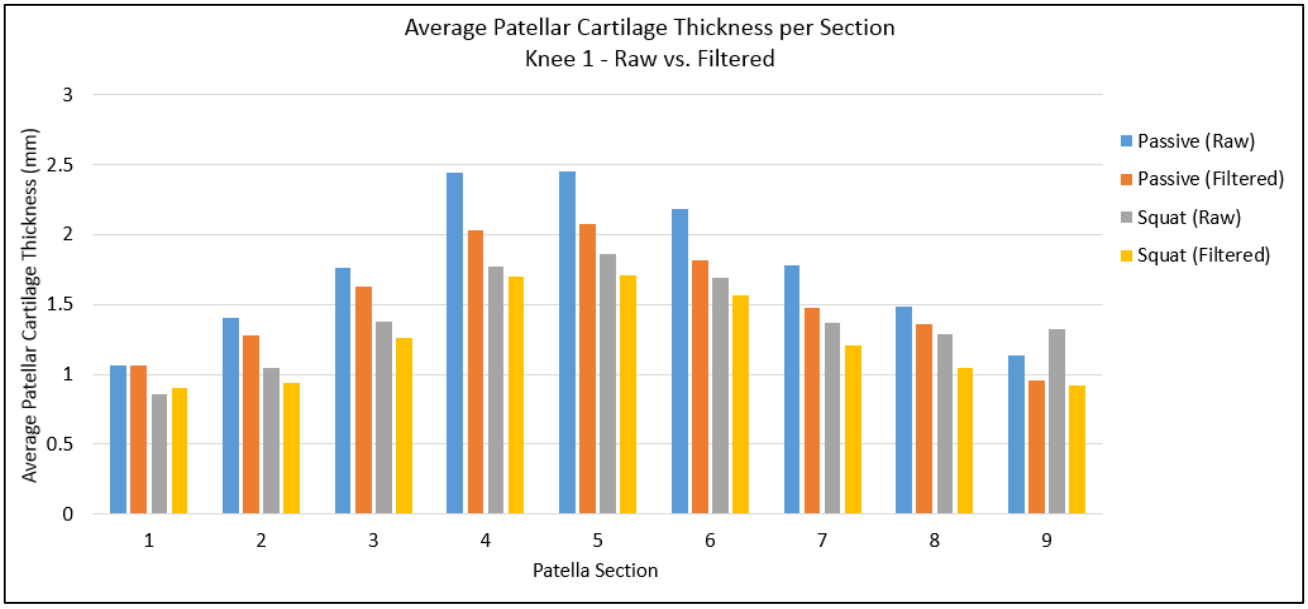

Figure 52: The average patellar cartilage thickness results per section for knee 2, model 2.1. The graph compares the unfiltered vs the filtered results for both the passive and squat motion.

In Appendix B.3, Table 17, the filtered sectional patellar cartilage thickness results for model 2.1 can be viewed. Table 7 summarises the average values calculated for all the cartilage sections for knee 2 (unfiltered and filtered results).

Table 7: Summary of the average values calculated for the patellar cartilage thickness results for knee 2.

	Passive			Squat		
	Model 2.1 (Unfiltered)	**Model 2.2 (Unfiltered)**	**Model 2.1 (Filtered)**	**Model 2.1 (Unfiltered)**	**Model 2.2 (Unfiltered)**	**Model 2.1 (Filtered)**
Average Cartilage Thickness (mm)	1.747	2.898	1.520	1.398	2.911	1.251
Cartilage Volume (mm^3)	2139.570	3319.910	2104.430	1502.630	2258.620	1386.950
Average Error (mm)	0.210	0.190	0.140	0.180	0.170	0.160
Standard Deviation (mm)	0.960	0.890	0.590	0.810	0.800	0.660

The results for the passive motion showed that an average of 12.99% (or an average of 0.227 mm) of the cartilage was removed during the filtering and smoothing step for the model 2.1. Also, the patellar cartilage resulting from the use of the model 2.1 had on average 39.71% (or a thickness average of 1.515 mm) less cartilage than the patellar cartilage resulting from using model 2.2.

The results for the squat movement showed that an average of 10.51% (0.147 mm) of cartilage was removed during the filtering and smoothing step for the model 2.1. Also, model 2.1 had on average 51.98% (1.513 mm) less cartilage than model 2.2. Finally, the estimated contact areas for the passive and squat motion of model 2.1 (knee 2) can be seen in Appendix C.3 and C.4, Figure 70 and Figure 71.

4.3 Patellofemoral Cartilage Compression

This section will detail the compression results for both knees through the application of each motion. These results relate to filtered models 1.1 and 2.1. The compression refers to results under the assumption that the femoral cartilage does not compress, thus the total compression of cartilage between the femur and patella.

4.3.1 Average Cartilage Compression for Knee 1

This section details the average compression that the patellar cartilage experiences due to its relating passive and squat motion for model 1.1 of knee 1. Figure 53 demonstrates a 3D surface plot of the layered surface cartilage results for the three states, indicating the relative compression due to the different motions.

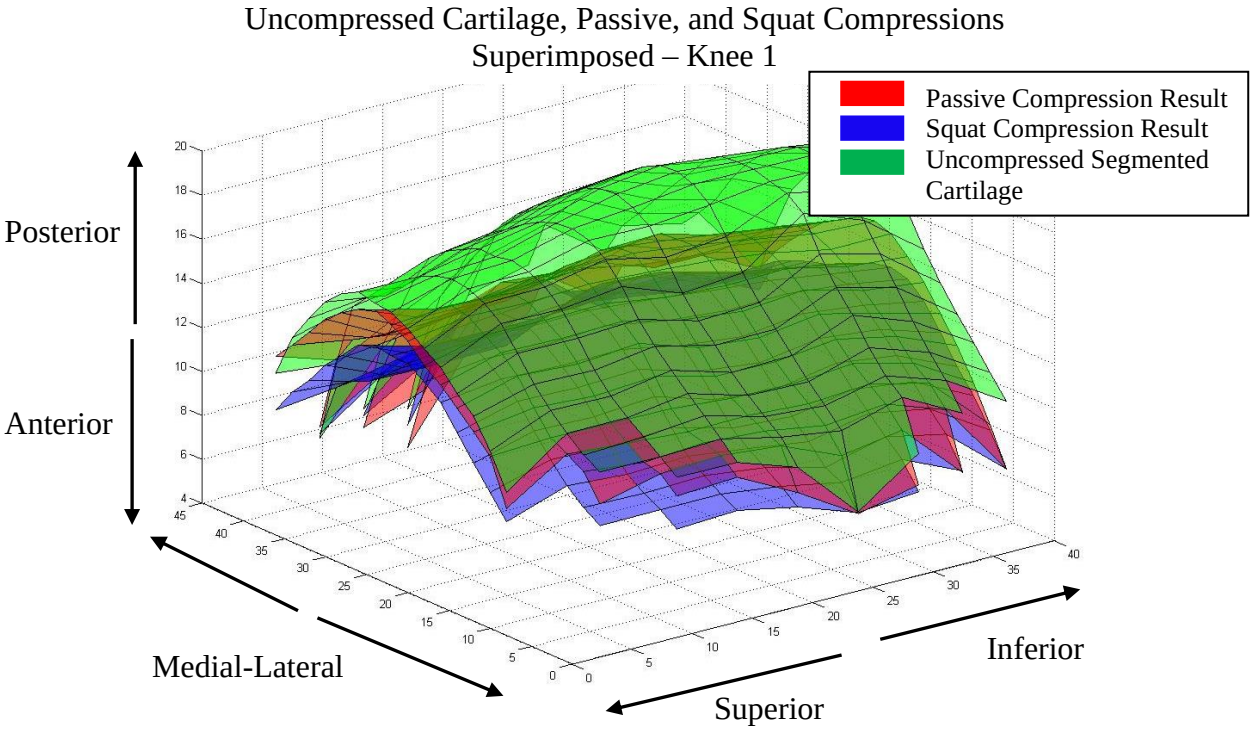

Figure 53: The surface plots of the compression results for knee 1 showing how much the passive and squat movement compressed the uncompressed segmented cartilage.

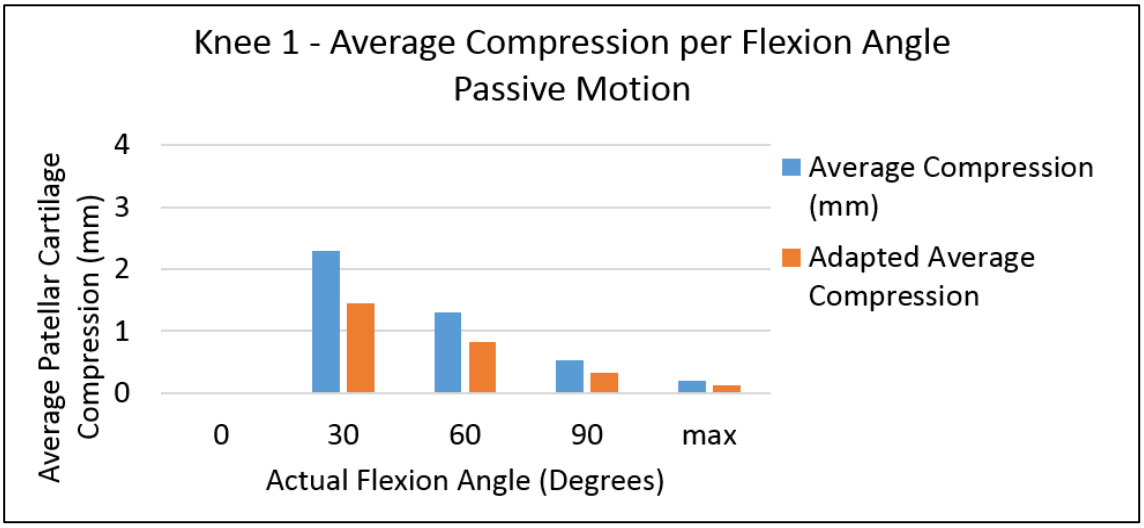

Figure 54: Average Cartilage Compression for model 1.1 of knee 1 for each degree of flexion investigated (Passive Motion)

Figure 54 and Figure 55 shows the average compression of the cartilage for each degree of flexion that was investigated for the passive and squat motions respectively.

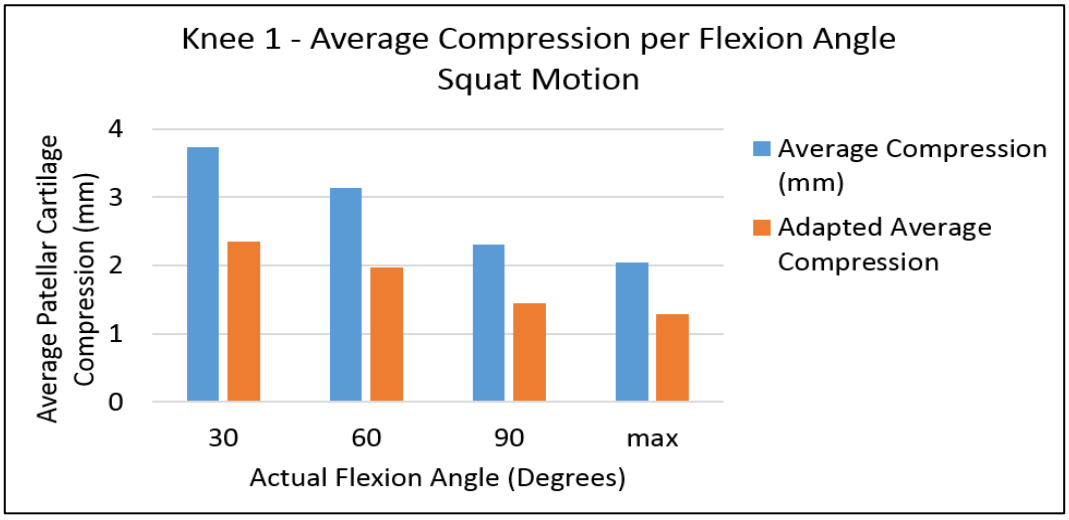

Figure 55: Average Cartilage Compression for model 1.1 of knee 1 for each degree of flexion investigated (Squat Motion)

Figure 56 shows the difference between the passive and squat motion results for the average cartilage compression per section of knee 1. See Appendix D, Table 20, for the calculated patellar cartilage compression results per section.

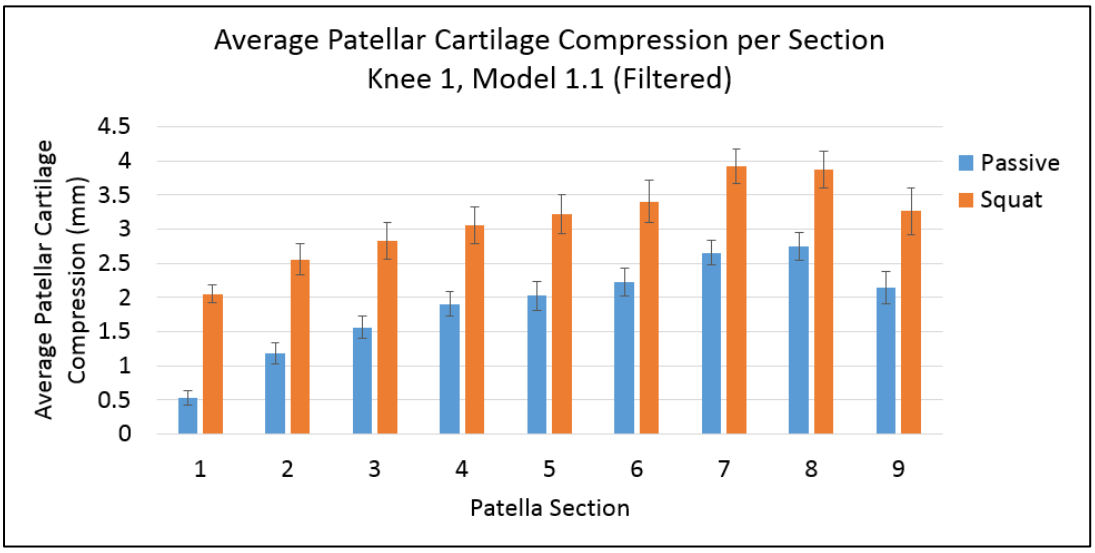

Figure 56: Plot indicating the average patellar cartilage compression per section for model 1.1 of knee 1. The plot indicates the difference in sectional compression between the passive and squat motions and showing the average error bars for each section.

The filtered average error and standard deviation for each section of the patellar cartilage for model 1.1 can be found in Appendix D.2, Table 21. Table 8 summarises the total average compression results.

Table 8: Summary of the average values calculated for the patellar cartilage compression results for knee 1, model 1.1.

	Passive	Squat
Average Cartilage Compression (mm)	1.87	3.13
Average Compression (%)	51.13	85.58
Average Error (mm)	0.18	0.26
Standard Deviation (mm)	0.76	1.11

4.3.2 Average Cartilage Compression for Knee 2

This section details the average compression that the patellar cartilage experiences due to its relating passive and squat motion for model 2.1 of knee 2. Figure 57 demonstrates a 3D surface plot of the layered surface cartilage results for the three states, indicating the relative compression due to the different motions.

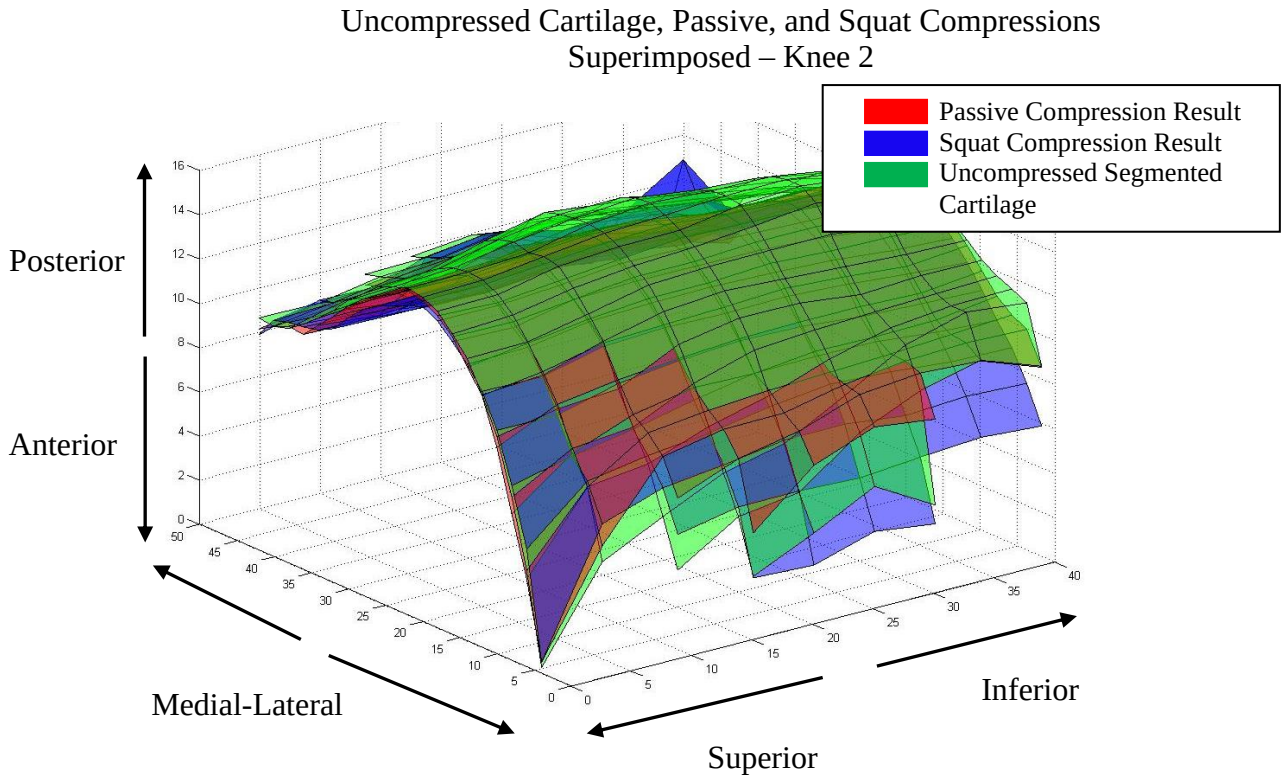

Figure 57: The surface plots of the compression results for knee 2 showing how much the passive and squat movement compressed the uncompressed segmented cartilage.

Figure 58 and Figure 59 shows the average compression of the cartilage for each degree of flexion that was investigated for the passive and squat motions respectively.

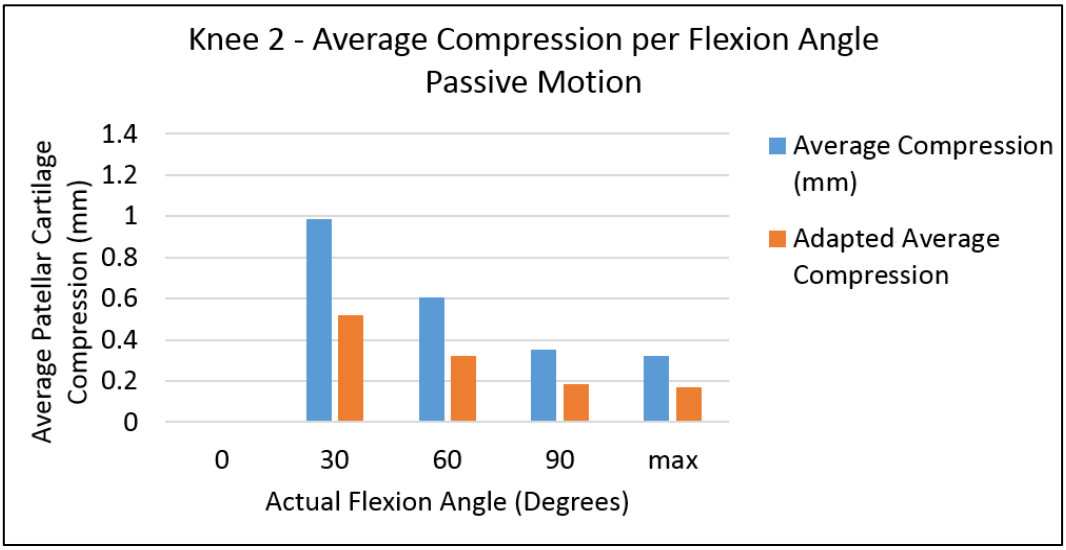

Figure 58: Average Cartilage Compression for model 2.1 of knee 2 for each degree of flexion investigated (Passive Motion)

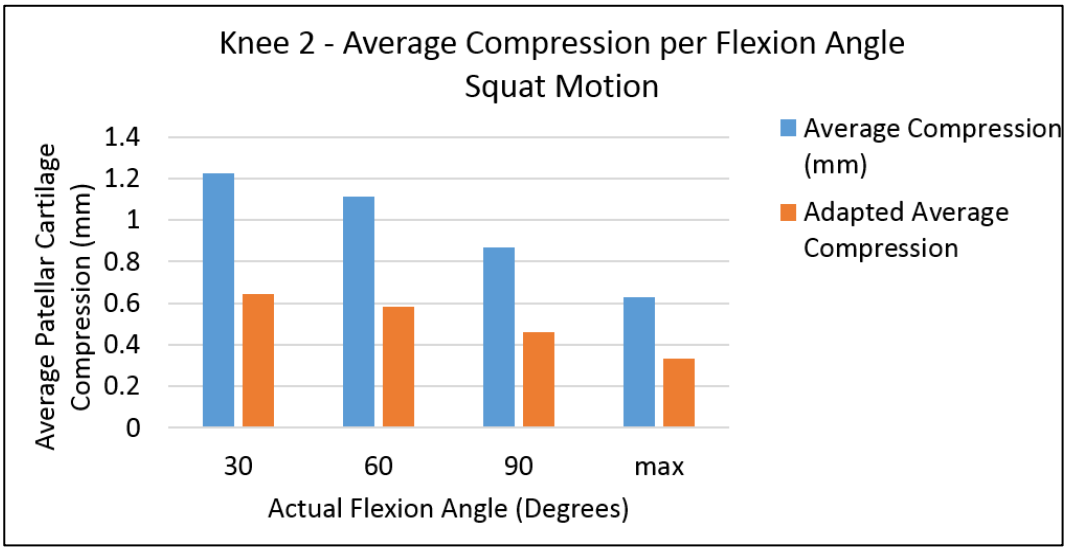

Figure 59: Average Cartilage Compression for model 2.1 of knee 2 for each degree of flexion investigated (Squat Motion)

Figure 60 shows the difference between the passive and squat motion results for the average cartilage compression per section of knee1. See Appendix D, Table 20, for the calculated patellar cartilage compression results per section.

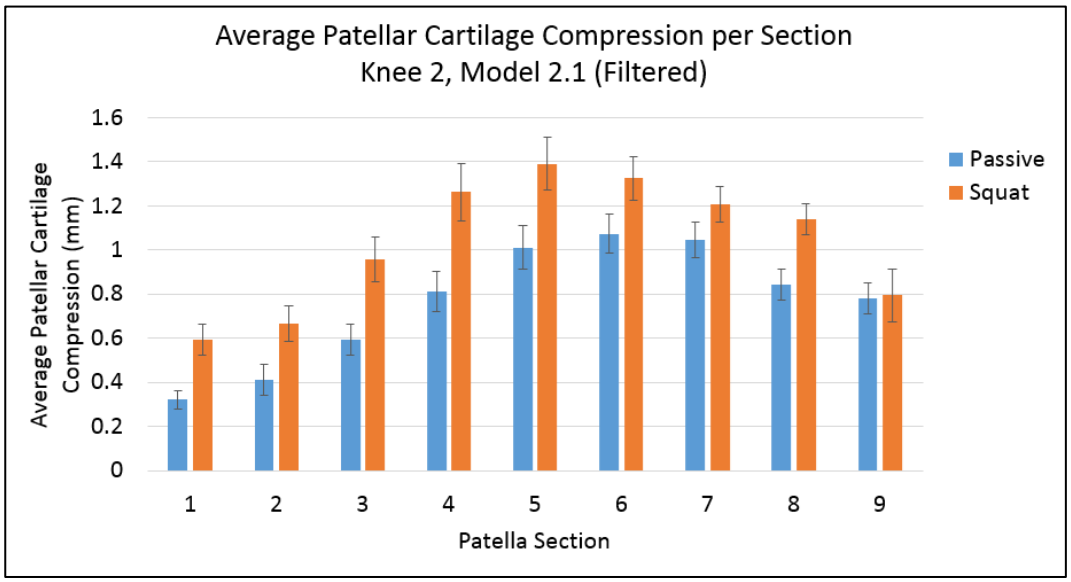

Figure 60: Plot indicating the average patellar cartilage compression per section for model 2.1 of knee 2. The plot indicates the difference in sectional compression between the passive and squat motions and showing the average error bars for each section.

The filtered average error and standard deviation for each section of the patellar cartilage for model 2.1 can be found in Appendix D.3, Table 22. Table 9 summarises the total average compression results.

Table 9: Summary of the average values calculated for the patellar cartilage compression results for knee 2, model 2.1

	Passive	Squat
Average Cartilage Compression (mm)	0.766	1.038
Average Compression (%)	34.24	46.4
Average Error (mm)	0.08	0.10
Standard Deviation (mm)	0.32	0.40

4.3.3 Relative Compression Ratio of Femoral to Patellar Cartilage

As mentioned previously, the initial compression outcomes were as a result of assuming that the femoral cartilage does not compress. This section documents the calculated ratio of cartilage between the patella and femur.

The average segmented patellar cartilage thickness for knee 1 was 3.657 mm and the femoral cartilage was 2.013 mm. This resulted in a ratio of 3.657:2.013 (Patella: Femur). The same ratio was determined for knee 2 with the resulting ratio of 2.237:2.01 (Patella: Femur).

4.3.4 Actual Compression of Patellar and Femoral Cartilage

The ratios determined in section 4.3.3 were applied to the total initial compressional results in Section 4.3 to determine the actual average compression that the patellar

and femoral cartilage undergoes while performing a specific movement. This section documents the resulting final compression results for both knee 1 and 2 undergoing the passive and squat movement.

When applying the ratio of 3.657:2.013 to the initial overall average compression results for the passive movement of knee 1, a final average cartilage compression of the original uncompressed patellar cartilage of 1.205 mm (32.95%) was calculated for the patellar cartilage and an average cartilage compression of 0.663 mm (32.94%) for the femoral cartilage. The final average cartilage compression for the squat movement was 2.019 mm (55.20%) for the patellar cartilage and 1.111 mm (55.19%) for the femoral cartilage. Refer to Figure 54 and Figure 55 to see the comparison between the total compression and the adapted patellar cartilage compression for model 1.1

The ratio of 2.237:2.01 was applied to the initial overall average compression results of knee 2. The final average cartilage compression of the original patellar cartilage for the passive movement was calculated as 0.403 mm (18.02%) of compression for the patellar cartilage and 0.362 mm (18.01%) of compression for the femoral cartilage. The squat movement resulted in a final average compression of 0.547 mm (24.45%) for the patellar cartilage and 0.491 mm (24.42%) for the femoral cartilage. Refer to Figure 58 and Figure 59 to see the comparison between the total compression and the adapted patellar cartilage compression for model 2.1.

4.4 Finite Element Model of the Patellar Cartilage

FEM models of the patellar cartilage were created to determine the resulting stresses on the patellar cartilage during a specific movement (passive or squat). These resulting stresses for both knee 1 and knee 2 (Models 1.1 and 2.1) will be documented in this section.

4.4.1 Patellar Stresses – Knee 1

In Appendix E.1 and E.2, Table 23 to Table 25 shows the resulting stresses obtained due to the pressure the passive movement places on the patellar cartilage and the patellar bone beneath, while Table 26 to Table 28 shows the resulting stresses due the squat movement.

Figure 61 shows box and whisker plots for the passive movement where the orange and grey boxes represent the stresses on the cartilage surface and the blue and green represents the stresses on the patellar bone. Each individual box and whisker chart gives the distribution of the recorded stresses at a specific compression and degree of flexion, but at different Poisson's Ratio's and Young's Moduli.

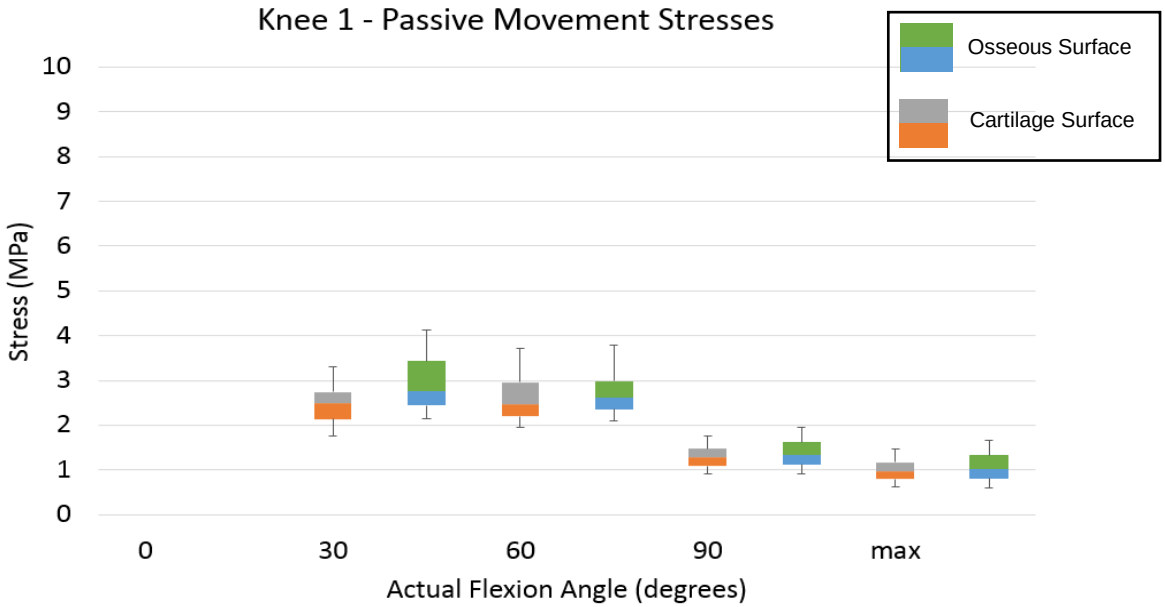

Figure 61: Box and whisker chart for the passive movement of knee 1. Grey and orange represents the stresses recorded on the cartilage surface and the green and blue the stresses on the patellar bone surface.

Figure 62 shows the same plots as shown for the passive movement, but for the squat movement instead.

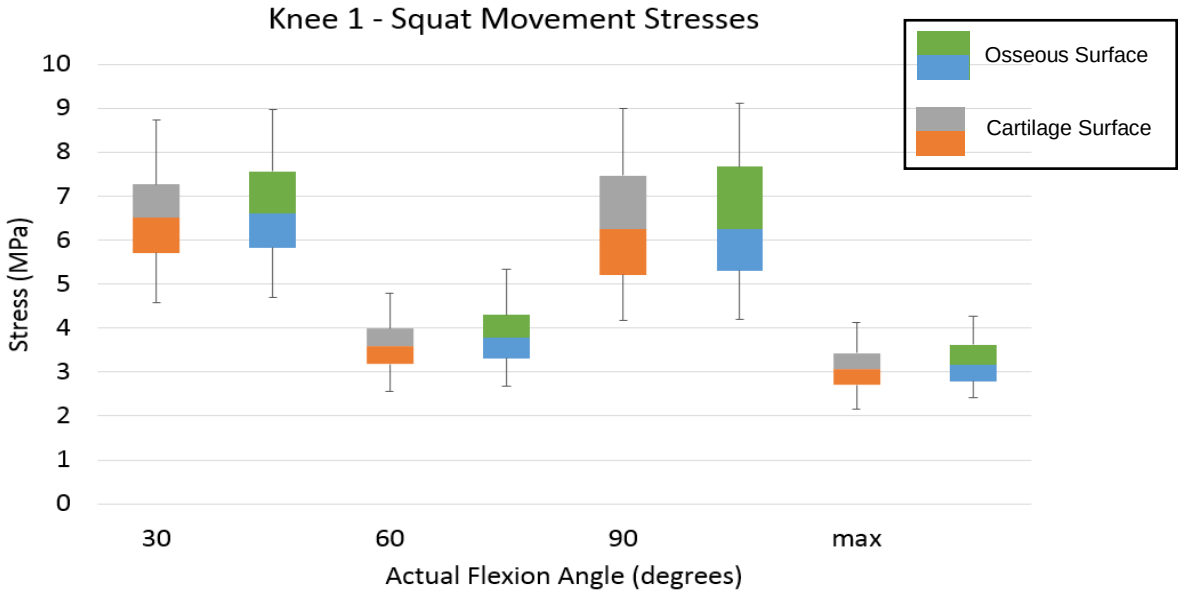

Figure 62: Box and whisker chart for the squat movement of knee 1. Grey and orange represents the stresses recorded on the cartilage surface and the green and blue the stresses on the patellar bone surface.

4.4.2 Patellar Stresses – Knee 2

In Appendix E.3 and E.4, the resulting stresses obtained for knee 2 from the FEM analysis can be found in Table 29 to Table 31 for the passive movement and Table 32 to Table 34 for the squat movement. The graphical results for the passive movement can be viewed in Figure 63. Figure 64 shows the box and whisker plots for the squat movement of knee 2.

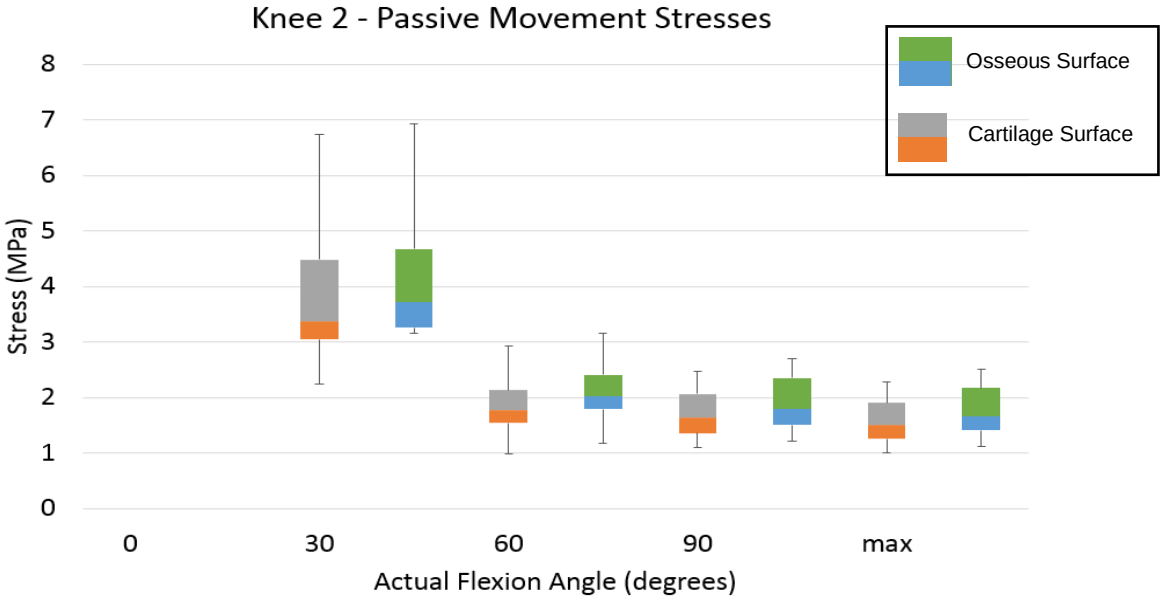

Figure 63: Box and whisker chart for the passive movement of knee 2. Grey and orange represents the stresses recorded on the cartilage surface and the green and blue the stresses on the patellar bone surface.

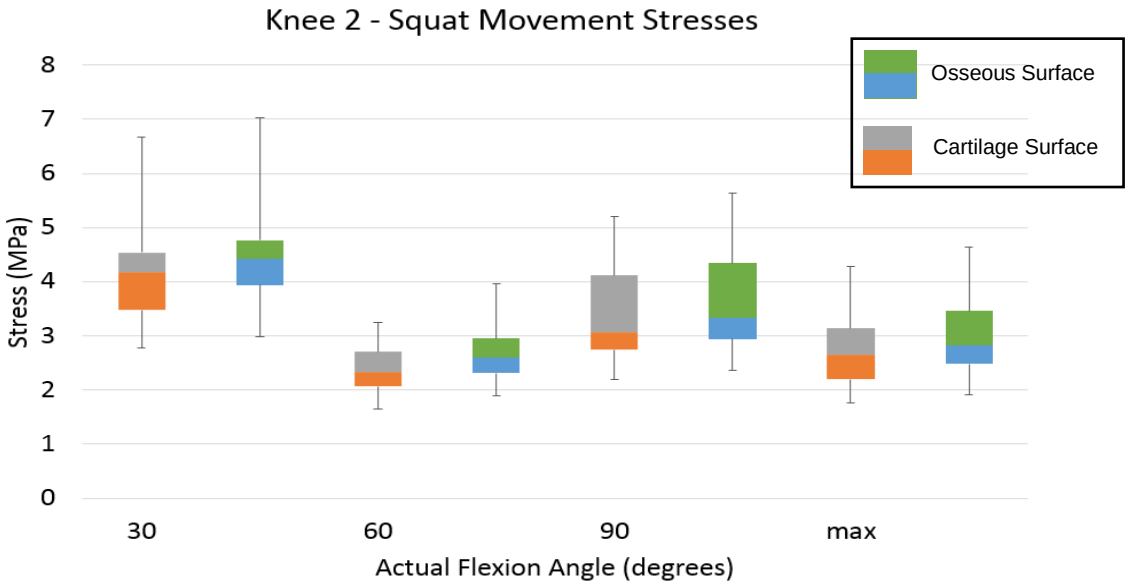

Figure 64: Box and whisker chart for the squat movement of knee 2. Grey and orange represents the stresses recorded on the cartilage surface and the green and blue the stresses on the patellar bone surface.

4.4.3 Mesh Analysis

Table 10 details the number of nodes and elements for the volumes meshes used during the FEM analysis of knee 1 and knee 2.

Table 10: Mesh analysis data for knee 1 and knee 2 as used during the FEM analysis.

Mesh Analysis for Knee 1 and 2		
	Knee 1	**Knee 2**
Mesh Type	Volume Mesh	Volume Mesh
Element Type	TET10	TET10
Number of Nodes	82295	132161
Number of Elements	44678	87978

4.4.4 Test for Mesh Convergence

The graph in Figure 65 shows the mesh convergence plot for knee 1 and 2 indicating the stresses under the same conditions, but for different mesh sizes.

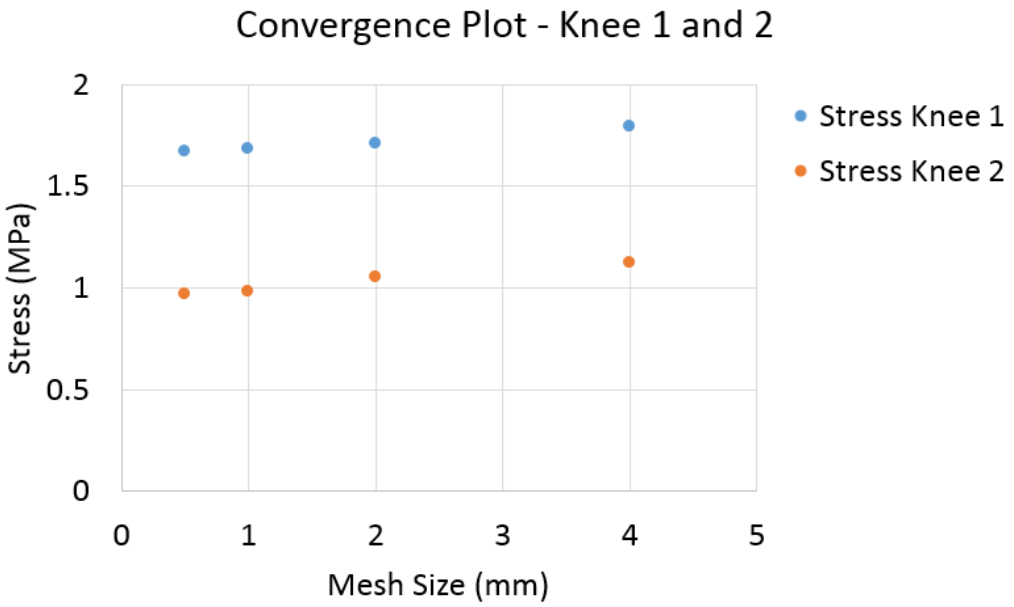

Figure 65: Test for convergence for knee 1 and 2

The stress values was calculated to be within a 6.7% range of each other for knee 1 and within a 13% range for knee 2.

Chapter 5

5 Discussion

5.1 Estimated Geometry Cartilage Results

This section discusses the final resulting cartilage that was estimated using the kinematic models and the designed cartilage estimation program as documented in section 4.2.

5.1.1 Segmented Uncompressed MRI Results

The most significant finding that could be seen from the results of the cartilage segmented from the MRI scans, were that the cartilage segmented for the patellae and femurs for both knees where segmented accurately. This means that the cartilage could be implemented in the estimation process.

The visual results of the segmented patellar cartilage for knee 2 (Figure 39) shows a substantial thickness difference when comparing the results to those for knee 1 in Figure 37. The results for knee 2 shows a much thinner patellar cartilage than the cartilage for knee 1.

It is noted from the chart in Figure 38 that the average sectional patellar cartilage thickness recorded from the segmented MRI data of knee 1 follows the trend of the average cartilage thickness as found in literature[48]. Also, the segmented cartilage stays within the minimum and maximum boundaries for patellar cartilage thickness. In Appendix A, the chart containing the data for the femur can be found. The chart comparing the average cartilage thicknesses for the femur (Figure 66) shows the same trend as the data in Figure 38, staying within the minimum and maximum cartilage thicknesses.

In Figure 40, it is noted that the segmented patellar cartilage for knee 2 closely follows the minimum recorded sectional thickness from literature, even falling below the minimum. The femur (Figure 67), however, lies well within the maximum and minimum range for segmented femoral cartilage closely following the average cartilage thickness (from literature) for most of the measured sections. This shows that the femoral cartilage for knee 2 was segmented close to the actual cartilage. The results for the segmented patellar cartilage indicate that the patellar cartilage thickness for knee 2 is below average and close to the minimum cartilage thickness as indicated by literature.

Knee 1 reported a 0.76 mm standard deviation (with a mean of 3.657 mm) for the patellar cartilage results, while knee 2 reported a standard deviation of 0.73 mm (with a mean of 2.237 mm). For both cases the standard deviation is small relative to the reported means, indicating that the data for both cases are closely clustered around the mean. Small standard errors were also reported for the segmented

patellar cartilage of both knees, indicating that the calculated mean is a reliable representation of the actual mean cartilage thickness.

Finally, the fact that the patellar cartilage for knee 2 does not lie close to the averages found in literature, indicates that the patellar cartilage was either poorly segmented, or that the patellar cartilage is just anatomically out of the standard average cartilage thickness range as indicated by literature. Since the cadaver donors' ages ranged from 76 to 95 years, the thin cartilage on knee 2 could possibly indicate that the knee was arthritic. The femoral cartilage for this model (knee 2) and the patellar and femoral cartilage for knee 1 was segmented with accuracy, it can thus be concluded that the thin patellar cartilage segmented for knee 2 is due to anatomical differences and not poorly segmented cartilage. This indicates that the uncompressed cartilage segmented from the MRI scans were accurately segmented and could be implemented in the estimation process.

5.1.2 Cartilage Estimation Results for Knee 1 and 2

It was found that the inverse kinematic analysis program designed was able to estimate the geometry of the patellar cartilage using kinematics and the uncompressed cartilage from the MRI scans.

The initial visual inspection of the estimated patellar cartilage results for the passive movement of both knees showed a well-shaped estimation of the patellar cartilage that agrees with the shape and location of patellar cartilage as found in literature [48]. The rough surfaces for the unfiltered results are as a result of ridges and surface inconsistencies overlooked during the segmentation process of the femoral cartilage which was then carried over to the patellar surface during the estimation process.

Upon the initial visual inspection of the squat results in Figure 42 and Figure 48, it is noted that the patellar cartilage has predominantly the same shape and location as was found produced by the passive movement. It was, however, noted that the thickness of the patellar cartilage was thinner for the results produced by the squat movement than for the results produced by the passive movement. This is as expected since the squat movement applies a greater pressure on the patellar cartilage than the passive movement which will result in a more compressed and thinner patellar cartilage result. Another important observation made, was that the patellar cartilage seems to intersect the patellar bone, which it should not. This is, however, due to the assumption that the femoral cartilage does not compress, made prior to running the patellar cartilage estimation program. The amount of compression seen in these initial results are the total compression that would take place for both the femoral and patellar cartilage, however the program only applies it to the patellar cartilage.

Estimated vs Segmented Femoral Cartilage

The estimated patellar cartilage that originates from using the author estimated femoral cartilage was included to compare whether the estimation of the femoral cartilage could be used in the overall estimation process instead of the femoral cartilage segmented from the MRI scans. For the passive movement, as deduced

from Figure 44A, it was found that for knee 1 the difference between the overall average patellar cartilage thicknesses of models 1.1 and 1.2 was 0.36 mm or 14.74%. A standard deviation of 0.82 mm for model 1.1 and 0.96 mm for model 1.2 indicated that for both models the data is clustered around the calculated mean. The standard errors calculated for all the investigated cases, showed similar results indicating that the calculated means was a relatively accurate reflection of the actual population means. This indicates that for knee 1, model 1.2 could have been used to recreate the patellar cartilage for the passive movement. Knee 2 (Figure 50A), however, showed an overall average patellar cartilage thickness difference of 1.515 mm or 39.71%. The standard deviations calculated for knee 2 showed that the data was once again clustered around the mean, but less so than for knee 1. Even though knee 1 and knee 2 showed the trend that the segmented cartilage resulted in a thinner overall average cartilage thickness, the big difference in thicknesses between model 2.1 and 2.2 shown by knee 2 indicates that it is difficult to create an accurate and consistent estimation of the femoral cartilage.

For the squat movement, it can be seen in Figure 44B that the segmented femoral cartilage (model 1.1) used to estimate the patellar cartilage for knee 1 resulted in a 0.903 mm (43.67%) thinner patellar cartilage thickness than when using the estimated femoral cartilage (model 1.2). Knee 2 (Figure 50B) showed a 1.513 mm (51.98%) thinner patellar cartilage thickness from using model 2.1 than using model 2.2. The standard deviations for the squat motions showed that the data for knee 1 was less densely clustered around the mean than for knee 2. Also, in general the squat results was less densely clustered around the mean than for the passive results. The difference between the cartilage thickness of the models created using the segmented femoral cartilage and the estimated femoral cartilage is large, further indicating that the use of the estimated femoral cartilage to determine the patellar cartilage is not accurate and reproducible.

Unfiltered vs Filtered Cartilage

The unfiltered and filtered data for the passive movement of knee 1 (model 1.1) is compared in Figure 46 and shows an average thickness difference of 0.311 mm or 14.95%, indicating that only a small percentage of material was removed during the smoothing and filtering process. On closer inspection of the data points of each section, the majority of the material was removed on the outer edges of the patellar cartilage (the medial and lateral edges) where the cartilage estimation program would start wrapping the created cartilage around the femoral condyles. Knee 2 (Figure 52) shows a similar removal of material during the smoothing and filtering of the unfiltered data (model 2.1) of 0.227 mm or 12.99%. This reduction in material found during the filtering process for both knees indicated that the filtering and smoothing process mostly removed material which improve the geometry of the final estimated cartilage.

One of the steps in the smoothing and filtering process is comparing the shape and curves of the resulting cartilage to the MRI segmented cartilage which gives a good indication of the general shape of the cartilage. During the smoothing process, the areas of the created patellar cartilage which are too thick as a result of the program

wrapping the cartilage around the femoral condyles, would be reduced. The thickness of the initial cartilage base material which is used to form and shape the final patellar cartilage, has an effect on how much the program wraps the cartilage around the femoral condyles. The thicker this initial estimation, the thicker the outside edges of the patellar cartilage would be since the femur is not in contact with the patella on these outer edges.

The smoothing and filtering process for the squat movement (Figure 46) removed an average of 0.507 mm (43.52%) of the created cartilage from the unfiltered results for knee 1 (model 1.1). As for the passive movement results, the filtering process for the squat removed the majority of the cartilage on the medial lateral edges. In the case of knee 1 the initial patellar cartilage estimation material was thicker than for the model during the passive movement, thus more material had to be removed. This, however does not have an effect on the majority of the resulting patellar cartilage. Knee 2 (Figure 52) only removed 0.147 mm (10.51%) of material from the unfiltered results during the filtering process indicating that the initial patellar material estimation for this model resulted in a close approximation of the patellar cartilage. This meant that little material had to be removed from the outer edges to estimate the geometry of the cartilage.

Finally, the standard deviations calculated for the filtered results for knee 1 and knee 2, both indicated that the filtered data was more densely clustered around the mean in comparison to the unfiltered data, showing that the filtering process increased the reliability of the results. Furthermore, the average errors for the filtered data of both knees was also smaller than the unfiltered data, further indicating that the filtering process improved mean results and created a more accurate reflection of the population mean.

Cartilage Volumes

The recorded cartilage volumes for knee 1 also indicated a reduction in volume from the passive to the squat motions. The same trend was seen for knee 2. Furthermore, the volume results for knee 1 and knee 2 for both motions identified that the cartilage estimated from the estimated femoral cartilage resulted in larger volumes than the cartilage estimated using the segmented femoral cartilage, further demonstrating that difficulty of accurately estimating the femoral cartilage.

Contact Areas

The contact areas for knees 1 and 2 where the patella and femur come into contact during the passive movement was identified to determine whether the created cartilage estimation program was able to create the correct indents in the cartilage at the correct contact areas and to see whether it follows the same shape and general placement as found in literature.

As found in literature [27], the femur is in contact with the superior section of the patella when it is at its maximum degree of flexion and as the degree of flexion decreases, the contact area on the patellar cartilage moves in the inferior direction. Although the pattern does not agree exactly with literature, it still follows the same trend in terms of decreasing degrees of flexion which comes in contact moving in

an inferior direction on the patellar cartilage surface. These results were seen for the passive movement of both knees. The areas showing no contact would be the areas where other degrees of flexion that were not specifically investigated, but still used during the estimation process, would have been in contact with the patellar cartilage.

Knee 2 shows less contact between the patella and femur at the designated degrees of flexion, but this could be due to fact that the patellar cartilage for knee 2 is much thinner than normal patellar cartilage thickness. Thinner cartilage allows for less compression, and since the program that estimates the cartilage uses the indentation the femur makes to create the cartilage, thinner cartilage would result in smaller contact areas.

The contact areas for both knees for the squat movement differ from the passive movement, but overall still conforms to the general established pattern. The contact areas for the squat movement moved in the superior direction in relation to the passive movement where the squat movement has a greater contact area between the patella and femur during the maximum degree of flexion as would be expected during a squat movement. The passive movement tend to show a greater interaction between the patellar and femur during the mid-range degrees of flexion, while the squat movement has a greater impact on the cartilage during the outer (minimum and maximum) degrees of flexion.

Passive vs Squat Motions

Overall, a difference is noted between the passive and squat movements in terms of the resulting thicknesses of the estimated patellar cartilage, with the squat movement resulting in a thinner patellar cartilage. This can be seen by the plots as shown in Figure 43 and Figure 45 for knee 1 and Figure 49 and Figure 51 for knee 2. Since the squat movement applies a greater pressure on the patella during the motion, it is to be expected that the cartilage estimated from the squat motion would be thinner than the cartilage estimated for the passive motion. The contact areas also exhibited differences between the passive and squat movement, which is as expected since the movements differ in terms of trajectories, degrees of freedom constrained, and amount of weight applied to the movement which would result in a different interaction between the femur and patella and thus contact areas.

5.2 Patellofemoral Cartilage Compression

The initial patellar cartilage compressional results documented, was the cartilage compression that was created and estimated under the assumption that the femoral cartilage does not compress, i.e. the total compression that both the femoral and patellar cartilage undergoes, but only applied to the patellar cartilage. This was done in an effort to simplify the designed program, and use the femur as little as possible during the estimation of the patellar cartilage.

5.2.1 Average Cartilage Compression for Knee 1 and 2

It was found that the squat motion consistently resulted in a larger compression than the passive motion. Also, larger compression values was reported at lower flexion angles.

Knee 1 reported a compression of 51.13% produced by the passive movement and 85.58% produced by the squat movement. These compression values seem quite large, indicating that half of the cartilage is compressed during the passive movement and over three-quarters of the original cartilage is compressed during the squat movement. However, the fact that these values refer to the total compression of both the femoral and patellar cartilage implies that these values will be smaller once the total compression is distributed between the femoral cartilage and patellar cartilage.

It is noted from Figure 56 that the squat movement for knee 1 results in a larger compression than the passive movement which is as expected since the squat movement applies greater forces to the patellofemoral joint than the passive movement. Figure 53 gives the 3D representation of the three cartilage layers which gives a good representation of the relative compression between the three layers of cartilage. This image shows a large compression from the uncompressed cartilage to the passive cartilage which is for the most part as a result of the uncompressible femoral cartilage assumption. However, the uncompressed cartilage from which the compression were measured could also have been over estimated during the segmentation of the MRI data.

In Figure 60, knee 2 presented compressional results considerably smaller than knee 1. The passive movement recorded an average compression of 34.24% and the squat movement resulted in a 46.40% compression. Figure 57 shows more densely stacked cartilage layers which could be as a result of the already notably thin original uncompressed cartilage for knee 2. The thinner the cartilage, the less compression will take place since the material structure of cartilage provides more resistance as the cartilage gets more compressed. Since the original cartilage is quite thin, the cartilage will provide much more resistance for the same amount of compression and thus will undergo less relative compression.

The compression for each flexion angle can be seen in Figure 54 and Figure 55 for the passive and squat motions of knee 1 and Figure 58 and Figure 59 for the passive and squat motions of knee 2. All four cases indicates that the compression experienced at a lower flexion angle is larger and decreases as the flexion angle increases. This is not as expected since the pressure increases with an increase in flexion angle, however, it should be noted that the patellofemoral contact areas at lower flexion angles are situated on the sections of the femur where there are relatively thick cartilage as opposed to the rest of the articulating surfaces. Thicker cartilage areas will result in larger compression results since the thicker the cartilage, the larger the relative compression will be.

Furthermore, since the compression data is calculated from the segmented MRI scans, any over or under segmentation of the MRI patellar cartilage could result in these inconsistencies. By comparing the relative compression between the passive

and squat motions, the inaccuracies that could possibly have been introduced through the use of the MRI data was removed. It was found that the relative compression between the passive and squat motions actually resulted in an increase in compression as the degree of flexion increases, which is as to be expected. It is also noted for the passive movement that there is no contact at zero degrees for both knees. This can be explained by the fact that during the collection of the experimental data, the patella was lifted away from the femur at zero degrees meaning there was no contact between the patella and femur at zero degrees during the experimental phase and thus would not show in the results.

Finally, the standard deviations calculated for the passive and squat motions for both knee 1 and 2 was very similar indicating that all the compressional data was closely clustered around their relating mean. Small standard errors was also calculated for all four cases signifying that calculated sample means was an accurate reflection of the actual population mean.

5.2.2 Actual Compression of Patellar and Femoral Cartilage

The compression ratios determined for knee 1 and 2 was used to determine the actual predicted patellar and femoral cartilage compression during the specific movements. When looking at each model's determined ratio, it is noted that the resulting smaller ratio produced for knee 2 indicates that the patellar cartilage for knee 2 will compress less relative to knee 1. Also, the application of the cartilage ratio decreases the amount that the patellar cartilage compresses.

When applying the determined cartilage ratio for knee 1 to its initial compression results, a 32.95% compression of the patellar cartilage was calculated for the passive movement and a 55.20% compression of the patellar cartilage was calculated for the squat movement. This showed a decrease in 18.18% compression for the passive movement and a 30.38% reduction in patellar cartilage compression for the squat movement by applying the cartilage ratio. These newly calculated patellar cartilage compression values represent the actual compression that the patella undergoes during the specific movements, now taking into account that the femoral cartilage also compresses during movement. The femoral cartilage compressed less than the patellar cartilage since the femoral cartilage is on average thinner than patellar cartilage.

The newly calculated actual compression for knee 2 resulted in an actual patellar cartilage compression of 18.02% for the passive movement, and 24.45% for the squat movement. This ratio applied to knee 2 resulted in a reduction 16.22% reduction in compression for the passive movement and a 21.95% reduction for the squat movement from the initial compression results. There is still a large difference in relative compression between knee 1 and knee 2, but as mentioned previously it could be attributed to how thin the original cartilage for knee 2 is.

The compression results is larger than expected, but could be attributed to the uncompressed cartilage. Even though the results indicated that the uncompressed cartilage was accurately segmented from the MRI scans as seen from their sectional averages, the accuracy of the MRI segmentation is still largely dependent on the

skill level of the individual segmenting the cartilage. This could introduce significant variability into the segmentation results. A small inaccuracy in the segmented results could significantly influence the representation of the compression results and result in larger compression results than expected. Therefore the compression results are not accurate enough to represent the actual compression that the patellofemoral joint experiences during these motions, but serves as a relative indication of the compressions that the patellofemoral joint experiences during movement. This is especially relevant to the compression changes between the passive and squat since it's not reliant on the segmented cartilage.

5.3 Finite Element Model of the Patellar Cartilage

The results recorded from the designed FEM models most significantly indicated that the stresses were higher for the squat motions than for the passive motions. Furthermore, it was deduced that the smaller values chosen for the Poisson's ratio and Young's Moduli resulted in stresses that vary less from the median. It was also noted that the stresses recorded on the osseous surfaces consistently resulted in higher stresses than the recorded on the cartilage surface.

Convergence plots, Figure 65 (Section 4.4.4), were created showing the stresses for different test cases where all the variables were kept the same, but the mesh size were changed. The stresses for knee 1 was within a 6.7% range of each other while the stresses for knee 2 were recorded to be in a 13% range of each other. The plots for both knees showed convergence, indicating that the 1mm meshes applied in the FEM analysis for both knees were small enough to produce accurate results, but not so small as to unnecessarily increase the simulation time without increasing the accuracy of the results.

It is difficult to relate the recorded results to stresses found in literature since the conditions under which the results were recorded were not exactly the same as found in literature. It is still, however, relevant to compare the results and see whether they are in the same general stress range as found in literature. Section 2.3 concluded that under normal everyday movement, the stresses on the cartilage would be in the range of 0.2 – 2.5 MPa, however, it further noted that these stresses can potentially peak to stresses in the range of 12 MPa. Since the median values all fall within the range, it can be assumed that reasonable assumptions and conditions were applied to the FEM analysis which provides some assurance in the accuracy of the stress results.

The box and whisker plots (Figure 61 to Figure 64) not only display the distribution of the stress values at a certain degree of flexion with varying Poisson's Ratio's and Young's Moduli, but also shows how the stress on the cartilage surface relates to the stress on the patellar bone. In general for all the models, it was found that the stress experienced on the patellar osseous surface was similar, but bigger than the stresses experienced at the articular cartilage surface.

Generally, the results does not produce any conclusive evidence to support using a certain Poisson's ratio and Young's Modulus over another, it does however tend to produce results in a more appropriate stress range when using lower values for the Poisson's Ratio's and Young's Modulus. Most of the box plots tend to have smaller lower quartiles than upper quartiles pointing to the fact that the average stresses tend to be below the medians. This also indicates that the lower values for the Poisson's Ratio's and Young's Moduli (which results in the lower stresses) produce stress that vary less than when using the higher values for these ratios. In most cases the lower 50% of the data is more tightly grouped than the upper 50%, indicating that higher combinations of the Poisson's Ratio's and Young's Moduli results in a bigger variation in stress and also more frequently results in un-relating stress spikes. This indicates again that the lower values v and E produces more consistent stress predictions.

The passive movement for both models indicates stresses at two or three measured degrees of flexion to be in the same stress range and the other degree of flexion to be in a smaller stress range. These differences could be attributed to the changes in contact area size and location, the amount of compression, and the cartilage thickness of the contact area being investigated.

Furthermore, we note for all cases that the stress tend to decrease at the maximum degree of flexion. Since the forces increase and contact areas decreases with an increase in flexion, it is expected to rather see a gradual increase in stress as the flexion angle increases. This sudden drop in stress can, however, be explained by the fact that as the knee moves into deep flexion, some of the load experienced by the patella is shared by the quadriceps tendon, decreasing the stress experienced by the patella during deep flexion.

The results also consistently indicate that the squat motions result in much larger stresses on both the articulating cartilage surface and the osseous surface. The deformation as a result of the passive motion could thus be a better option to implement in potentially improving patellar replacements since the smaller deformation would results in smaller stresses on the remaining patellar bone while still implementing deformation to the patellar replacement in the hopes of improving prosthesis comfort and fit.

5.4 Accuracy of Method

Determining the overall accuracy of a novel method like the one described in this thesis is generally quite difficult since there are no real data and results that it can be compared to due to the unique nature of the method. This leaves the researcher with the option of determining the accuracy of each subsequent step of the process, and also attempt to compare the consequent data from that section to that from literature if possible. The combination of these accuracies might be able to provide some insight into the overall accuracy of the method used.

The method used to determine the kinematic model results documented in section 4.1 is a process that has been used numerous times with great degree of success

[67], [68]. The main uncertainties are introduced during the process of capturing the data during the experimental process, however, this process has also been proven to be accurate [66]. The other factor to consider is the creation of the model in ADAMS, however, the models created was able to very accurately reproduce the relevant movement which leads to a resulting accuracy certainty of 0.95.

The next step in the method to be investigated was the process of segmenting the MRI cartilage. The method greatly relied on accurate cartilage segmentation since a minor inaccuracy in the cartilage will greatly affect the final estimated cartilage and thus the resulting compression. This is exceptionally prevalent with segmenting the femoral cartilage since the estimation of the patellar cartilage is directly related to the thickness and shape of the femoral cartilage. The main reason variability is introduced into the segmentation of the MRI, is due to lack of segmentation experience. The segmentation process in itself is a difficult process which requires extensive experience to guarantee accurate results. Due to the experience level of the individual that segmented the MRI data, a degree of inaccuracy was introduced during this step even though great effort was made to improve and provide reasonably accurate segmented cartilage. This resulted in an accuracy certainty of 0.8.

Furthermore, the actual process of estimating the cartilage had various steps involved which could introduce inaccuracies into the final results, however great care was taken to minimise the likelihood of inaccuracies being introduced. The final step in the process also provides a step to validate that the process that was performed produced the required results. This step included a final evaluation of the estimated patellar cartilage against the femoral cartilage at the varying degrees of flexion where it was ensured that there was no intersection between the patellar cartilage and femoral cartilage and that the cartilage conformed to the shape of the femur through its varying degrees of flexion. It was estimated that this step of the process could results in an accuracy certainty of 0.7.

It was determined that the designed method was able to perform as initially intended by creating and estimating the compressed patellar cartilage from the kinematics of the knee by creating cartilage that conformed to the shape of the opposing femoral contact area at the varying degrees of flexion. It was, however, noted that the use of the segmented MRI cartilage for the femur was very important to guarantee accuracy of the process since the estimated patellar cartilage is predominantly dependant on the thickness and shape of the femoral cartilage. Overall, an accuracy certainty of 53.2% was calculated for the process. This result is a rough estimate, but still provides adequate assurance that the method could be a means of determining cartilage compression.

Chapter 6

6 Conclusion

6.1 Overview

This project aimed at creating a method for using kinematics to estimate the geometry of the patellar articular cartilage with as little as possible use of MRI data. Furthermore, the estimated cartilage was used to determine the compression that the cartilage experiences during passive and squat movements and the stresses on the cartilage as a result of the relating compression. The project specifically endeavoured to use kinematics to recreate the cartilage in an attempt to find a different means to cartilage recreation and compression prediction than standard MRI segmentation of compressed cartilage or *in-vivo* measurements of disarticulated cadaver specimens. By using kinematics, only the kinematic measurements and a single MRI scan is necessary which provides a different means of determining patient specific compression of the cartilage in the patellofemoral joint. The use of kinematics also allows the determination of the cartilage in compression in live patients without a magnitude of MRI scans as would normally be necessary.

Determining the compression of the cartilage due to movement produces valuable insight into the way that cartilage reacts during movement. This information can be used towards improving the materials used in patellar implants in an effort to find materials which would perform more like actual cartilage. Replacing the stiff unyielding materials currently being used by a more yielding and biocompatible material which can compress with movement, or allow for some compression, could aid in decreasing anterior knee pain. The stresses determined from the resulting compression could further provide deeper insight into patellofemoral pain and allow for patient specific inspection of the patella in order to determine the cause of the discomfort or pain.

6.2 Objectives

The objectives identified to successfully complete the project were as follows:

Objective 1: Estimate the Geometry of the Patellofemoral Cartilage.

The estimation process requires accurate segmentation of the femoral cartilage since the patellar cartilage being estimated is directly dependant on the shape and thickness of the femoral cartilage. The MRI segmentation process, however, is a difficult manual process greatly dependant on the amount of experience and the skill level of the individual segmenting the MRI data. Section 4.2.1, nonetheless, is able to provide results indicating that the segmented cartilage for both models was done with acceptable accuracy for use in the project. The resulting average

thicknesses of the segmented cartilage for the femur and the patella were compared to literature and found to all, except the patellar cartilage for knee 2, be within the determine thickness range as indicated by literature. The patellar cartilage for knee 2 was found to be just under the minimum determined thickness range for patellar cartilage, however, since the other three structures were segmented with acceptable accuracy, it was assumed that this difference recorded for the patella of knee 2 was simply due to an anatomical abnormality specific to the cadaver knee that was originally measured. Visually, this thickness difference between the patellar cartilage of knee 1 and knee 2 was very noticeable, however, this was possibly due to the patellar cartilage for knee 2 being arthritic. From these results, it was concluded that the patellar and femoral cartilage was segmented accurately enough to be used in the patellar estimation process.

Initially the segmented femoral cartilage and the femoral cartilage estimated using a crude manual technique in 3-Matic was both applied to each model and their two movements. This was to be able to determine whether it would be necessary to use MRI data for the project. Since it was already established that the MRI segmented cartilage was segmented with reasonable accuracy, the results using the 3-Matic estimated femoral cartilage was compared to that of the MRI segmented femoral cartilage results. It was found for both knees for each of the movements, that there was a difference between the segmented and estimated femoral cartilage models. Sections 4.2.2 and 4.2.3 showed that for the passive movements, for example, a recorded difference of 14.74% for knee 1 and 39.71% for knee 2 could be seen. Knee 1 showed a small difference between the two models concluding that the specific estimated femoral cartilage could have been used to estimate the patellar cartilage, however, the substantial difference recorded for knee 2 shows that this technique did not produce consistent and accurate results and could not without further technique refinement be used to produce the femoral cartilage. The squat movement for knee 1 recorded a 43.67% difference between the segmented and estimated femoral cartilage results, while knee 2 reported a difference of 51.98%. These results further proves that the estimation of the femoral cartilage using 3-Matic is not accurate and reproducible, and should not be used in the estimation process which shows that to ensure an accurately reproduced estimated patellar cartilage, a MRI scan of the femoral cartilage is necessary.

Since the models using the estimated femoral cartilage was concluded as being inaccurate and inconsistent, it was determined that the project should continue with the resulting patellar cartilage models where the MRI segmented femoral cartilage was used. The first initial results of the estimated patellar cartilages recorded from the estimation model needed to be further filtered as established by the inspection of the data distribution and visual comparison of the geometry for the cartilage. The main reason for this was to smooth out any surface abnormalities which were propagated onto the newly estimated patellar cartilage surface due to the presence of surface protrusions and ridges on the femoral cartilage surface due to segmentation process. The other reason for filtering and smoothing the cartilage was due to the way that the estimation program creates the patellar cartilage. The written program creates the patellar cartilage by shaping an extra added piece of

material on the patellar surface to take on the shape of the opposing femoral surface. This, however, results in the created patellar surface to start to wrap around the femoral condyles which causes the patellar cartilage to have thicker cartilage on the Medial-Lateral edges and from literature, it is known that patellar cartilage does not take on that shape. Therefore, the extreme excess created on the outer edges of the patella was filtered away. The passive movement, for example, showed that a very small amount of material was filtered away. Knee 1 only filtered away 14.95% of the cartilage and knee 2 filtered away 12.99%. The squat movement for knee 2 showed similar results with a reduction of 10.51%. Knee 1 showed a substantial reduction of 43.52%, but it was noted upon closer inspection that most of the material removed was from the outer edges. The amount of cartilage removed from the initial results, as shown in sections 4.2.2 and 4.2.3, demonstrated that the filtering process only removed cartilage which would ultimately aid in improving the geometry if the cartilage.

Visual inspection of the resulting patellar cartilage (Figure 41 and Figure 47) showed promising results, since the shape and location of the cartilage closely adhered to that defined by literature. The contact areas between the patella and femur at the various degrees of flexion were also estimated from the results and compared to literature. It was found that the contact areas differed slightly from literature, but followed the same pattern as seen in literature. This lead to the conclusion that the estimated program was able to relay the passive and squat movements onto the geometry of the cartilage and shape the cartilage accordingly. Also, for both models, the squat resulted in a thinner resulting patellar cartilage in relation to the passive movement, from which can be concluded that the squat applied larger forces onto the patellar cartilage than the passive movement.

Finally, from the results recorded in section 4.2, it was concluded that the patellar estimation program created is a viable option to produce estimations of the geometry of the patellar cartilage using the kinematics of each subsequent movement. It was, however, also noted that the program has two big limitations which could introduce inaccuracies into the end results. This included the fact that the final patellar cartilage results are directly dependant on an precise femoral cartilage reproduction at the very beginning of the process which means that at least one MRI scan of the knee needs to be performed to be able to properly use the written program. The second limitation is the amount of manual filtering that needs to be done in order to correct the fact that the program wraps the material around the femoral condyles. Nevertheless, the program is still able to reproduce the geometry of the patellar cartilage based on the kinematics of a specific movement.

Objective 2: Determine the Deformation and Compression of the Estimated Patellofemoral Cartilage.

Initial results for the recreated patellar cartilage were estimated under the assumption that the femoral cartilage does not compress in order to simplify the estimation program. This means that the initial patellar cartilage compression results investigated (sections 4.3.1 and 4.3.2), showed the total compression of both the femoral and patellar cartilage applied to the patellar cartilage. Consequently, the

initial results showed extremely large compression percentages for the models, clearly showing a difference between the passive and squat motions (see Figure 56 and Figure 60). The large compression results, however, leads to the conclusion that the assumption of the femoral cartilage not compressing was a poor assumption greatly influencing the outcome of the compression results. Nevertheless the total deformation and compression could still be determined using the inverse kinematic analysis program.

Furthermore, the application of the cartilage ratios solved the problem presented by the uncompressible femoral cartilage assumption. For example, the passive movement for knee 1 initially reported a 51.13% compression of the uncompressed cartilage during the passive movement, and a massive 85.58% compression of the uncompressed cartilage during the squat movement. After applying the cartilage thickness ratio, these values decreased from 51.13% to 30.93% and from 85.58% to 51.84%. This is still quite high for the type of compression being experienced, however, it is important to note that even a significantly small variation in the thickness of the uncompressed patellar cartilage has a major effect on the recorded compression results.

Knee 2 showed much smaller initial compression values of 34.24% for the passive movement and 46.40% for the squat movement which reduced to 20.20% and 33.74% respectively after the application of the cartilage thickness ratio. The big difference in the compression results for knee 1 and knee 2 could be attributed to the below average thin cartilage thickness of knee 2. This meant that less compression would take place since the deeper the compression moves into the layers of the cartilage, the more resistance is presented against the force, and the less compression takes place.

The reduction in compression noticed by applying the cartilage ratio was able to reduce the amount of compression experienced by the patellofemoral joint, leading to the conclusion that the cartilage ratio improved the deformation and compression results and resulted in a more accurate representation of the actual deformation that the patellofemoral cartilage experiences.

Finally, it can be concluded from the compressional results that the method was able to determine the compression and deformation of the cartilage during the passive and squat movements, as seen by the differences shown by the charts in sections 4.2 and 4.3 between the uncompressed, passive, and squat models. Furthermore, it can be concluded that with additional refinement the designed method could potentially become a new non-invasive technique to investigate the compression of patellofemoral cartilage. In addition, a definitive difference in the compression and deformation of the patellar cartilage was noted between the passive and squat movements which leads to the conclusion that the two movements affect the cartilage differently and by investigating and taking this difference into account during patellar replacements, proper replacement materials can be investigated.

Objective 3: Determine the Stresses Present due to the Compression of the Patellofemoral Cartilage.

From the results in section 4.4, it was found that the mean values for the stresses for both models were within the range of stresses as identified by literature from which it can be concluded that the assumptions and conditions applied during the FEM analysis was sufficient. The bigger the Poisson's ratio and Young's Moduli, the bigger the resulting stresses experienced by the cartilage and the more widely spread the stress distribution was. It was also noted from the box and whisker plots that the lower v and E values more consistently produced results that fall well within the stress range determined by literature. Also, the lower values for v and E, especially the combination of $v = 0.4$ and $E = 8$ MPa, produce stress results that are more constant and tightly grouped than bigger values, resulting in less unexplainable stress spikes. This leads to the conclusion that smaller v and E values were more appropriate for the stress analysis.

Furthermore, the results indicated that higher stresses were present on the osseous surfaces of the patella than on the cartilage surface indicating that large compressions experienced by the patella could potentially results in pain experienced on the osseous surfaces of the patella. The larger stresses reported by the squat motion as opposed to the passive motion indicates that if the thickness of the patellar replacement is reduced to take into account the squat motion, the patient is more likely to experience pain after the replacement. A good middle ground would thus be to reduce the thickness of the patellar replacement to that of the passive motion providing patellar replacement which takes some deformation into account, but not enough to significantly increase the chances of the patient experiencing patellar pain.

6.3 Limitations

Certain limitations of using the patellar cartilage estimation model have been identified. The principal limitation of the designed process is the fact that MRI scans are still necessary for an accurate estimation of the patellar cartilage. At least one complete MRI scan of the knee during a relaxed state is necessary for accurate results. Furthermore, the accuracy of the compression results is greatly dependant on the accuracy of the segmentation of the femoral and patellar cartilage from the MRI scan and thus the experience level of the individual segmenting the MRI scans.

Lastly, the process involves multiple steps and processes with a substantial amount of manual work necessary to produce the end results. This decreases the reproducibility and accuracy of the estimated cartilage since it allows for human error to be introduced during the process. It is also very difficult to validate the results for the project since there is no known literature to compare the results to.

6.4 Future Work

The following areas have been identified where the patellar cartilage estimation model can be improved:

- Automate the entire process to reduce the variabilities that are introduced by the manual processes.
- Develop an automatic and quicker measuring process.
- Focus on, and develop a way of estimating the femoral cartilage accurately enough to be able to eliminate the need to use any MRI scans.
- Introduce more models and movements into the process to be able to obtain statistically relevant results to determine the accuracy and effectiveness of the designed process in more detail.

6.5 Contribution to Field

This project was able to provide an initial novel design model with which compressed patellar cartilage can be estimated by using kinematics and minimal MRI scans. The designed model proved that the use of kinematics to determine the geometry and compression of cartilage during the movement of the knee can be seen as a viable option to create and investigate compression of patellar cartilage without disarticulating the knee. It also provides information regarding the cartilage under compression which could be further utilised in improving the materials currently being utilised for patellar implants by making them more compliant. This could result in the implant performing more like actual cartilage during movement thus reducing the chance of pain related complications occurring.

Certain stages of the project can be improved, but it created the base for future work to expand on the idea of using kinematics for cartilage recreation and determining motion specific cartilage compression. Certain assumptions were made during the project in order to reduce the complexity of the process, however, even with these assumptions made, the model was still able to produce promising results which could be of great benefit in prosthesis design and injury management.

7 References

[1] T. M. G. J. van Eijden, E. Kouwenhoven, J. Verburg, and W. a. Weijs, "A Mathematical Model of the Patellofemoral Joint," *J. Biomech.*, vol. 19, no. 3, pp. 219–229, 1986.

[2] S. Hirokawa, "Three-Dimensional Mathematical Model Analysis of the Patellofemoral Joint," *J Biomech.*, vol. 24, no. 8, pp. 659–671, 1991.

[3] S. D. Kwak, W. W. Colman, and G. A. Ateshian, "Anatomy of the Human Patellofemoral Joint Articular Cartilage: Surface Curvature Analysis," *J. Orthop. Res.*, vol. 15, no. 3, pp. 468–472, 1997.

[4] A. Losch, F. Eckstein, and M. Haubner, "A Non-Invasive Technique for 3-Dimensional Assessment of Articular Cartilage Thickness Based on MRI Part 1: Development of a Computational Method," *Magn. Reson. Imaging*, vol. 15, no. 7, pp. 795–804, 1997.

[5] J. S. Wayne, C. W. Brodrick, and N. Mukherjee, "Measurement of Articular Cartilage Thickness in the Articulated Knee.," *Ann. Biomed. Eng.*, vol. 26, no. 1, pp. 96–102, 1998.

[6] D. E. Shepherd and B. B. Seedhom, "Thickness of Human Articular Cartilage in Joints of the Lower Limb," *Ann. Rheum. Dis.*, vol. 58, no. 1, pp. 27–34, 1999.

[7] Z. Cohen, D. McCarthy, D. Kwak, P. Legrand, F. Fogarasi, E. Ciaccio, and G. A. Ateshian, "Knee Cartilage Topography , Thickness , and Contact Areas from MRI : In-Vitro Calibration and In-Vivo Measurements," *J. Osteoarthr. Res. Soc. Int.*, vol. 7, pp. 95–109, 1999.

[8] H. U. Stäubli, U. Dürrenmatt, B. Porcellini, and W. Rauschning, "Anatomy and Surface Geometry of the Patellofemoral Joint in the Axial Plane.," *J. Bone Joint Surg. Br.*, vol. 81, no. 3, pp. 452–458, 1999.

[9] J. A. Feller, A. a. Amis, J. T. Andrish, E. a. Arendt, P. J. Erasmus, and C. M. Powers, "Surgical Biomechanics of the Patellofemoral Joint," *Arthrosc. J. Arthrosc. Relat. Surg.*, vol. 23, no. 5, pp. 542–553, 2007.

[10] O. S. Schindler, "Basic Kinematics and Biomechanics of the Patellofemoral Joint Part 2: The Patella in Total Knee Arthroplasty," *Acta Orthop. Belg.*, vol. 78, no. 1, pp. 11–29, 2012.

[11] C. K. Fitzpatrick, D. P. FitzPatrick, and D. D. Auger, "Size and Shape of the Resection Surface Geometry of the Osteoarthritic Knee in Relation to Total

Knee Replacement Design.," *J. Eng. Med.*, vol. 222, no. 6, pp. 923–932, 2008.

[12] P. S. Walker, J. M. Sussman-Fort, G. Yildirim, and J. Boyer, "Design Features of Total Knees for Achieving Normal Knee Motion Characteristics," *J. Arthroplasty*, vol. 24, no. 3, pp. 475–483, 2009.

[13] P. S. Walker, "Application of a Novel Design Method for Knee Replacements to Achieve Normal Mechanics," *Knee*, pp. 6–11, 2012.

[14] D. J. Berry, "Patellofemoral Arthroplasty in Arthritis Patients," vol. 6, no. 1, pp. 1–8, 2012.

[15] T. Luyckx, K. Didden, H. Vandenneucker, L. Labey, B. Innocenti, and J. Bellemans, "Is There a Biomechanical Explanation for Anterior Knee Pain in Patients with Patella Alta?," *J. Bone Jt. Surg. - Br. Vol.*, vol. 91-B, no. 3, pp. 344–350, 2009.

[16] S. Zffagnini, D. Dejour, and E. A. Arendt, *Patellofemoral Pain, Instability, and Arthritis*. 2010.

[17] M. Bollier and J. P. Fulkerson, "The Role of Trochlear Dysplasia in Patellofemoral Instability," *The Journal of the American Academy of Orthopaedic Surgeons*, vol. 19, no. 1. pp. 8–16, 2011.

[18] C. K. Fitzpatrick, M. a. Baldwin, P. J. Laz, D. P. FitzPatrick, A. L. Lerner, and P. J. Rullkoetter, "Development of a Statistical Shape Model of the Patellofemoral Joint for Investigating Relationships between Shape and Function," *J. Biomech.*, vol. 44, no. 13, pp. 2446–2452, 2011.

[19] L. M. Smoger, C. K. Fitzpatrick, C. W. Clary, A. J. Cyr, L. P. Maletsky, P. J. Rullkoetter, and P. J. Laz, "Statistical Modeling to Characterize Relationships between Knee Anatomy and Kinematics," *J. Orthop. Res.*, vol. 33, no. 11, pp. 1620–1630, 2015.

[20] G. Wibeeg, "Roentgenographs and Anatomic Studies on the Femoropatellar Joint : With Special Reference to Chondromalacia Patellae," *Acta Orthop Scand*, vol. 12, no. May, pp. 319–410, 1941.

[21] A. M. Ahmed, D. L. Burke, and A. Hyder, "Force Analysis of the Patellar Mechanism," *J. Orthop. Res.*, vol. 5, pp. 69–85, 1987.

[22] F. Eckstein, B. Lemberger, T. Stammberger, K. H. Englmeier, and M. Reiser, "Patellar Cartilage Deformation In Vivo after Static versus Dynamic Loading," *J. Biomech.*, vol. 33, pp. 819–825, 2000.

[23] S.-K. S.-K. Han, S. Federico, M. Epstein, and W. Herzog, "An Articular Cartilage Contact Model Based on Real Surface Geometry," *J. Biomech.*, vol. 38, no. 1, pp. 179–184, 2005.

[24] J. H. Yoo, S. R. Yi, and J. H. Kim, "The Geometry of Patella and Patellar Tendon Measured on Knee MRI," *Surg. Radiol. Anat.*, vol. 29, no. 8, pp. 623–628, 2007.

[25] I. McEwan, L. Herrington, and J. Thom, "The Validity of Clinical Measures of Patella Position," *Man. Ther.*, vol. 12, no. 3, pp. 226–230, 2007.

[26] C. L. Phillips, D. a T. Silver, P. J. Schranz, and V. Mandalia, "The Measurement of Patellar Height: a Review of the Methods of Imaging.," *J. Bone Joint Surg. Br.*, vol. 92, no. 8, pp. 1045–1053, 2010.

[27] A. Fox, F. Wanivenhaus, and S. Rodeo, "The Basic Science of the Patella: Structure, Composition, and Function," *J. Knee Surg.*, vol. 25, no. 02, pp. 127–142, 2012.

[28] M. D. Ellington, B. N. Robin, D. C. Jupiter, and B. C. Allen, "Plateau-Patella Angle in Evaluation of Patellar Height in Osteoarthritis," *Knee*, vol. 21, pp. 699–702, 2014.

[29] P. Raux, P. Townsend, R. Miegel, R. Rose, and E. Radin, "Trabecular Architecture of the Human Patella," *J. Biomech.*, vol. 8, pp. 1–7, 1975.

[30] G. E. Kempson, H. Muir, C. Pollard, and M. Tuke, "The Tensile Properties of the Cartilage of the Human Femoral Condyles Related to the Content of Collagen and Glycosaminoglycans," *Biochim. Biophys. Acta*, vol. 297, pp. 456–472, 1973.

[31] M. I. Froimson, A. Ratcliffe, T. R. Gardner, and V. Mow, "Differences in Patellofemoral Joint Cartilage Material Properties and their Significance to the Etiology of Cartilage Surface Fibrillation," *Osteoarthr. Cartil.*, vol. 5, pp. 377–386, 1997.

[32] D. Elliott, S. Kydd, C. Perry, and L. Setton, "Direct Measurement of the Poisson's Ratio of Human Articular Cartilage in Tension," 1999.

[33] C. Herberhold, S. Faber, T. Stammberger, M. Steinlechner, R. Putz, K. H. Englmeier, M. Reiser, and F. Eckstein, "In situ Measurement of Articular Cartilage Deformation in Intact Femoropatellar Joints under Static Loading," *J. Biomech.*, vol. 32, pp. 1287–1295, 1999.

[34] R. Andresen, S. Radmer, H. König, D. Banzer, K. Wolf, S. Radmer, H. König, D. Banzer, and K. Wolf, "MR Diagnosis of Retropatellar Chondral Lesions Under Compression," *Acta radiol.*, vol. 37, pp. 91–97, 1996.

[35] T. Stammberger, F. Eckstein, K. Englmeier, and M. Reiser, "Determination of 3D Cartilage Thickness Data From MR Imaging : Computational Method and Reproducibility in the Living," *Magn. Reson. Med.*, vol. 41, pp. 529–536, 1999.

[36] Y. Wilkie and C. Kerr, "Knee Stability," 2010. [Online]. Available: http://kneestability.weebly.com/index.html. [Accessed: 28-Jul-2016].

[37] J. P. Goldblatt and J. C. Richmond, "Anatomy and Biomechanics of the Knee," *Oper. Tech. Sports Med.*, vol. 11, no. 3, pp. 172–186, 2003.

[38] J. Rich, D. E. Dean, and R. H. Powers, *Forensic Medicine of the lower Extremity: Human Identification and Trauma Analysis of the thigh, leg, and foot*. Totowa: The Humana Press Inc.

[39] Barnard Health Care - Forensic Radiology, "Bony Landmarks Femur and Tibia," 2016. [Online]. Available: http://www.barnardhealth.us/forensic-radiology/femur.html. [Accessed: 29-Jul-2016].

[40] Dictionary.com, "Ligament," *Dictionary.com*, 2016. [Online]. Available: http://www.dictionary.com/browse/ligament. [Accessed: 29-Jul-2016].

[41] Dictionary.com, "Tendon," *Dictionary.com*, 2016. [Online]. Available: http://www.dictionary.com/browse/tendon?s=t. [Accessed: 29-Jul-2016].

[42] Epomedicine, "Applied Anatomy of the Knee Joint," *Epomedicine*, 2016. [Online]. Available: http://epomedicine.com/medical-students/applied-anatomy-of-knee-joint/. [Accessed: 29-Jul-2016].

[43] K. Tecklenburg, D. Dejour, C. Hoser, and C. Fink, "Bony and Cartilaginous Anatomy of the Patellofemoral Joint," *Knee Surgery, Sport. Traumatol. Arthrosc.*, vol. 14, no. 3, pp. 235–240, 2006.

[44] S. D. Masouros, A. M. J. Bull, and A. A. Amis, "Biomechanics of the Knee Joint," *Orthop. Trauma*, vol. 24, no. 2, pp. 84–91, 2016.

[45] A. M. Ahmed, D. L. Burke, and A. Hyder, "Force Analysis of the Patellar Mechanism.," *J. Orthop. Res.*, vol. 5, pp. 69–85, 1987.

[46] G. a Ateshian, W. H. Warden, J. J. Kim, R. P. Grelsamer, and V. C. Mow, "Finite Deformation Biphasic Material Properties of Bovine Articular

Cartilage from Confined Compression Experiments," *J. Biomech.*, vol. 30, no. 97, pp. 1157–1164, 1997.

[47] J. H. Brechter and C. M. Powers, "Patellofemoral Stress During Walking in Persons with and without Patellofemoral Pain," *Med. Sci. Sports Exerc.*, vol. 34, no. 10, pp. 1582–1593, 2002.

[48] G. a. Ateshian, L. J. Soslowsky, and V. C. Mow, "Quantitation of Articular Surface Topography and Cartilage Thickness in Knee Joints using Stereophotogrammetry," *J. Biomech.*, vol. 24, no. 8, pp. 761–776, 1991.

[49] L. Enzor, "Chondrocytes: Definition & Function," *Study.com*. [Online]. Available: http://study.com/academy/lesson/chondrocytes-definition-function-quiz.html. [Accessed: 03-Aug-2016].

[50] Farlex Partner Medical Dictionary, "Proteoglycan," *Farlex Inc*, 2012. [Online]. Available: http://medical-dictionary.thefreedictionary.com/proteoglycan. [Accessed: 03-Aug-2016].

[51] K. E. Kadler, D. F. Holmes, J. a Trotter, and J. a Chapman, "Collagen Fibril Formation," *J. Biochem.*, vol. 316, pp. 1–11, 1996.

[52] S. Pal, "Mechanical Properties of Biological Materials," in *Design of Artificial Human Joints & Organs*, 1st ed., New York: Springer US, 2014, pp. 23–40.

[53] G. E. Kempson, M. a. R. Freeman, and S. a. V. Swanson, "The Determination of a Creep Modulus for Articular Cartilage from Indentation Test on the Human Femoral Head," *J. Biomech.*, vol. 4, pp. 239–250, 1971.

[54] W. C. Hayes, L. M. Keer, G. Herrmann, and L. F. Mockros, "A Mathematical Analysis for Indentation Tests of Articular Cartilage," *J. Biomech.*, vol. 5, pp. 541–551, 1972.

[55] R. Y. Hori and L. F. Mockros, "Indentation Tests of Human Articular Cartilage," *J. Biomech.*, vol. 9, pp. 259–268, 1976.

[56] G. E. Kempson, C. J. Spivey, S. a V Swanson, and M. a R. Freeman, "Patterns of Cartilage Stiffness on Normal and Degenerate Human Femoral Heads," *J. Biomech.*, vol. 4, pp. 597–609, 1971.

[57] Farlex Partner Medical Dictionary, *Radiograph*. Farlex, 2012.

[58] North Central Surgical Center, "What's the difference betwen an X-ray, CT scan and MRI?," 2015. [Online]. Available:

http://www.northcentralsurgical.com/blog/whats-the-difference-between-an-x-ray-ct-scan-and-mri-140.html. [Accessed: 04-Aug-2016].

[59] Materialise, "Mimics 16.0." [Online]. Available: http://biomedical.materialise.com/mimics. [Accessed: 05-Aug-2016].

[60] MSC software Corporation, "Adams," *MSC Software*. USA.

[61] K. Nishimura, T. Tanabe, M. Kimura, A. Harasawa, K. Karita, and T. Matsushita, "Measurement of Articular Cartilage Volumes in the Normal Knee by Magnetic Resonance Imaging: Can Cartilage Volumes be Estimated from Physical Characteristics?," *J. Orthop. Sci.*, vol. 10, pp. 246–252, 2005.

[62] F. Eckstein, J. Westhoff, H. Sittek, K.-P. Maag, M. Haubner, S. Faber, K.-H. Englmeier, and M. Reiser, "In Vivo Reproducibility of Three Dimensional Cartilage Volume and Thickness with MR Imaging," *Am. J. Roentgenol.*, vol. 170, no. 3, pp. 593–597, 1998.

[63] P. A. Hardy, P. Nammalwar, and S. Kuo, "Measuring the Thickness of Articular Cartilage from MR Images," *J. Magn. Reson. Imaging*, vol. 13, no. 1, pp. 120–126, 2001.

[64] M. Boocock, P. McNair, F. Cicuttini, A. Stuart, and T. Sinclair, "The Short-Term Effects of Running on the Deformation of Knee Articular Cartilage and its Relationship to Biomechanical Loads at the Knee," *Osteoarthr. Cartil.*, vol. 17, no. 7, pp. 883–890, 2009.

[65] C. Herberhold, T. Stammberger, S. Faber, R. Putz, K. Englmeier, M. Reiser, and F. Eckstein, "An MR-Based Technique for Quantifying the Deformation of Articular Cartilage During Mechanical Loading in an Intact Cadaver Joint," *Magn. Reson. Med.*, vol. 39, no. 5, pp. 843–850, 1998.

[66] H. Delport, L. Labey, B. Innocenti, and J. Bellemans, "Restoration of Constitutional Alignment in TKA Leads to More Physiological Strains in the Collateral Ligaments," *Knee Surgery, Sport. Traumatol. Arthrosc.*, vol. 23, pp. 2159–2169, 2015.

[67] F. Marin, N. Hoang, P. Aufaure, and M. C. Ho Ba Tho, "In-Vivo Intersegmental Motion of the Cervical Spine using an Inverse Kinematics Procedure," *Clin. Biomech.*, vol. 25, no. 5, pp. 389–396, 2010.

[68] C. S. Shin, A. M. Chaudhari, and T. P. Andriacchi, "The Effect of Isolated Valgus Moments on ACL Strain during Single-Leg Landing: A Simulation Study," *J. Biomech.*, vol. 42, no. 3, pp. 280–285, 2009.

[69] Cape Ortho & Spine, “Cape Ortho & Spine: Hip & Knee,” 2010. [Online]. Available: http://capeortho-spine.co.za/doctorgroup/hip-and-knee/. [Accessed: 27-Jul-2016].

[70] R. C. Schafer, “Body Alignment, Posture, and Gait,” in *Clinical Biomechanics: Musculoskeletal Actions and Reactions*, 2nd Editio., Williams & Wilkins, 1987.

[71] N. Joseph, “Film Critique of the Lower Extremity - Part 2,” 2006. [Online]. Available: https://www.ceessentials.net/article27.html. [Accessed: 04-Aug-2016].

[72] A. J. Towbin, “Radiology,” 2009. [Online]. Available: http://blog.cincinnatichildrens.org/radiology/difference-between-mri-and-ct/. [Accessed: 04-Aug-2016].

Appendix A Segmented Cartilage Thickness Charts

A.1 Knee 1 – Model S120331

Femur:

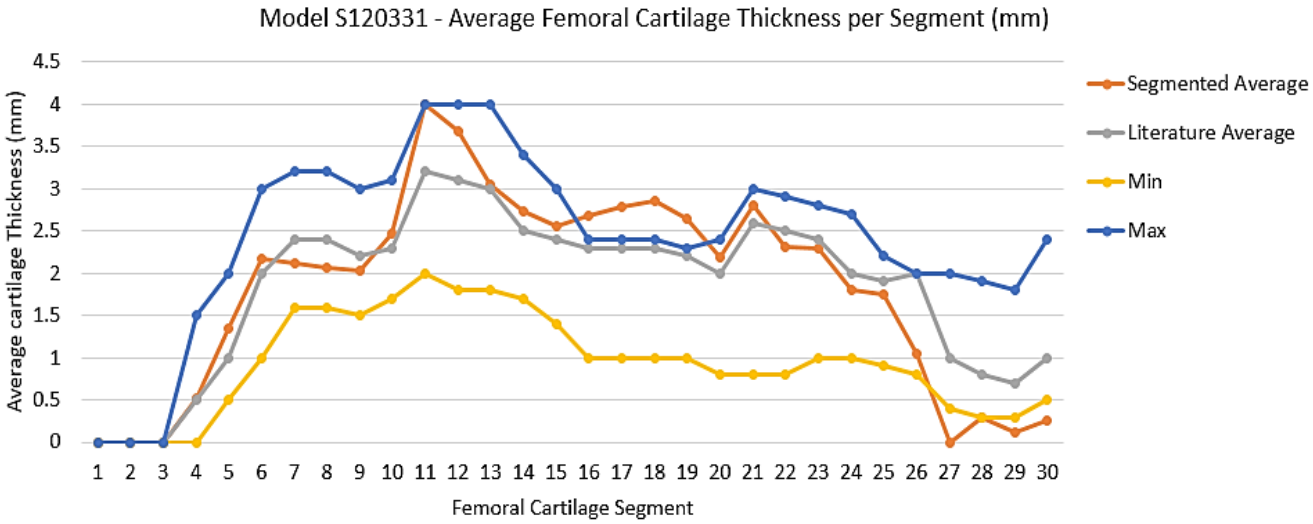

Figure 66: Chart comparing the average, minimum and maximum cartilage thickness per section as found in literature, to the average cartilage thickness of knee 1 segmented from the MRI data for the femur.

A.2 Knee 2 - Model S120324

Femur:

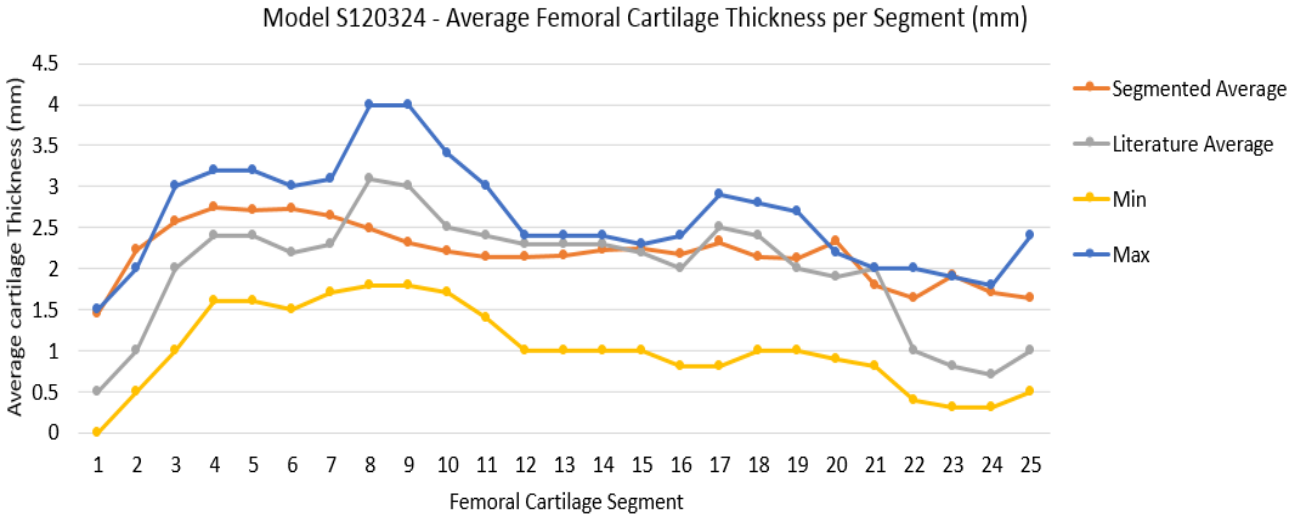

Figure 67: Chart comparing the average, minimum and maximum cartilage thickness per section as found in literature, to the average cartilage thickness of knee 2 segmented from the MRI data for the femur

Appendix B Average Cartilage Thickness Results per Section (mm)

B.1 Raw and Unfiltered Data – Knee 1

Table 11: Average Patellar Cartilage Thickness (mm) Results per Section - Raw Unfiltered Data (Knee 1)

	Model 1.1		Model 1.2	
Section	**Passive**	**Squat**	**Passive**	**Squat**
1	1.656	0.539	2.279	1.642
2	1.923	0.731	2.355	1.776
3	2.320	1.020	2.546	2.098
4	2.844	1.554	2.935	2.410
5	3.371	2.050	3.423	2.983
6	3.053	1.837	3.410	2.855
7	2.247	1.314	2.491	2.187
8	0.939	0.763	1.583	1.434
9	0.384	0.674	0.952	1.231
Average	**2.082**	**1.165**	**2.442**	**2.068**

Table 12: Sectional average error and standard deviation for the estimated patellar cartilage thickness of knee 1, model 1.1 of the passive and squat motions (Unfiltered).

	Passive		Squat	
Section	**Average Error (mm)**	**Standard Deviation (mm)**	**Average Error (mm)**	**Standard Deviation (mm)**
1	0.25	0.93	0.32	1.19
2	0.23	0.95	0.29	1.2
3	0.15	0.66	0.2	0.87
4	0.19	0.89	0.25	1.15
5	0.19	0.83	0.22	1
6	0.32	1.44	0.32	1.43
7	0.18	0.79	0.27	1.16
8	0.09	0.36	0.21	0.87
9	0.13	0.51	0.21	0.82
Average	**0.19**	**0.82**	**0.25**	**1.08**

Table 13: Sectional average error and standard deviation for the estimated patellar cartilage thickness of knee 1, model 1.2 of the passive and squat motions (Unfiltered).

	Passive		Squat	
Section	**Average Error (mm)**	**Standard Deviation (mm)**	**Average Error (mm)**	**Standard Deviation (mm)**
1	0.21	0.78	0.24	0.88
2	0.21	0.87	0.22	0.91
3	0.14	0.63	0.17	0.75
4	0.18	0.82	0.18	0.84
5	0.2	0.89	0.25	1.11
6	0.34	1.52	0.42	1.87
7	0.3	1.3	0.33	1.43
8	0.23	0.94	0.24	0.98
9	0.22	0.87	0.29	1.12
Average	**0.23**	**0.96**	**0.26**	**1.10**

B.2 Raw and Unfiltered Data – Knee 2

Table 14: Average Patellar Cartilage Thickness (mm) Results per Section - Raw Unfiltered Data (Knee 2)

	Model 2.1		Model 2.2	
Section	**Passive**	**Squat**	**Passive**	**Squat**
1	1.066	0.857	2.059	2.162
2	1.403	1.046	2.658	2.463
3	1.763	1.375	3.121	2.840
4	2.446	1.768	3.471	3.352
5	2.449	1.858	3.766	3.553
6	2.186	1.695	3.615	3.445
7	1.783	1.370	2.923	2.929
8	1.489	1.292	2.777	2.800
9	1.136	1.324	1.694	2.655
Average	**1.747**	**1.398**	**2.898**	**2.911**

Table 15: Sectional average error and standard deviation for the estimated patellar cartilage thickness of knee 2, model 2.1 of the passive and squat motions (Unfiltered).

	Passive		Squat	
Section	**Average Error (mm)**	**Standard Deviation (mm)**	**Average Error (mm)**	**Standard Deviation (mm)**
1	0.19	0.81	0.16	0.7
2	0.18	0.77	0.22	0.97
3	0.18	0.83	0.16	0.73
4	0.23	1.11	0.13	0.63
5	0.23	1.11	0.14	0.68
6	0.23	1.11	0.16	0.78
7	0.24	1.15	0.16	0.76
8	0.19	0.85	0.18	0.81
9	0.19	0.89	0.27	1.23
Average	**0.21**	**0.96**	**0.18**	**0.81**

Table 16: Sectional average error and standard deviation for the estimated patellar cartilage thickness of knee 2, model 2.2 of the passive and squat motions (Unfiltered).

	Passive		Squat	
Section	**Average Error (mm)**	**Standard Deviation (mm)**	**Average Error (mm)**	**Standard Deviation (mm)**
1	0.25	1.08	0.22	0.95
2	0.22	0.94	0.22	0.94
3	0.2	0.94	0.19	0.87
4	0.15	0.73	0.17	0.84
5	0.18	0.85	0.13	0.62
6	0.2	0.94	0.13	0.65
7	0.2	0.97	0.17	0.79
8	0.18	0.85	0.11	0.49
9	0.16	0.75	0.23	1.05
Average	**0.19**	**0.89**	**0.17**	**0.8**

B.3 Filtered and Smoothed Data – Knee 1 and Knee 2

Table 17: Average Patellar Cartilage Thickness (mm) Results per Section - Smoothed and Filtered Data (Knee 1 and 2)

	Knee 1			Knee 2		
Section	**Passive**	**Squat**	**Uncompressed**	**Passive**	**Squat**	**Uncompressed**
1	2.059	0.544	2.592	1.061	0.905	1.345
2	2.018	0.643	3.201	1.275	0.936	1.678
3	1.916	0.653	3.481	1.627	1.262	2.064
4	2.052	0.9	3.955	2.030	1.698	2.755
5	2.670	1.473	4.696	2.074	1.713	2.967
6	2.455	1.278	4.681	1.820	1.562	2.892
7	1.702	0.432	4.353	1.478	1.212	2.448
8	0.832	0	3.576	1.360	1.045	2.258
9	0.234	0	2.380	0.959	0.924	1.724
Average	***1.771***	***0.658***	***3.657***	***1.520***	***1.251***	***2.237***

Table 18: Sectional average error and standard deviation for the estimated patellar cartilage thickness of knee 1, model 1.1 of the passive and squat motions (Filtered).

	Passive		**Squat**	
Section	**Average Error (mm)**	**Standard Deviation (mm)**	**Average Error (mm)**	**Standard Deviation (mm)**
1	0.15	0.56	0.21	0.78
2	0.17	0.72	0.23	0.94
3	0.17	0.75	0.26	1.12
4	0.2	0.89	0.27	1.24
5	0.16	0.71	0.26	1.18
6	0.19	0.85	0.23	1.03
7	0.16	0.69	0.19	0.84
8	0.12	0.5	0.2	0.84
9	0.08	0.3	0.19	0.75
Average	**0.16**	**0.66**	**0.23**	**0.97**

Table 19: Sectional average error and standard deviation for the estimated patellar cartilage thickness of knee 2, model 2.1 of the passive and squat motions (Filtered).

	Passive		Squat	
Section	**Average Error (mm)**	**Standard Deviation (mm)**	**Average Error (mm)**	**Standard Deviation (mm)**
1	0.12	0.46	0.12	0.41
2	0.14	0.51	0.14	0.56
3	0.13	0.5	0.12	0.48
4	0.12	0.54	0.11	0.45
5	0.14	0.62	0.13	0.55
6	0.14	0.64	0.15	0.68
7	0.15	0.71	0.22	0.89
8	0.16	0.7	0.22	0.83
9	0.15	0.66	0.25	1.07
Average	**0.14**	**0.59**	**0.16**	**0.66**

Appendix C Contact Areas

C.1 Knee 1 - Passive

30 degrees flexion

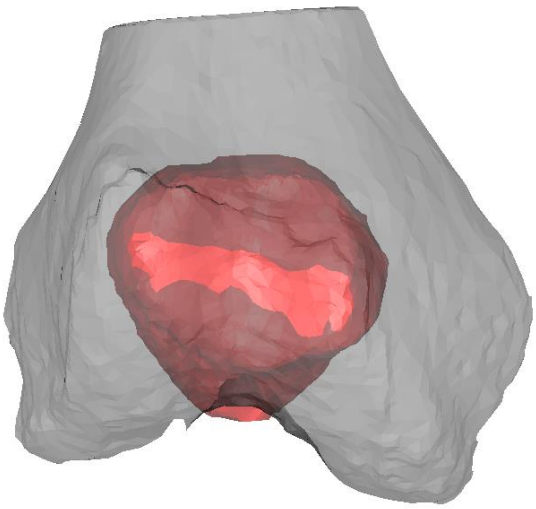

60 degrees flexion

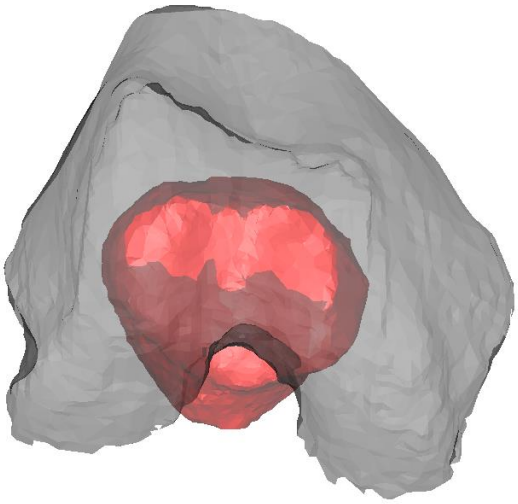

90 degrees flexion

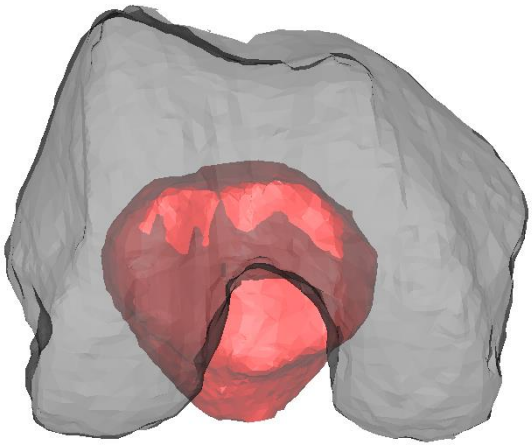

Maximum degrees flexion

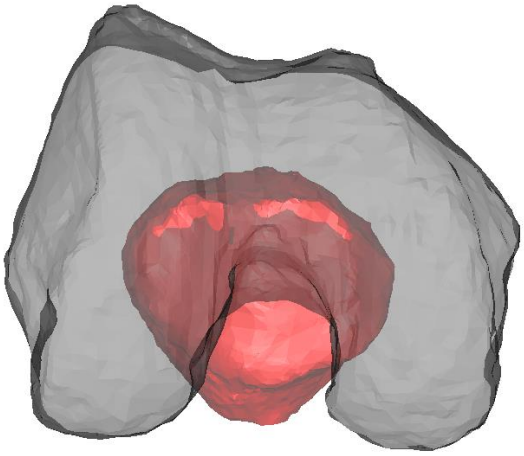

Figure 68: Estimated patellofemoral contact areas for the passive movement of knee 1 for actual degrees of flexion 30, 60, 90, and maximum.

C.2 Knee 1 – Squat

30 degrees flexion

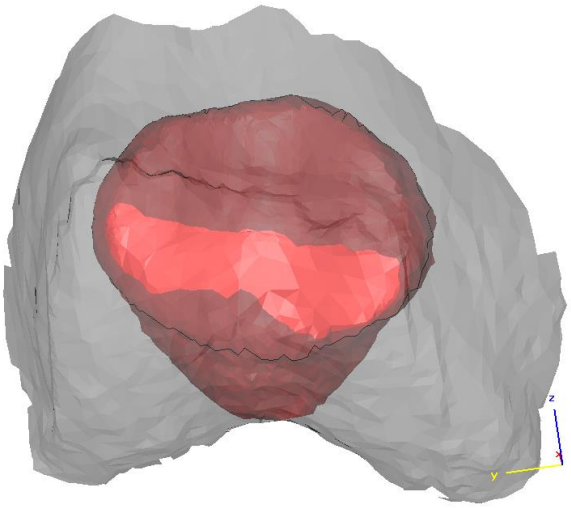

60 degrees flexion

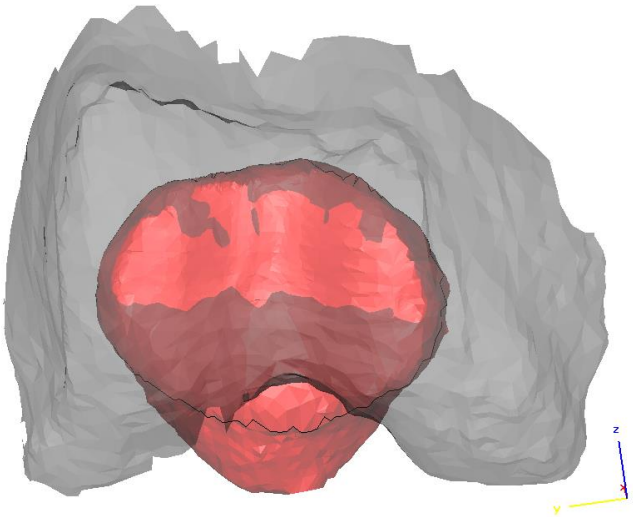

90 degrees flexion

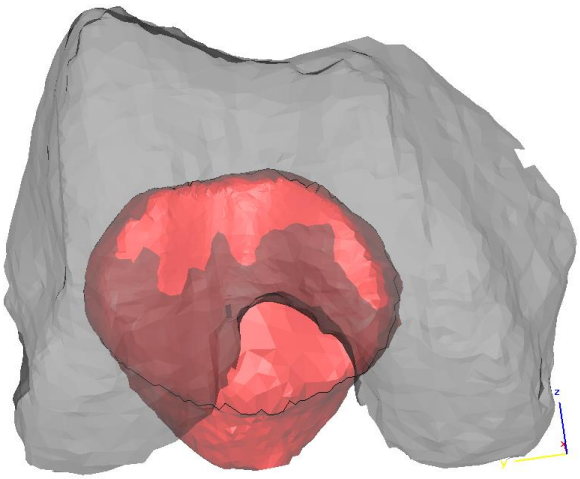

Maximum degrees flexion

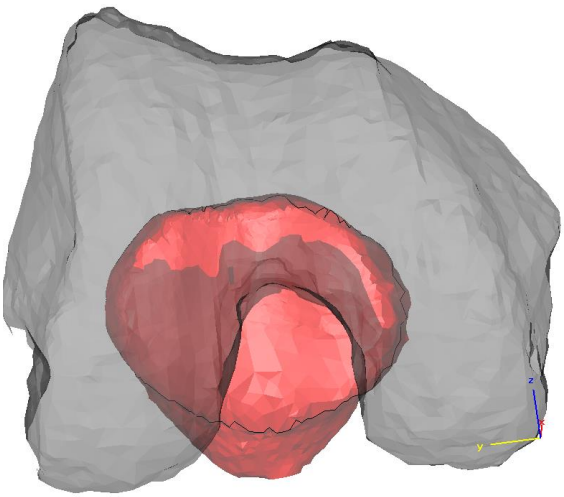

Figure 69: Estimated patellofemoral contact areas for the squat movement of knee 1 for actual degrees of flexion 30, 60, 90, and maximum.

C.3 Knee 2 – Passive

30 degrees flexion

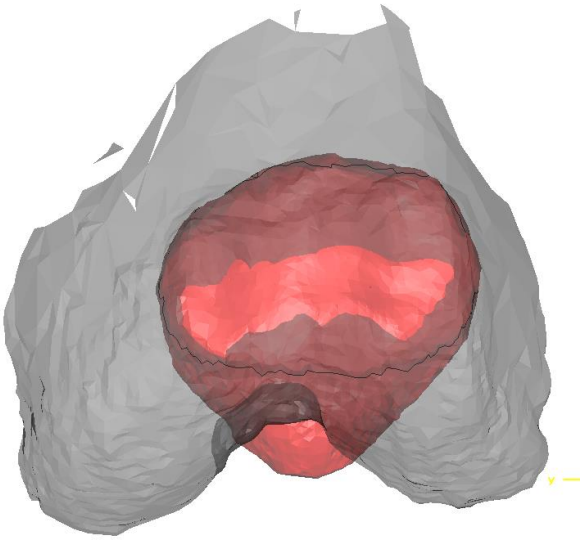

60 degrees flexion

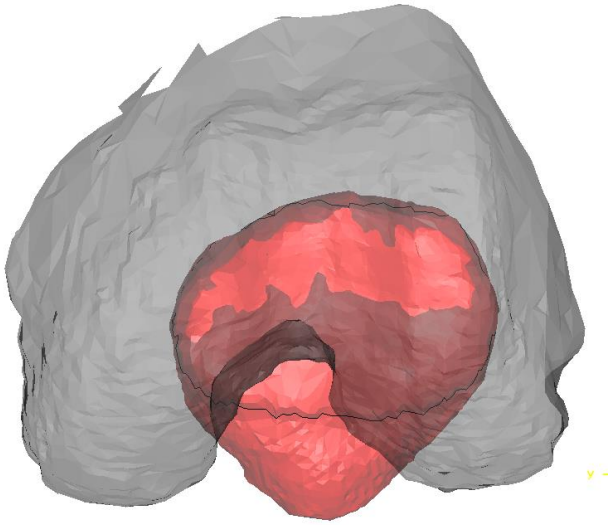

90 degrees flexion

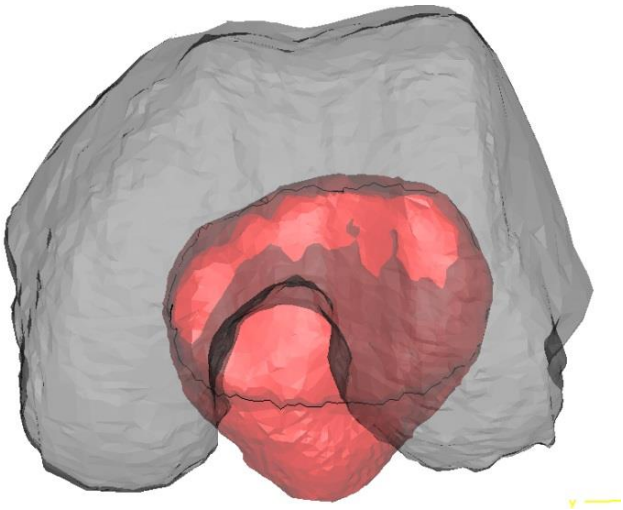

Maximum degrees flexion

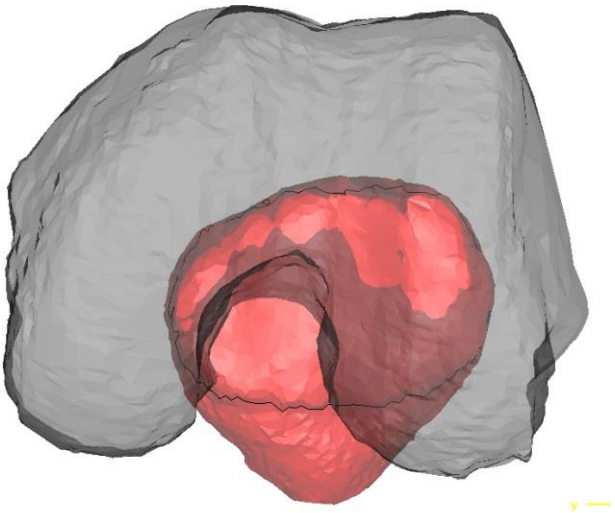

Figure 70: Estimated patellofemoral contact areas for the passive movement of knee 2 for actual degrees of flexion 30, 60, 90, and maximum.

C.4 Knee 2 – Squat

30 degrees flexion

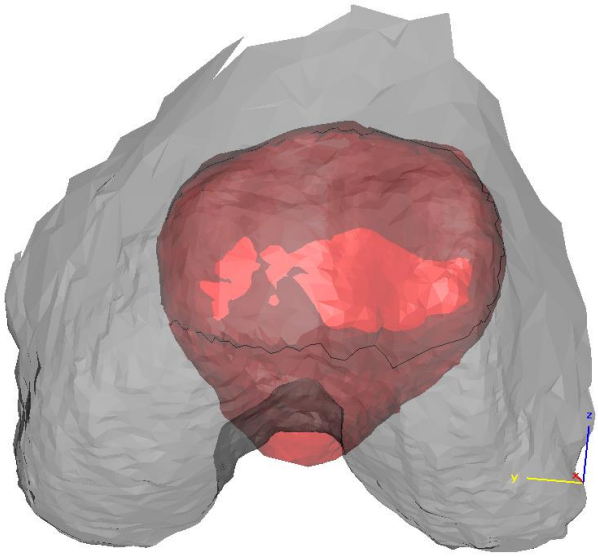

60 degrees flexion

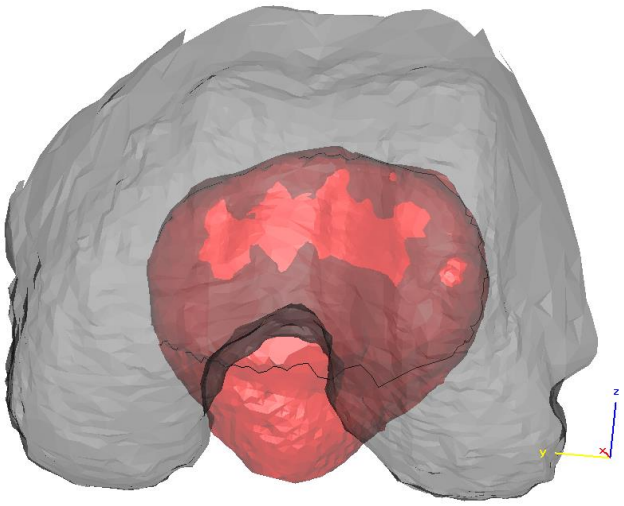

90 degrees flexion

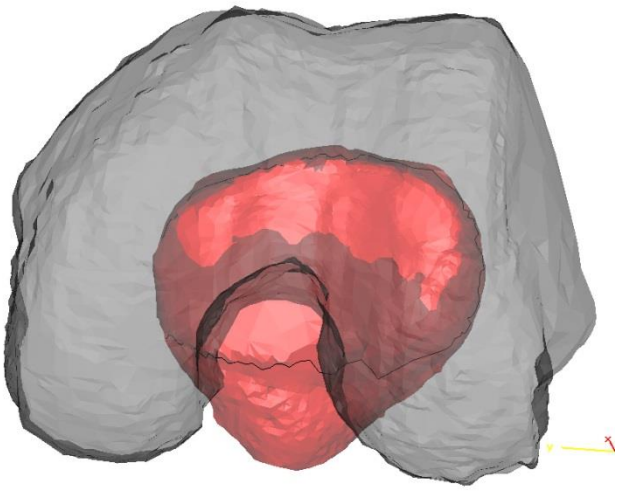

Maximum degrees flexion

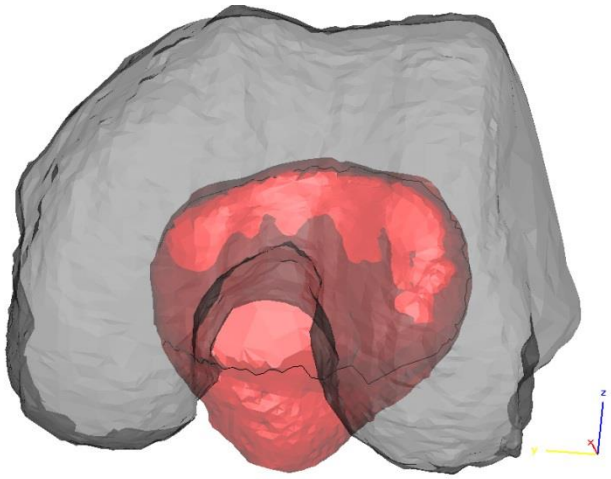

Figure 71: Estimated patellofemoral contact areas for the squat movement of knee 2 for actual degrees of flexion 30, 60, 90, and maximum.

Appendix D Sectional Compression Results

D.1 Sectional Compression Results – Knee 1 and 2

Table 20: Sectional patellar cartilage compression (mm) results for knee 1 and knee 2 for their passive and squat movements.

	Knee 1		Knee 2	
Section	**Passive**	**Squat**	**Passive**	**Squat**
1	0.533	2.048	0.322	0.594
2	1.183	2.557	0.413	0.666
3	1.565	2.828	0.593	0.958
4	1.903	3.055	0.811	1.263
5	2.027	3.223	1.012	1.391
6	2.226	3.403	1.074	1.325
7	2.652	3.922	1.045	1.207
8	2.744	3.871	0.843	1.140
9	2.146	3.264	0.780	0.796
Average Compression (mm)	1.87	3.13	0.766	1.038
Average Compression (%)	51.13	85.58	34.24	46.40

D.2 Average Value Compression Results per Section - Knee 1

Table 21: Sectional average errors and standard deviations for the estimated patellar cartilage compression of knee 1, model 1.1 of the passive and squat motions (Filtered).

	Passive		Squat	
Section	**Average Error (mm)**	**Standard Deviation (mm)**	**Average Error (mm)**	**Standard Deviation (mm)**
1	0.11	0.39	0.13	0.49
2	0.15	0.62	0.23	0.96
3	0.16	0.7	0.27	1.17
4	0.18	0.75	0.27	1.25
5	0.21	0.92	0.29	1.29
6	0.21	0.96	0.31	1.37
7	0.18	0.79	0.25	1.07
8	0.2	0.81	0.27	1.13
9	0.23	0.89	0.34	1.3
Average	**0.18**	**0.76**	**0.26**	**1.11**

D.3 Average Value Compression Results per Section - Knee 2

Table 22: Sectional average errors and standard deviations for the estimated patellar cartilage compression of knee 2, model 2.1 of the passive and squat motions (Filtered).

	Passive		Squat	
Section	**Average Error (mm)**	**Standard Deviation (mm)**	**Average Error (mm)**	**Standard Deviation (mm)**
1	0.04	0.17	0.07	0.24
2	0.07	0.24	0.08	0.32
3	0.07	0.29	0.1	0.42
4	0.09	0.4	0.13	0.55
5	0.1	0.42	0.12	0.51
6	0.09	0.39	0.1	0.46
7	0.08	0.35	0.08	0.35
8	0.07	0.3	0.07	0.27
9	0.07	0.32	0.12	0.5
Average	**0.08**	**0.32**	**0.10**	**0.40**

Appendix E FEM Analysis Stress Results

E.1 Knee 1 – Passive Movement

Table 23: Stress results from FEM analysis for the passive movement of knee 1 at *E* = 8 MPa showing the stress on the cartilage and osseous surfaces.

Passive Stress (MPa)							
		E = 8 MPa					
Degree of flexion	Average Adapted Compression (mm)	*v* = 0.4		*v* = 0.45		*v* = 0.48	
		Cartilage surface	Osseous Surface	Cartilage surface	Osseous Surface	Cartilage surface	Osseous Surface
0	-	-	-	-	-	-	-
30	1.39	1.959	1.469	2.135	1.6	2.2	2.75
60	0.78	1.565	1.77	2.205	2.405	2.575	2.825
90	0.32	0.874	0.884	1.02	1.065	1.174	1.344
Max	-	-	-	-	-	-	-

Table 24: Stress results from FEM analysis for the passive movement of knee 1 at E = 10 MPa showing the stress on the cartilage and osseous surfaces.

Passive Stress (MPa)							
		E = 10 MPa					
Degree of flexion	Average Adapted Compression (mm)	*v* = 0.4		*v* = 0.45		*v* = 0.48	
		Cartilage surface	Osseous Surface	Cartilage surface	Osseous Surface	Cartilage surface	Osseous Surface
0	-	-	-	-	-	-	-
30	1.39	2.11	2.445	2.5	2.665	2.745	3.435
60	0.78	1.955	1.965	2.465	2.62	3.09	3.18
90	0.32	1.093	1.123	1.274	1.369	1.467	1.622
Max	-	-	-	-	-	-	-

Table 25: Stress results from FEM analysis for the passive movement of knee 1 at E = 12 MPa showing the stress on the cartilage and osseous surfaces.

Passive Stress (MPa)							
		E = 12 MPa					
Degree of flexion	Average Adapted Compression (mm)	v = 0.4		v = 0.45		v = 0.48	
		Cartilage surface	Osseous Surface	Cartilage surface	Osseous Surface	Cartilage surface	Osseous Surface
0	-	-	-	-	-	-	-
30	1.39	2.735	2.935	3.2	4	3.3	4.125
60	0.78	2.345	2.355	2.955	2.985	3.705	3.785
90	0.32	1.313	1.328	1.528	1.688	1.761	1.951
Max	-	-	-	-	-	-	-

E.2 Knee 1 – Squat Movement

Table 26: Stress results from FEM analysis for the squat movement of knee 1 at E = 8 MPa showing the stress on the cartilage and osseous surfaces.

Squat Stress (MPa)							
		E = 8 MPa					
Degree of flexion	Average Adapted Compression (mm)	ν = 0.4		ν = 0.45		ν = 0.48	
		Cartilage surface	Osseous Surface	Cartilage surface	Osseous Surface	Cartilage surface	Osseous Surface
0	2.26	4.575	4.695	5.205	5.325	5.8	6.05
30	1.9	2.555	2.69	2.875	3.12	3.195	3.55
60	1.39	4.165	4.19	5.025	5.11	6	6.1
90	-	-	-	-	-	-	-
Max	1.24	2.165	2.42	2.455	2.595	2.745	2.945

Table 27: Stress results from FEM analysis for the squat movement of knee 1 at E = 10 MPa showing the stress on the cartilage and osseous surfaces.

Squat Stress (MPa)							
		E = 10 MPa					
Degree of flexion	Average Adapted Compression (mm)	ν = 0.4		ν = 0.45		ν = 0.48	
		Cartilage surface	Osseous Surface	Cartilage surface	Osseous Surface	Cartilage surface	Osseous Surface
0	2.26	5.715	5.835	6.505	6.62	7.265	7.565
30	1.9	3.185	3.32	3.585	3.795	3.985	4.295
60	1.39	5.215	5.31	6.28	6.395	7.475	7.675
90	-	-	-	-	-	-	-
Max	1.24	2.705	2.79	3.065	3.165	3.435	3.625

Table 28: Stress results from FEM analysis for the squat movement of knee 1 at E = 12 MPa showing the stress on the cartilage and osseous surfaces.

Squat Stress (MPa)							
		E = 12 MPa					
Degree of flexion	Average Adapted Compression (mm)	v = 0.4		v = 0.45		v = 0.48	
		Cartilage surface	Osseous Surface	Cartilage surface	Osseous Surface	Cartilage surface	Osseous Surface
0	2.26	6.865	7.015	7.805	7.955	8.725	8.975
30	1.9	3.825	3.925	4.305	4.53	4.785	5.345
60	1.39	6.255	6.265	7.535	7.685	9	9.125
90	-	-	-	-	-	-	-
Max	1.24	3.255	3.265	3.68	3.925	4.12	4.265

E.3 Knee 2 – Passive Movement

Table 29: Stress results from FEM analysis for the passive movement of knee 2 at E = 8 MPa showing the stress on the cartilage and osseous surfaces.

Passive Stress (MPa)							
		E = 8 MPa					
Degree of flexion	Average Adapted Compression (mm)	ν = 0.4		ν = 0.45		ν = 0.48	
		Cartilage surface	Osseous Surface	Cartilage surface	Osseous Surface	Cartilage surface	Osseous Surface
0	-	-	-	-	-	-	-
30	0.520	2.25	3.15	3.045	3.35	3.585	3.81
60	0.319	0.987	1.182	1.1395	1.37	1.561	1.826
90	0.184	1.094	1.209	1.219	1.329	1.651	1.796
Max	0.169	1.012	1.127	1.131	1.241	1.525	1.67

Table 30: Stress results from FEM analysis for the passive movement of knee 2 at E = 10 MPa showing the stress on the cartilage and osseous surfaces.

Passive Stress (MPa)							
		E = 10 MPa					
Degree of flexion	Average Adapted Compression (mm)	ν = 0.4		ν = 0.45		ν = 0.48	
		Cartilage surface	Osseous Surface	Cartilage surface	Osseous Surface	Cartilage surface	Osseous Surface
0	-	-	-	-	-	-	-
30	0.520	2.815	3.215	3.15	3.255	4.485	4.68
60	0.319	1.543	1.793	1.776	2.021	2.438	2.758
90	0.184	1.363	1.508	1.525	1.695	2.065	2.41
Max	0.169	1.263	1.408	1.412	1.582	1.908	2.253

Table 31: Stress results from FEM analysis for the passive movement of knee 2 at E = 12 MPa showing the stress on the cartilage and osseous surfaces.

Passive Stress (MPa)							
		E = 12 MPa					
Degree of flexion	Average Adapted Compression (mm)	v = 0.4		v = 0.45		v = 0.48	
		Cartilage surface	Osseous Surface	Cartilage surface	Osseous Surface	Cartilage surface	Osseous Surface
0	-	-	-	-	-	-	-
30	0.520	3.375	3.725	4.57	4.675	6.745	6.92
60	0.319	1.85	2.105	2.132	2.407	2.925	3.155
90	0.184	1.958	2.093	2.196	2.356	2.478	2.693
Max	0.169	1.513	1.663	2.029	2.169	2.292	2.512

E.4 Knee 2 – Squat Movement

Table 32: Stress results from FEM analysis for the squat movement of knee 2 at E = 8 MPa showing the stress on the cartilage and osseous surfaces.

Squat Stress (MPa)							
		E = 8 MPa					
Degree of flexion	Average Adapted Compression (mm)	ν = 0.4		ν = 0.45		ν = 0.48	
		Cartilage surface	Osseous Surface	Cartilage surface	Osseous Surface	Cartilage surface	Osseous Surface
0	0.645	2.785	2.99	3.025	3.285	4.455	4.695
30	0.585	1.653	1.888	1.867	2.107	2.16	2.385
60	0.458	2.195	2.36	2.455	2.675	2.775	3.005
90	-	-	-	-	-	-	-
Max	0.322	1.761	1.911	2.095	2.39	2.845	3.305

Table 33: Stress results from FEM analysis for the squat movement of knee 2 at E = 10 MPa showing the stress on the cartilage and osseous surfaces.

Squat Stress (MPa)							
		E = 10 MPa					
Degree of flexion	Average Adapted Compression (mm)	ν = 0.4		ν = 0.45		ν = 0.48	
		Cartilage surface	Osseous Surface	Cartilage surface	Osseous Surface	Cartilage surface	Osseous Surface
0	0.645	3.48	3.935	3.78	4.26	5.565	6.1
30	0.585	2.065	2.315	2.335	2.595	2.7	2.955
60	0.458	2.745	2.945	3.065	3.325	3.465	3.805
90	-	-	-	-	-	-	-
Max	0.322	2.2	2.48	2.615	2.795	3.56	3.925

Table 34: Stress results from FEM analysis for the squat movement of knee 2 at E = 12 MPa showing the stress on the cartilage and osseous surfaces.

Squat Stress (MPa)							
		E = 12 MPa					
Degree of flexion	Average Adapted Compression (mm)	v = 0.4		v = 0.45		v = 0.48	
		Cartilage surface	Osseous Surface	Cartilage surface	Osseous Surface	Cartilage surface	Osseous Surface
0	0.645	4.18	4.425	4.54	4.77	6.67	7.035
30	0.585	2.48	2.9	2.8	3.305	3.24	3.97
60	0.458	4.12	4.34	4.6	5.105	5.195	5.645
90	-	-	-	-	-	-	-
Max	0.322	2.645	2.82	3.14	3.46	4.275	4.645